Drug Design, Development and Therapy

Dovepress
open access to scientific and medical research

Open Access Full Text Article

ORIGINAL RESEARCH

Plumbagin suppresses epithelial to mesenchymal transition and stemness via inhibiting Nrf2-mediated signaling pathway in human tongue squamous cell carcinoma cells

This article was published in the following Dove Press journal:
Drug Design, Development and Therapy
5 October 2015
Number of times this article has been viewed

Shu-Ting Pan,[1] Yiru Qin,[2] Zhi-Wei Zhou,[2,3] Zhi-Xu He,[3] Xueji Zhang,[4] Tianxin Yang,[5] Yin-Xue Yang,[6] Dong Wang,[7] Shu-Feng Zhou,[2] Jia-Xuan Qiu[1]

[1]Department of Oral and Maxillofacial Surgery, The First Affiliated Hospital of Nanchang University, Nanchang, Jiangxi, People's Republic of China; [2]Department of Pharmaceutical Sciences, College of Pharmacy, University of South Florida, Tampa, FL, USA; [3]Guizhou Provincial Key Laboratory for Regenerative Medicine, Stem Cell and Tissue Engineering Research Center and Sino-US Joint Laboratory for Medical Sciences, Guiyang Medical University, Guiyang, Guizhou, People's Republic of China; [4]Research Center for Bioengineering and Sensing Technology, University of Science and Technology Beijing, Beijing, People's Republic of China; [5]Department of Internal Medicine, University of Utah and Salt Lake Veterans Affairs Medical Center, Salt Lake City, UT, USA; [6]Department of Colorectal Surgery, General Hospital of Ningxia Medical University, Yinchuan, Ningxia, People's Republic of China; [7]Cancer Center, Daping Hospital and Research Institute of Surgery, Third Military Medical University, Chongqing, People's Republic of China

Correspondence: Jia-Xuan Qiu
Department of Oral and Maxillofacial Surgery, The First Affiliated Hospital of Nanchang University, 17 Yongwai Main St, Nanchang, Jiangxi 330006, People's Republic of China
Tel +86 791 8869 5069
Fax +86 791 8869 2745
Email qiujiaxuan@163.com

Shu-Feng Zhou
Department of Pharmaceutical Sciences, College of Pharmacy, University of South Florida, 12901 Bruce B Downs Boulevard, Tampa, FL 33612, USA
Tel +1 813 974 6276
Fax +1 813 905 9885
Email szhou@health.usf.edu

Abstract: Tongue squamous cell carcinoma (TSCC) is the most common malignancy in oral and maxillofacial tumors with highly metastatic characteristics. Plumbagin (5-hydroxy-2-methyl-1, 4-naphthoquinone; PLB), a natural naphthoquinone derived from the roots of *Plumbaginaceae* plants, exhibits various bioactivities, including anticancer effects. However, the potential molecular targets and underlying mechanisms of PLB in the treatment of TSCC remain elusive. This study employed stable isotope labeling by amino acids in cell culture (SILAC)-based quantitative proteomic approach to investigate the molecular interactome of PLB in human TSCC cell line SCC25 and elucidate the molecular mechanisms. The proteomic data indicated that PLB inhibited cell proliferation, activated death receptor-mediated apoptotic pathway, remodeled epithelial adherens junctions pathway, and manipulated nuclear factor erythroid 2-related factor 2 (Nrf2)-mediated oxidative stress response signaling pathway in SCC25 cells with the involvement of a number of key functional proteins. Furthermore, we verified these protein targets using Western blotting assay. The verification results showed that PLB markedly induced cell cycle arrest at G_2/M phase and extrinsic apoptosis, and inhibited epithelial to mesenchymal transition (EMT) and stemness in SCC25 cells. Of note, *N*-acetyl-l-cysteine (NAC) and l-glutathione (GSH) abolished the effects of PLB on cell cycle arrest, apoptosis induction, EMT inhibition, and stemness attenuation in SCC25 cells. Importantly, PLB suppressed the translocation of Nrf2 from cytosol to nucleus, resulting in an inhibition in the expression of downstream targets. Taken together, these results suggest that PLB may act as a promising anticancer compound via inhibiting Nrf2-mediated oxidative stress signaling pathway in SCC25 cells. This study provides a clue to fully identify the molecular targets and decipher the underlying mechanisms of PLB in the treatment of TSCC.

Keywords: PLB, SILAC, EMT, stemness, Nrf2, tongue squamous cell carcinoma

Introduction

Tongue squamous cell carcinoma (TSCC) is the most prevalent type of oral and maxillofacial tumor, with an estimated 14,320 new cases and 2,190 deaths in the US in 2015.[1] The most important etiological factors are tobacco, excessive consumption of alcohol, and betel quid usage, which act separately or synergistically.[2] It has been reported that TSCC is more commonly found in males, with a percentage of 72.0% of all TSCC cases, compared with a percentage of 28.0% in females.[1] Of note, the incidence of TSCC in young white women is significantly increasing, according to the Surveillance, Epidemiology, and End Results program data from 1973 to 2010 in the US.[3] Because of the mobility and masticatory function of the tongue, TSCC is inclined to spread locally, involving perioral structures, and metastasize to local

regional lymph nodes. For this reason, TSCC always demonstrates a much more aggressive behavior than other kinds of oral and maxillofacial tumors.[4] Although there has been advancement in the sequential therapies, including radiation, surgery, and chemotherapy, the patients still suffer from serious relapse and the 5-year survival rate shows no inspiring progress.[5] It requires the development of novel therapeutics with improved therapeutic effect and reduced side effect for TSCC treatment.

It has been revealed that acquisition of epithelial to mesenchymal transition (EMT) and induction of cancer stem cell (CSC)-like properties are closely involved in the initiation, development, progression, metastasis, and relapse of solid tumors.[6,7] Normal epithelial cells show apical–basal polarity maintained by apical tight junctions and basolateral adherens junctions. The loss of epithelial property and acquisition of mesenchymal features enables cancer cells to metastasize easily and quickly. The reverse process of mesenchymal to epithelial transition (MET) can also occur. Cancer progression is affected by the balance between EMT and MET.[8,9] Thus, interfering with the EMT process may help regress cancer metastasis. On the other hand, the proliferation of tumors is driven by a bulk of dedicated stem cells, the CSCs. CSCs, also known as cancer-initiating cells, are involved in cancer cell renewal and differentiation.[10] CSCs can display EMT characteristics such as loss of adhesion protein E-cadherin.[11] It is reported that CSCs play an important role in chemotherapy resistance due to the self-renewal ability. Multiple oncogenes are involved in the maintenance of stemness and tumorigenicity of CSCs, such as Octamer-4 (Oct-4), Bmi-1, Nanog, and sex-determing region Y-box 2 (Sox-2).[12–15] Hence, targeting the CSCs shows great therapeutic potential in cancer therapy.[16]

Plumbagin (5-hydroxy-2-methyl-1, 4-naphthoquinone; PLB) is isolated from the root of *Plumbago zeylanica* L, *Juglans regia*, *Juglans cinerea*, and *Juglans nigra*, with a variety of pharmacological activities including anti-inflammatory, antiatherosclerotic, antibacterial, antifungal, and anticancer activities in in vitro and in vivo models.[17] Notably, PLB shows a potent ability in killing cancer cells with minimal side effects.[18] Previous studies from our and other groups have shown that PLB regulates various cellular processes such as cell cycle, apoptosis, autophagy, and cellular redox status.[19–21] PLB also induces cancer cell apoptosis and autophagy by inhibition of nuclear factor kappa B (NF-κB) activation and phosphatidylinositide 3-kinase (PI3K)/protein kinase B (Akt)/mTOR signaling pathway.[21–25] Besides, PLB can efficiently facilitate reactive oxygen species (ROS) generation, which also contributes to the cancer cell killing effect.[26–28] However, the full spectrum of the molecular targets and therapeutic effects of PLB in TSCC are not clear.

Accumulating evidence shows that stable isotope labeling by amino acids in cell culture (SILAC)-based quantitative proteomic approach has the capability of revealing the potential targets of a given compound or drug.[29,30] In this study, we aimed at elucidating the possible mechanisms for PLB's anticancer effect in the treatment of TSCC using a SILAC-based quantitative proteomic approach to take a panoramic view of PLB in a TSCC cell line (SCC25). The corresponding verifications were also performed. In addition, we also carried out separate experiments to investigate the relationship between PLB-induced ROS generation and PLB-mediated cell cycle arrest, apoptosis induction, EMT inhibition, and stemness attenuation.

Materials and methods

Chemicals and reagents

Dulbecco's Modified Eagle's Medium (DMEM) and Ham's F12 medium were obtained from Corning Cellgro Inc. (Herndon, VA, USA). Fetal bovine serum (FBS), PLB, dimethyl sulfoxide (DMSO), hydrocortisone, *N*-acetyl-L-cysteine (NAC, a ROS scavenger), L-glutathione (GSH, a ROS scavenger), ammonium persulfate, D-glucose, propidium iodide (PI), ribonuclease, protease and phosphatase inhibitor cocktails, radioimmunoprecipitation assay buffer (RIPA), bovine serum albumin (BSA), Tris base, sodium dodecyl sulfate (SDS), ethylenediaminetetraacetic acid, Dulbecco's phosphate-buffered saline (PBS), dithiothreitol (DTT), $^{13}C_6$-L-lysine, L-lysine, $^{13}C_6$ $^{15}N_4$-L-arginine, and L-arginine were purchased from Sigma-Aldrich (St Louis, MO, USA). FASP™ protein digestion kit was bought from Protein Discovery Inc. (Knoxville, TN, USA). The Annexin V:PE apoptosis detection kit was purchased from BD Pharmingen Biosciences (San Jose, CA, USA). Ionic Detergent Compatibility Reagent (IDCR) kit, nuclear and cytoplasmic extraction kit, Pierce bicinchoninic acid (BCA) protein assay kit, skimmed milk, and Western blotting substrate were bought from Thermo Fisher Scientific (Waltham, MA, USA). The polyvinylidene difluoride (PVDF) membrane was purchased from Bio-Rad (Hercules, CA, USA). Primary antibodies against human CDK1/cdc2, Cyclin B1, cdc25, Fas (TNFRSF6)-associated via death domain (FADD), TNF1 receptor-associated death domain (TRADD), TRAIL-R2 (DR5), cleaved caspase-3 (CC3), E-cadherin, N-cadherin, Snail, Slug, zinc finger E-box-binding homeobox 1 (TCF8/ZEB1), vimentin, β-Catenin, zona occludens protein 1 (ZO-1), claudin-1, Oct-4, Bmi-1, Nanog, Sox-2, and

glutathione *S*-transferase (GST) were purchased from Cell Signaling Technology Inc. (Beverly, MA, USA). Primary antibodies against nuclear factor erythroid 2-related factor 2 (Nrf2), NAD(P)H quinone oxidoreductase 1 (NQO1), and heat shock protein 90 (HSP90) were purchased from Santa Cruz Biotechnology Inc. (Santa Cruz, CA, USA). The antibodies against human β-actin and Histone H3 were obtained from Santa Cruz Biotechnology Inc.

Cell line and cell culture

The TSCC cell line SCC25 was obtained from the American Type Culture Collection (Manassas, VA, USA) and cultured in a 1:1 mixture of DMEM and Ham's F12 medium containing 1.2 g/L sodium bicarbonate, 2.5 mM L-glutamine, 15 mM HEPES, and 0.5 mM sodium pyruvate and was supplemented with 400 ng/mL hydrocortisone and 10% heat-inactivated FBS. The cells were maintained at 37°C in a 5% CO_2/95% air humidified incubator. PLB was dissolved in DMSO with a stock concentration of 100 mM and was freshly diluted to the desired concentrations with the culture medium. The final concentration of DMSO was at 0.05% (v/v, volume per volume). The control cells received only the vehicle. No ethics approval was required for the use of this cell line this paper.

SILAC quantitative proteomics

Quantitative proteomic experiments were performed using SILAC as described previously.[31–33] Briefly, SCC25 cells were cultured in the medium with or without stable isotope-labeled amino acids ($^{13}C_6$ L-lysine and $^{13}C_6{}^{15}N_4$ L-arginine). SCC25 cells were passaged for five times by changing medium or splitting cells. Then, cells with stable isotope-labeled amino acids were treated with 5 μM PLB for 24 hours. Following that, the cell samples were harvested and lysed with hot lysis buffer (100 mM Tris base, 4% SDS, and 100 mM DTT). The proteins were denatured at 95°C for 5 minutes and sonicated at 20% amplitude (AMPL) for 3 seconds with 6 pulses. Later, the samples were centrifuged at 15,000× *g* for 20 minutes and the supernatant was collected in clean tubes. The protein concentration was determined using the IDCR kits. Then, equal amounts of heavy and light protein sample were combined to reach a total volume of 30–60 μL containing 300–600 μg proteins. The combined protein sample was digested using FASP™ protein digestion kit. After proteins were digested, the resultant sample was acidified to pH of 3 and desalted using a C_{18} solid-phase extraction column. The samples were then concentrated using vacuum concentrator at 45°C for 120 minutes and the peptide mixtures (5 μL) were subject to the hybrid linear ion trap-Orbitrap (LTQ Orbitrap XL, Thermo Scientific Inc.). Liquid chromatography-tandem mass spectrometry (LC-MS/MS) was performed using a 10 cm long 75 μm (inner diameter) reversed-phase column packed with 5 μm diameter C_{18} material with 300 Å pore size (New Objective, Woburn, MA, USA), with a gradient mobile phase of 2%–40% acetonitrile in 0.1% formic acid at 200 μL/minute for 125 minutes. The Orbitrap full MS scanning was performed at a mass (*m/z*) resolving power of 60,000, with positive polarity in profile mode ($M+H^+$). Peptide SILAC ratio was calculated using MaxQuant version 1.2.0.13. The SILAC ratio was determined by averaging all peptide SILAC ratios from peptides identified of the same protein. The protein IDs were identified using Scaffold 4.3.2 from Proteome Software Inc. (Portland, OR, USA) and the pathway was analyzed using Ingenuity Pathway Analysis (IPA) from QIAGEN (Redwood City, CA, USA).

Cell cycle distribution analysis

The effect of PLB on cell cycle distribution of SCC25 cells was determined by flow cytometry using PI as the DNA stain as described previously.[20] Briefly, SCC25 cells were treated with PLB at concentrations of 0.1, 1, and 5 μM for 24 hours. In separate experiments, SCC25 cells were treated with 5 μM PLB for 6, 24, and 48 hours. In addition, the effect of ROS scavengers (GSH and NAC)[34] on PLB-induced G_2/M arrest was also examined. Cells were trypsinized and resuspended in 1 mL serum-free medium. Subsequently, the cells were fixed with 3 mL 70% ethanol at −20°C overnight. The cells were stained using 50 μg/mL PI. A total number of 1×10^4 cells was subject to cell cycle analysis using a flow cytometer (Becton Dickinson Immunocytometry Systems, San Jose, CA, USA). Finally, the raw data were analyzed by ModFitLT software (version 3.2.1) (Verity Software House, Topsham, MA, USA).

Quantification of cellular apoptosis

We used Annexin V:PE apoptosis detection kit to measure apoptotic cells after the cells were treated with 0.1, 1, and 5 μM PLB for 24 hours. In separate experiments, SCC25 cells were treated with 5 μM PLB for 6, 24, and 48 hours. In addition, the effect of GSH and NAC on PLB-induced apoptosis was also examined. Briefly, cells were trypsinized and washed twice with cold PBS, and then resuspended in 1× binding buffer with 5 μL of PE Annexin V and 5 μL of 7-amino-actinomycin D at a concentration of 1×10^5/mL cells in a total volume of 100 μL. The cells were gently mixed and incubated in the dark for 15 minutes at room temperature. Following that, a quota of 1× binding buffer (400 μL) was added to each test tube and the number of apoptotic cells

was quantified by flow cytometry (BD LSR II Analyzer) within 1 hour.

Western blotting assay

The levels of various cellular proteins were determined using Western blotting assays. The SCC25 cells were incubated with PLB at 0.1, 1, and 5 μM for 24 hours. In separate experiments, SCC25 cells were treated with 5 μM PLB for 6, 24, and 48 hours. After PLB treatment, cells were washed twice with precold PBS and lysed with the RIPA buffer containing the protease inhibitor and phosphatase inhibitor cocktails. In addition, we extracted the nuclear proteins according to the instruction given in the nuclear and cytoplasmic extraction kit. Protein concentrations were measured using the Pierce BCA protein assay kit. Equal amounts of protein samples at 20 μg were electrophoresed on 7%–12% sodium dodecyl sulfate–polyacrylamide gel electrophoresis (SDS-PAGE) minigel after thermal denaturation for 5 minutes at 95°C. Proteins were transferred onto immobilon PVDF membrane at 80 V for 3 hours at 4°C. Subsequently, membranes were blocked with 5% BSA and probed with indicated primary antibody overnight at 4°C and then blotted with respective secondary antibody. Visualization was performed using the Bio-Rad system. Cytosolic protein level was normalized to the matching densitometric value of β-actin, and nuclear protein level was normalized to the matching densitometric value of Histone H3.

Statistical analysis

Data are presented as the mean ± standard deviation (SD). Multiple comparisons were evaluated by one-way analysis of variance (ANOVA), followed by Tukey's multiple comparison. A value of $P<0.05$ was considered statistically significant. All the assays were performed in triplicate.

Results

Summary of proteomic response to PLB treatment in SCC25 cells

We first performed SILAC-based proteomics to evaluate the potential molecular targets of PLB in SCC25 cells. PLB increased the expression level of 143 protein molecules, but decreased the expression level of 255 protein molecules in SCC25 cells (Tables 1 and 2). Subsequently, these proteins were subject to IPA. The results showed that 101 signaling pathways were potentially regulated by PLB in SCC25 cells (Table 3 and Figure 1). The top ten targeted signaling

Table 1 Proteins upregulated by PLB in SCC25 cells

Fold change	ID	Symbol	Entrez gene name	Location	Type(s)
16.699	Q9Y4L1	HYOU1	Hypoxia upregulated 1	Cytoplasm	Other
6.339	Q86UP2	KTN1	Kinectin 1 (kinesin receptor)	Plasma membrane	Transmembrane receptor
5.171	P07996	THBS1	Thrombospondin 1	Extracellular space	Other
4.993	Q9H3K6	BOLA2/BC	BolA family member 2	Cytoplasm	Other
4.304	Q9NY33	DPP3	Dipeptidyl-peptidase 3	Cytoplasm	Peptidase
3.861	P12277	CKB	Creatine kinase, brain	Cytoplasm	Kinase
3.794	P14866	HNRNPL	Heterogeneous nuclear ribonucleoprotein L	Nucleus	Other
3.14	H0Y4R1	IMPDH2	IMP (inosine 5′-monophosphate) dehydrogenase 2	Cytoplasm	Enzyme
3.022	Q9NZB2	FAM120A	Family with sequence similarity 120A	Cytoplasm	Other
2.667	Q9P2E9	RRBP1	Ribosome binding protein 1	Cytoplasm	Other
2.61	Q9BQE3	TUBA1C	Tubulin, alpha 1c	Cytoplasm	Other
2.289	P62136	PPP1CA	Protein phosphatase 1, catalytic subunit, alpha isozyme	Cytoplasm	Phosphatase
2.164	P23284	PPIB	Peptidylprolyl isomerase B (cyclophilin B)	Cytoplasm	Enzyme
2.142	P14923	JUP	Junction plakoglobin	Plasma membrane	Other
2.136	P38646	HSPA9	Heat shock 70 kDa protein 9 (mortalin)	Cytoplasm	Other
2.052	C9JZR2	CTNND1	Catenin (cadherin-associated protein), delta 1	Nucleus	Other
1.978	O43852	CALU	Calumenin	Cytoplasm	Other
1.871	Q01082	SPTBN1	Spectrin, beta, non-erythrocytic 1	Plasma membrane	Other
1.864	P50454	SERPINH1	Serpin peptidase inhibitor, clade H (heat shock protein 47), member 1, (collagen binding protein 1)	Extracellular space	Other
1.753	Q13751	LAMB3	Laminin, beta 3	Extracellular space	Transporter
1.742	Q13158	FADD	Fas (TNFRSF6)-associated via death domain	Cytoplasm	Other
1.732	Q9UHX1	PUF60	Poly-U binding splicing factor 60 kDa	Nucleus	Other
1.718	P32320	CDA	Cytidine deaminase	Nucleus	Enzyme
1.695	P05556	ITGB1	Integrin, beta 1 (fibronectin receptor, beta polypeptide, antigen CD29 includes MDF2, MSK12)	Plasma membrane	Transmembrane receptor

(*Continued*)

Table 1 (*Continued*)

Fold change	ID	Symbol	Entrez gene name	Location	Type(s)
1.682	P04844	RPN2	Ribophorin II	Cytoplasm	Enzyme
1.615	P17844	DDX5	DEAD (Asp-Glu-Ala-Asp) box helicase 5	Nucleus	Enzyme
1.612	O14579	COPE	Coatomer protein complex, subunit epsilon	Cytoplasm	Transporter
1.581	Q13409	DYNC1/2	Dynein, cytoplasmic 1, intermediate chain 2	Cytoplasm	Other
1.576	Q13753	LAMC2	Laminin, gamma 2	Extracellular space	Other
1.556	Q96QK1	VPS35	Vacuolar protein sorting 35 (*S. cerevisiae*)	Cytoplasm	Transporter
1.536	P04181	OAT	Ornithine aminotransferase	Cytoplasm	Enzyme
1.535	E7EPN9	PRRC2C	Proline-rich coiled-coil 2C	Other	Other
1.534	P22102	GART	Phosphoribosylglycinamide formyltransferase, phosphoribosylglycinamide synthetase, phosphoribosylaminoimidazole synthetase	Cytoplasm	Enzyme
1.518	P45974	USP5	Ubiquitin specific peptidase 5 (isopeptidase T)	Cytoplasm	Peptidase
1.508	P62263	RPS14	Ribosomal protein S14	Cytoplasm	Translation regulator
1.474	P08779	KRT16	Keratin 16	Cytoplasm	Other
1.463	P62701	RPS4X	Ribosomal protein S4, X-linked	Cytoplasm	Other
1.454	P31939	ATIC	5-Aminoimidazole-4-carboxamide ribonucleotide formyltransferase/IMP cyclohydrolase	Cytoplasm	Enzyme
1.442	Q6NZI2	PTRF	Polymerase I and transcript release factor	Nucleus	Transcription regulator
1.439	B1AH77	RAC2	Ras-related C3 botulinum toxin substrate 2 (rho family, small GTP binding protein Rac2)	Cytoplasm	Enzyme
1.412	P05787	KRT8	Keratin 8	Cytoplasm	Other
1.41	P60228	EIF3E	Eukaryotic translation initiation factor 3, subunit E	Cytoplasm	Other
1.408	A1A4Z1	IQUB	IQ motif and ubiquitin domain containing	Cytoplasm	Other
1.405	Q15459	SF3A1	Splicing factor 3a, subunit 1, 120 kDa	Nucleus	Other
1.404	O95817	BAG3	BCL2-associated athanogene 3	Cytoplasm	Other
1.398	F5GWP8	KRT17	Keratin 17	Cytoplasm	Other
1.396	O00303	EIF3F	Eukaryotic translation initiation factor 3, subunit F	Cytoplasm	Translation regulator
1.388	P11021	HSPA5	Heat shock 70 kDa protein 5 (glucose-regulated protein, 78 kDa)	Cytoplasm	Enzyme
1.374	Q07065	CKAP4	Cytoskeleton-associated protein 4	Cytoplasm	Other
1.367	P49411	TUFM	Tu translation elongation factor, mitochondrial	Cytoplasm	Translation regulator
1.363	K7EK07	H3F3A/ H3F3B	H3 histone, family 3A	Nucleus	Other
1.36	P15924	DSP	Desmoplakin	Plasma membrane	Other
1.357	P20700	LMNB1	Lamin B1	Nucleus	Other
1.324	P14625	HSP90B1	Heat shock protein 90 kDa beta (Grp94), member 1	Cytoplasm	Other
1.315	F8VY35	NAP1L1	Nucleosome assembly protein 1-like 1	Nucleus	Other
1.314	F8VZX2	PCBP2	Poly(rC) binding protein 2	Nucleus	Other
1.302	P42224	STAT1	Signal transducer and activator of transcription 1, 91 kDa	Nucleus	Transcription regulator
1.286	P35613	BSG	Basigin (Ok blood group)	Plasma membrane	Transporter
1.268	Q9UQ80	PA2G4	Proliferation-associated 2G4, 38 kDa	Nucleus	Transcription regulator
1.258	K7EJ78	RPS15	Ribosomal protein S15	Cytoplasm	Other
1.254	F8VPF3	PDE6H	Phosphodiesterase 6H, cGMP-specific, cone, gamma	Cytoplasm	Enzyme
1.252	P32969	RPL9	Ribosomal protein L9	Cytoplasm	Other
1.243	P09972	ALDOC	Aldolase C, fructose-bisphosphate	Cytoplasm	Enzyme
1.243	P26038	MSN	Moesin	Plasma membrane	Other
1.234	P68366	TUBA4A	Tubulin, alpha 4a	Cytoplasm	Other
1.232	P23526	AHCY	Adenosylhomocysteinase	Cytoplasm	Enzyme
1.224	P31949	S100A11	S100 calcium binding protein A11	Cytoplasm	Other
1.22	R4GNH3	PSMC3	Proteasome (prosome, macropain) 26S subunit, ATPase, 3	Nucleus	Transcription regulator
1.215	Q12906	ILF3	Interleukin enhancer binding factor 3, 90 kDa	Nucleus	Transcription regulator
1.214	P46777	RPL5	Ribosomal protein L5	Cytoplasm	Other
1.21	H0YA96	HNRNPD	Heterogeneous nuclear ribonucleoprotein D (AU-rich element RNA binding protein 1, 37kDa)	Nucleus	Transcription regulator
1.209	P22314	UBA1	Ubiquitin-like modifier activating enzyme 1	Cytoplasm	Enzyme
1.199	P02786	TFRC	Transferrin receptor	Plasma membrane	Transporter
1.198	P02545	LMNA	Lamin A/C	Nucleus	Other

(*Continued*)

Table 1 (*Continued*)

Fold change	ID	Symbol	Entrez gene name	Location	Type(s)
1.17	Q08211	DHX9	DEAH (Asp-Glu-Ala-His) box helicase 9	Nucleus	Enzyme
1.163	P31153	MAT2A	Methionine adenosyltransferase II, alpha	Cytoplasm	Enzyme
1.162	P55072	VCP	Valosin containing protein	Cytoplasm	Enzyme
1.16	P62979	RPS27A	Ribosomal protein S27a	Cytoplasm	Other
1.16	P31947	SFN	Stratifin	Cytoplasm	Other
1.159	P23381	WARS	Tryptophanyl-tRNA synthetase	Cytoplasm	Enzyme
1.154	P46940	IQGAP1	IQ motif containing GTPase activating protein 1	Cytoplasm	Other
1.153	Q13177	PAK2	p21 protein (Cdc42/Rac)-activated kinase 2	Cytoplasm	Kinase
1.148	Q9Y446	PKP3	Plakophilin 3	Plasma membrane	Other
1.147	H0YLC2	PSMA4	Proteasome (prosome, macropain) subunit, alpha type, 4	Cytoplasm	Peptidase
1.144	P25705	ATP5A1	ATP synthase, H+ transporting, mitochondrial F1 complex, alpha subunit 1, cardiac muscle	Cytoplasm	Transporter
1.143	Q14697	GANAB	Glucosidase, alpha; neutral AB	Cytoplasm	Enzyme
1.137	P06576	ATP5B	ATP synthase, H+ transporting, mitochondrial F1 complex, beta polypeptide	Cytoplasm	Transporter
1.136	P07355	ANXA2	Annexin A2	Plasma membrane	Other
1.136	Q99460	PSMD1	Proteasome (prosome, macropain) 26S subunit, non-ATPase, 1	Cytoplasm	Other
1.133	P07858	CTSB	Cathepsin B	Cytoplasm	Peptidase
1.129	Q9UMS4	PRPF19	Pre-mRNA processing factor 19	Nucleus	Enzyme
1.127	P31948	STIP1	Stress-induced phosphoprotein 1	Cytoplasm	Other
1.126	P05783	KRT18	Keratin 18	Cytoplasm	Other
1.125	P20618	PSMB1	Proteasome (prosome, macropain) subunit, beta type, 1	Cytoplasm	Peptidase
1.123	P30101	PDIA3	Protein disulfide isomerase family A, member 3	Cytoplasm	Peptidase
1.122	P04083	ANXA1	Annexin A1	Plasma membrane	Enzyme
1.115	Q96FW1	OTUB1	OTU deubiquitinase, ubiquitin aldehyde binding 1	Cytoplasm	Enzyme
1.115	P55735	SEC13	SEC13 homolog (*S. cerevisiae*)	Cytoplasm	Transporter
1.111	P09936	UCHL1	Ubiquitin carboxyl-terminal esterase L1 (ubiquitin thiolesterase)	Cytoplasm	Peptidase
1.108	O60506	SYNCRIP	Synaptotagmin binding, cytoplasmic RNA interacting protein	Nucleus	Other
1.104	P02533	KRT14	Keratin 14	Cytoplasm	Other
1.103	P36952	SERPINB5	Serpin peptidase inhibitor, clade B (ovalbumin), member 5	Extracellular space	Other
1.103	O43399	TPD52L2	Tumor protein D52-like 2	Cytoplasm	Other
1.099	P50991	CCT4	Chaperonin containing TCP1, subunit 4 (delta)	Cytoplasm	Other
1.096	P11142	HSPA8	Heat shock 70 kDa protein 8	Cytoplasm	Enzyme
1.096	P40926	MDH2	Malate dehydrogenase 2, NAD (mitochondrial)	Cytoplasm	Enzyme
1.096	P31946	YWHAB	Tyrosine 3-monooxygenase/tryptophan 5-monooxygenase activation protein, beta	Cytoplasm	Transcription regulator
1.094	Q92597	NDRG1	N-myc downstream regulated 1	Nucleus	Kinase
1.086	H7C5W9	ATP2A2	ATPase, Ca^{2+} transporting, cardiac muscle, slow twitch 2	Cytoplasm	Transporter
1.086	P13489	RNH1	Ribonuclease/angiogenin inhibitor 1	Cytoplasm	Other
1.083	P31930	UQCRC1	Ubiquinol-cytochrome c reductase core protein 1	Cytoplasm	Enzyme
1.08	P17655	CAPN2	Calpain 2, (m/II) large subunit	Cytoplasm	Peptidase
1.08	P34932	HSPA4	Heat shock 70 kDa protein 4	Cytoplasm	Other
1.076	P62241	RPS8	Ribosomal protein S8	Cytoplasm	Other
1.071	P13647	KRT5	Keratin 5	Cytoplasm	Other
1.07	P02538	KRT6A	Keratin 6A	Other	Other
1.058	P61981	YWHAG	Tyrosine 3-monooxygenase/tryptophan 5-monooxygenase activation protein, gamma	Cytoplasm	Other
1.057	P04075	ALDOA	Aldolase A, fructose-bisphosphate	Cytoplasm	Enzyme
1.053	Q96AG4	LRRC59	Leucine rich repeat containing 59	Cytoplasm	Other
1.05	P23219	PTGS1	Prostaglandin-endoperoxide synthase 1 (prostaglandin G/H synthase and cyclooxygenase)	Cytoplasm	Enzyme
1.05	P27348	YWHAQ	Tyrosine 3-monooxygenase/tryptophan 5-monooxygenase activation protein, theta	Cytoplasm	Other

(*Continued*)

Table 1 (*Continued*)

Fold change	ID	Symbol	Entrez gene name	Location	Type(s)
1.046	P00387	CYB5R3	Cytochrome b5 reductase 3	Cytoplasm	Enzyme
1.046	Q9UL46	PSME2	Proteasome (prosome, macropain) activator subunit 2 (PA28 beta)	Cytoplasm	Peptidase
1.037	P06748	NPM1	Nucleophosmin (nucleolar phosphoprotein B23, numatrin)	Nucleus	Transcription regulator
1.036	P36578	RPL4	Ribosomal protein L4	Cytoplasm	Enzyme
1.033	P28066	PSMA5	Proteasome (prosome, macropain) subunit, alpha type, 5	Cytoplasm	Peptidase
1.032	P08238	HSP90AB1	Heat shock protein 90 kDa alpha (cytosolic), class B member 1	Cytoplasm	Enzyme
1.03	P52907	CAPZA1	Capping protein (actin filament) muscle Z-line, alpha 1	Cytoplasm	Other
1.03	P16152	CAR1	Carbonyl reductase 1	Cytoplasm	Enzyme
1.028	Q14019	COTL1	Coactosin-like F-actin binding protein 1	Cytoplasm	Other
1.027	P04632	CAPNS1	Calpain, small subunit 1	Cytoplasm	Peptidase
1.026	P19105	MYL12A	Myosin, light chain 12A, regulatory, nonsarcomeric	Cytoplasm	Other
1.024	P12814	ACTN1	Actinin, alpha 1	Cytoplasm	Other
1.021	P50395	GD12	GDP dissociation inhibitor 2	Cytoplasm	Other
1.02	Q01518	CAP1	CAP, adenylate cyclase-associated protein 1 (yeast)	Plasma membrane	Other
1.018	J3KPE3	GNB2L1	Guanine nucleotide binding protein (G protein), beta polypeptide 2-like 1	Cytoplasm	Enzyme
1.014	Q99880	HIST1H2BL	Histone cluster 1, H2bl	Nucleus	Other
1.012	P27695	APEX1	APEX nuclease (multifunctional DNA repair enzyme) 1	Nucleus	Enzyme
1.007	P68371	TUBB4B	Tubulin, beta 4B class IVb	Cytoplasm	Other
1.006	F5GZS6	SLC3A2	Solute carrier family 3 (amino acid transporter heavy chain), member 2	Plasma membrane	Transporter
1.004	O15371	EIF3D	Eukaryotic translation initiation factor 3, subunit D	Cytoplasm	Other
1.002	D6RG13	RPS3A	Ribosomal protein S3A	Nucleus	Other
1.001	M0R2L9	RPS19	Ribosomal protein S19	Cytoplasm	Other

Abbreviation: PLB, plumbagin.

Table 2 Proteins downregulated by PLB in SCC25 cells

Fold change	ID	Symbol	Entrez gene name	Location	Type(s)
−3.32	P52306	RAP1GDS1	RAP1, GTP-GDP dissociation stimulator 1	Cytoplasm	Other
−2.964	P29966	MARCKS	Myristoylated alanine-rich protein kinase C substrate	Plasma membrane	Other
−2.937	P04264	KRT1	Keratin 1	Cytoplasm	Other
−2.79	Q15942	ZYX	Zyxin	Plasma membrane	Other
−2.644	P35527	KRT9	Keratin 9	Other	Other
−2.642	P80723	BASP1	Brain abundant, membrane attached signal protein 1	Nucleus	Transcription regulator
−2.561	B8ZZQ6	PTMA	Prothymosin, alpha	Nucleus	Other
−2.542	P25786	PSMA1	Proteasome (prosome, macropain) subunit, alpha type, 1	Cytoplasm	Peptidase
−2.476	P35637	FUS	FUS RNA binding protein	Nucleus	Transcription regulator
−2.439	P16989	YBX3	Y box binding protein 3	Nucleus	Transcription regulator
−2.394	K7EL20	EIF3G	Eukaryotic translation initiation factor 3, subunit G	Cytoplasm	Other
−2.346	P13726	F3	Coagulation factor III (thromboplastin, tissue factor)	Plasma membrane	Transmembrane receptor
−2.3	Q08J23	NSUN2	NOP2/Sun RNA methyltransferase family, member 2	Nucleus	Enzyme
−2.244	P47895	ALDH1A3	Aldehyde dehydrogenase 1 family, member A3	Cytoplasm	Enzyme
−2.128	P26358	DNMT1	DNA (cytosine-5-)-methyltransferase 1	Nucleus	Enzyme
−2.111	Q15582	TGFBI	Transforming growth factor, beta-induced, 68 kDa	Extracellular space	Other
−2.081	P30153	PPP2R1A	Protein phosphatase 2, regulatory subunit A, alpha	Cytoplasm	Phosphatase
−2.052	P06744	GPI	Glucose-6-phosphate isomerase	Extracellular space	Enzyme
−2.018	Q5JXT2	NOP56	NOP56 ribonucleoprotein	Nucleus	Other
−2.013	P53621	COPA	Coatomer protein complex, subunit alpha	Cytoplasm	Transporter
−1.946	Q16777	HIST2H2AC	Histone cluster 2, H2ac	Nucleus	Other

(*Continued*)

Table 2 (*Continued*)

Fold change	ID	Symbol	Entrez gene name	Location	Type(s)
−1.921	C9JNR4	RHOA	Ras family member A	Cytoplasm	Enzyme
−1.921	F8VWS0	RPLP0	Ribosomal protein, large, P0	Cytoplasm	Other
−1.915	P09211	GSTP1	Glutathione *S*-transferase pi 1	Cytoplasm	Enzyme
−1.88	Q06830	PRDX1	Peroxiredoxin 1	Cytoplasm	Enzyme
−1.87	P11498	PC	Pyruvate carboxylase	Cytoplasm	Enzyme
−1.86	P33176	KIF5B	Kinesin family member 5B	Cytoplasm	Other
−1.858	I7HJJ0	SLC25A6	Solute carrier family 25 (mitochondrial carrier; adenine nucleotide translocator), member 6	Cytoplasm	Transporter
−1.856	P52566	ARHGDIB	Rho GDP dissociation inhibitor (GDI) beta	Cytoplasm	Other
−1.844	P67809	YBX1	Y box binding protein 1	Nucleus	Transcription regulator
−1.764	Q9UKY7	CDV3	CDV3 homolog (mouse)	Cytoplasm	Other
−1.764	B7Z972	PCMT1	Protein-L-isoaspartate (D-aspartate) *O*-methyltransferase	Cytoplasm	Enzyme
−1.737	E9PBS1	PAICS	Phosphoribosylaminoimidazole carboxylase, phosphoribosylaminoimidazole succinocarboxamide synthetase	Cytoplasm	Enzyme
−1.727	P13010	XRCC5	X-ray repair complementing defective repair in Chinese hamster cells 5 (double-strand-break rejoining)	Nucleus	Enzyme
−1.723	P26368	U2AF2	U2 small nuclear RNA auxiliary factor 2	Nucleus	Other
−1.722	P28074	PSMB5	Proteasome (prosome, macropain) subunit, beta type, 5	Cytoplasm	Peptidase
−1.715	P15374	UCHL3	Ubiquitin carboxyl-terminal esterase L3 (ubiquitin thiolesterase)	Cytoplasm	Peptidase
−1.709	P68104	EEF1A1	Eukaryotic translation elongation factor 1 alpha 1	Cytoplasm	Translation regulator
−1.698	J3KTF8	ARHGDIA	Rho GDP dissociation inhibitor (GDI) alpha	Cytoplasm	Other
−1.694	O75367	H2AFY	H2A histone family, member Y	Nucleus	Other
−1.663	P63010	AP2B1	Adaptor-related protein complex 2, beta 1 subunit	Plasma membrane	Transporter
−1.655	B4DUR8	CCT3	Chaperonin containing TCP1, subunit 3 (gamma)	Cytoplasm	Other
−1.646	P13667	PDIA4	Protein disulfide isomerase family A, member 4	Cytoplasm	Enzyme
−1.638	P23229	ITGA6	Integrin, alpha 6	Plasma membrane	Transmembrane receptor
−1.632	F8VZ29	UBE2N	Ubiquitin-conjugating enzyme E2N	Cytoplasm	Enzyme
−1.631	Q9UHI5	SLC7A8	Solute carrier family 7 (amino acid transporter light chain, L system), member 8	Plasma membrane	Transporter
−1.629	F8W726	UBAP2L	Ubiquitin associated protein 2-like	Other	Other
−1.617	Q9HB71	CACYBP	Calcyclin binding protein	Nucleus	Other
−1.614	Q12905	ILF2	Interleukin enhancer binding factor 2	Nucleus	Transcription regulator
−1.599	O43390	HNRNPR	Heterogeneous nuclear ribonucleoprotein R	Nucleus	Other
−1.599	E9PK47	PYGL	Phosphorylase, glycogen, liver	Cytoplasm	Enzyme
−1.579	Q6NYC8	PPP1R18	Protein phosphatase 1, regulatory subunit 18	Other	Other
−1.574	O60884	DNAJA2	DNAJ (Hsp40) homolog, subfamily A, member 2	Nucleus	Enzyme
−1.566	E9PDF6	MYO1B	Myosin IB	Cytoplasm	Other
−1.565	Q02878	RPL6	Ribosomal protein L6	Cytoplasm	Other
−1.562	P05386	RPLP1	Ribosomal protein, large, P1	Cytoplasm	Other
−1.56	E9PLD0	RAB1B	RAB1B, member RAS oncogene family	Cytoplasm	Other
−1.556	Q14247	CTTN	Cortactin	Plasma membrane	Other
−1.554	P42704	LRPPRC	Leucine-rich pentatricopeptide repeat containing	Cytoplasm	Other
−1.549	Q9H4M9	EHD1	EH-domain containing 1	Cytoplasm	Other
−1.498	P30084	ECHS1	Enoyl CoA hydratase, short chain, 1, mitochondrial	Cytoplasm	Enzyme
−1.498	P49915	GMPS	Guanine monphosphate synthase	Nucleus	Enzyme
−1.496	Q86VP6	CAND1	Cullin-associated and neddylation-dissociated 1	Cytoplasm	Transcription regulator
−1.49	P49588	AARS	Alanyl-tRNA synthetase	Cytoplasm	Enzyme
−1.482	P62314	SNRPD1	Small nuclear ribonucleoprotein D1 polypeptide 16 kDa	Nucleus	Other
−1.474	P20290	BTF3	Basic transcription factor 3	Nucleus	Transcription regulator
−1.473	Q9ULV4	CORO1C	Coronin, actin binding protein, 1C	Cytoplasm	Other
−1.468	P51858	HDGF	Hepatoma-derived growth factor	Extracellular space	Growth factor
−1.468	G3V1A1	RPL8	Ribosomal protein L8	Other	Other
−1.466	Q9UHD8	SEPT9	Septin 9	Cytoplasm	Enzyme

(*Continued*)

Table 2 (*Continued*)

Fold change	ID	Symbol	Entrez gene name	Location	Type(s)
−1.461	P55060	CSE1L	CSE1 chromosome segregation 1-like (yeast)	Nucleus	Transporter
−1.46	P61978	HNRNPK	Heterogeneous nuclear ribonucleoprotein K	Nucleus	Other
−1.457	P84077	ARF1	ADP-ribosylation factor 1	Cytoplasm	Enzyme
−1.452	P62081	RPS7	Ribosomal protein S7	Cytoplasm	Other
−1.447	K7EJ57	TOMM40	Translocase of outer mitochondrial membrane 40 homolog (yeast)	Cytoplasm	Ion channel
−1.443	Q9Y5B9	SUPT16H	Suppressor of Ty 16 homolog (*S. cerevisiae*)	Nucleus	Transcription regulator
−1.434	P49327	FASN	Fatty acid synthase	Cytoplasm	Enzyme
−1.432	P30086	PEBP1	Phosphatidylethanolamine binding protein 1	Cytoplasm	Other
−1.421	C9J9K3	RPSA	Ribosomal protein SA	Cytoplasm	Translation regulator
−1.421	Q12874	SF3A3	Splicing factor 3a, subunit 3, 60 kDa	Nucleus	Other
−1.42	P43490	NAMPT	Nicotinamide phosphoribosyltransferase	Extracellular space	Cytokine
−1.41	Q14444	CAPRIN1	Cell cycle associated protein 1	Plasma membrane	Other
−1.409	P13928	ANXA8/ ANXA8L1	Annexin A8-like 1	Plasma membrane	Other
−1.408	Q9UK76	HN1	Hematological and neurological expressed 1	Nucleus	Other
−1.404	P00367	GLUD1	Glutamate dehydrogenase 1	Cytoplasm	Enzyme
−1.402	Q14764	MVP	Major vault protein	Nucleus	Other
−1.391	Q9NTK5	OLA1	Obg-like ATPase 1	Cytoplasm	Other
−1.391	P08670	VIM	Vimentin	Cytoplasm	Other
−1.387	P07195	LDHB	Lactate dehydrogenase B	Cytoplasm	Enzyme
−1.384	P07384	CAPN1	Calpain 1, (mu/I) large subunit	Cytoplasm	Peptidase
−1.378	Q5T7C4	HMGB1	High mobility group box 1	Nucleus	Transcription regulator
−1.374	P55884	EIF3B	Eukaryotic translation initiation factor 3, subunit B	Cytoplasm	Translation regulator
−1.367	Q15417	CNN3	Calponin 3, acidic	Cytoplasm	Other
−1.367	Q96AE4	FUBP1	Far upstream element (FUSE) binding protein 1	Nucleus	Transcription regulator
−1.366	F8W1N5	NACA	Nascent polypeptide-associated complex alpha subunit	Cytoplasm	Transcription regulator
−1.364	Q32Q12	NME1-NME2	NME1-NME2 readthrough	Cytoplasm	Other
−1.361	P21796	VDAC1	Voltage-dependent anion channel 1	Cytoplasm	Ion channel
−1.359	P54136	RARS	Arginyl-tRNA synthetase	Cytoplasm	Enzyme
−1.359	Q9H2G2	SLK	STE20-like kinase	Nucleus	Kinase
−1.359	Q12792	TWF1	Twinfilin actin-binding protein 1	Cytoplasm	Kinase
−1.354	Q7KZF4	SND1	Staphylococcal nuclease and tudor domain containing 1	Nucleus	Enzyme
−1.347	P20042	EIF2S2	Eukaryotic translation initiation factor 2, subunit 2 beta, 38 kDa	Cytoplasm	Translation regulator
−1.344	Q14204	DYNC1H1	Dynein, cytoplasmic 1, heavy chain 1	Cytoplasm	Peptidase
−1.34	K7EIP4	LAMA3	Laminin, alpha 3	Extracellular space	Other
−1.337	P24534	EEF1B2	Eukaryotic translation elongation factor 1 beta 2	Cytoplasm	Translation regulator
−1.331	P61353	RPL27	Ribosomal protein L27	Cytoplasm	Other
−1.33	P41250	GARS	Glycyl-tRNA synthetase	Cytoplasm	Enzyme
−1.326	P04080	CSTB	Cystatin B (stefin B)	Cytoplasm	Peptidase
−1.326	G8JLD5	DNM1L	Dynamin 1-like	Cytoplasm	Enzyme
−1.317	P04792	HSPB1	Heat shock 27 kDa protein 1	Cytoplasm	Other
−1.315	P12956	XRCC6	X-ray repair complementing defective repair in Chinese hamster cells 6	Nucleus	Enzyme
−1.308	P0CW22	RPS17	Ribosomal protein S17	Cytoplasm	Other
−1.306	Q13283	G3BP1	GTPase activating protein (SH3 domain) binding protein 1	Nucleus	Enzyme
−1.306	Q15181	PPA1	Pyrophosphatase (inorganic) 1	Cytoplasm	Enzyme
−1.302	P14618	PKM	Pyruvate kinase, muscle	Cytoplasm	Kinase
−1.297	P27797	CALR	Calreticulin	Cytoplasm	Transcription regulator
−1.287	P48643	CCT5	Chaperonin containing TCP1, subunit 5 (epsilon)	Cytoplasm	Other
−1.286	P61158	ACTR3	ARP3 actin-related protein 3 homolog (yeast)	Plasma membrane	Other
−1.286	Q07021	C1QBP	Complement component 1, q subcomponent binding protein	Cytoplasm	Transcription regulator

(*Continued*)

Table 2 (*Continued*)

Fold change	ID	Symbol	Entrez gene name	Location	Type(s)
−1.283	P41091	EIF2S3	Eukaryotic translation initiation factor 2, subunit 3 gamma, 52 kDa	Cytoplasm	Translation regulator
−1.28	P26639	TARS	Threonyl-tRNA synthetase	Nucleus	Enzyme
−1.279	P43243	MATR3	Matrin 3	Nucleus	Other
−1.278	B4DS13	EIF4B	Eukaryotic translation initiation factor 4B	Cytoplasm	Translation regulator
−1.277	P09914	IFIT1	Interferon-induced protein with tetratricopeptide repeats 1	Cytoplasm	Other
−1.277	Q15084	PDIA6	Protein disulfide isomerase family A, member 6	Cytoplasm	Enzyme
−1.276	P52292	KPNA2	Karyopherin alpha 2 (RAG cohort 1, importin alpha 1)	Nucleus	Transporter
−1.271	P12004	PCNA	Proliferating cell nuclear antigen	Nucleus	Enzyme
−1.269	P13639	EEF2	Eukaryotic translation elongation factor 2	Cytoplasm	Translation regulator
−1.267	F5H018	RAN	RAN, member RAS oncogene family	Nucleus	Enzyme
−1.265	P40121	CAPG	Capping protein (actin filament), gelsolin-like	Nucleus	Other
−1.264	E7EQR4	EZR	Ezrin	Plasma membrane	Other
−1.264	P43686	PSMC4	Proteasome (prosome, macropain) 26S subunit, ATPase, 4	Nucleus	Peptidase
−1.263	P63241	EIF5A	Eukaryotic translation initiation factor 5A	Cytoplasm	Translation regulator
−1.261	B1AK85	CAPZB	Capping protein (actin filament) muscle Z-line, beta	Cytoplasm	Other
−1.254	Q14974	KPNB1	Karyopherin (importin) beta 1	Nucleus	Transporter
−1.253	P07237	P4HB	Prolyl 4-hydroxylase, beta polypeptide	Cytoplasm	Enzyme
−1.251	B4DLR8	NQO1	NAD(P)H dehydrogenase, quinone 1	Cytoplasm	Enzyme
−1.251	O60664	PLIN3	Perilipin 3	Cytoplasm	Other
−1.251	P54725	RAD23A	RAD23 homolog A (*S. cerevisiae*)	Nucleus	Other
−1.25	P18669	PGAM1	Phosphoglycerate mutase 1 (brain)	Cytoplasm	Phosphatase
−1.248	P05141	SLC25A5	Solute carrier family 25 (mitochondrial carrier; adenine nucleotide translocator), member 5	Cytoplasm	Transporter
−1.247	P55263	ADK	Adenosine kinase	Nucleus	Kinase
−1.245	P49321	NASP	Nuclear autoantigenic sperm protein (histone-binding)	Nucleus	Other
−1.244	P22626	HNRNPA2B1	Heterogeneous nuclear ribonucleoprotein A2/B1	Nucleus	Other
−1.243	P01892	HLA-A	Major histocompatibility complex, class I, A	Plasma membrane	Other
−1.242	P54727	RAD23B	RAD23 homolog B (*S. cerevisiae*)	Nucleus	Other
−1.239	P07737	PFN1	Profilin 1	Cytoplasm	Other
−1.237	P21333	FLNA	Filamin A, alpha	Cytoplasm	Other
−1.236	P06733	ENO1	Enolase 1, (alpha)	Cytoplasm	Enzyme
−1.234	P09382	LGALS1	Lectin, galactoside-binding, soluble, 1	Extracellular space	Other
−1.232	P35998	PSMC2	Proteasome (prosome, macropain) 26S subunit, ATPase, 2	Nucleus	Peptidase
−1.23	P52272	HNRNPM	Heterogeneous nuclear ribonucleoprotein M	Nucleus	Other
−1.229	P06396	GSN	Gelsolin	Extracellular space	Other
−1.229	Q99714	HSD17B10	Hydroxysteroid (17-beta) dehydrogenase 10	Cytoplasm	Enzyme
−1.227	P30044	PRDX5	Peroxiredoxin 5	Cytoplasm	Enzyme
−1.224	P00491	PNP	Purine nucleoside phosphorylase	Nucleus	Enzyme
−1.223	P39023	RPL3	Ribosomal protein L3	Cytoplasm	Other
−1.221	P37802	TAGLN2	Transgelin 2	Cytoplasm	Other
−1.22	Q7L2H7	EIF3M	Eukaryotic translation initiation factor 3, subunit M	Other	Other
−1.22	P62906	RPL10A	Ribosomal protein L10a	Nucleus	Other
−1.219	P62937	PPIA	Peptidylprolyl isomerase A (cyclophilin A)	Cytoplasm	Enzyme
−1.215	P11766	ADH5	Alcohol dehydrogenase 5 (class III), chi polypeptide	Cytoplasm	Enzyme
−1.213	Q09666	AHNAK	AHNAK nucleoprotein	Nucleus	Other
−1.207	E7ETK0	RPS24	Ribosomal protein S24	Cytoplasm	Other
−1.205	Q03135	CAV1	Caveolin 1, caveolae protein, 22 kDa	Plasma membrane	Transmembrane receptor
−1.203	P35606	COPB2	Coatomer protein complex, subunit beta 2 (beta prime)	Cytoplasm	Transporter
−1.203	P52209	PGD	Phosphogluconate dehydrogenase	Cytoplasm	Enzyme
−1.203	Q13200	PSMD2	Proteasome (prosome, macropain) 26S subunit, non-ATPase, 2	Cytoplasm	Other
−1.198	P60842	EIF4A1	Eukaryotic translation initiation factor 4A1	Cytoplasm	Translation regulator

(*Continued*)

Table 2 (*Continued*)

Fold change	ID	Symbol	Entrez gene name	Location	Type(s)
−1.198	P18124	RPL7	Ribosomal protein L7	Nucleus	Transcription regulator
−1.193	P05161	ISG15	ISG15 ubiquitin-like modifier	Extracellular space	Other
−1.184	A0A075B730	EPPK1	Epiplakin 1	Cytoplasm	Other
−1.184	Q02790	FKBP4	FK506 binding protein 4, 59 kDa	Nucleus	Enzyme
−1.184	M0R0F0	RPS5	Ribosomal protein S5	Cytoplasm	Other
−1.183	P35221	CTNNA1	Catenin (cadherin-associated protein), alpha 1, 102 kDa	Plasma membrane	Other
−1.179	Q01105	SET	SET nuclear proto-oncogene	Nucleus	Phosphatase
−1.175	P05387	RPLP2	Ribosomal protein, large, P2	Cytoplasm	Other
−1.174	Q00839	HNRNPU	Heterogeneous nuclear ribonucleoprotein U (scaffold attachment factor A)	Nucleus	Transporter
−1.173	O15143	ARPC1B	Actin related protein 2/3 complex, subunit 1B, 41 kDa	Cytoplasm	Other
−1.173	P23528	CFL1	Cofilin 1 (non-muscle)	Nucleus	Other
−1.173	A2A2Y8	COL17A1	Collagen, type XVII, alpha 1	Extracellular space	Other
−1.171	E7EQV3	PABPC1	Poly(A) binding protein, cytoplasmic 1	Cytoplasm	Translation regulator
−1.171	F8W7C6	RPL10	Ribosomal protein L10	Cytoplasm	Other
−1.158	Q14980	NUMA1	Nuclear mitotic apparatus protein 1	Nucleus	Other
−1.157	P27824	CANX	Calnexin	Cytoplasm	Other
−1.155	Q14134	TRIM29	Tripartite motif containing 29	Cytoplasm	Transcription regulator
−1.154	E9PCY7	HNRNPH1	Heterogeneous nuclear ribonucleoprotein H1 (H)	Nucleus	Other
−1.153	O00299	CLIC1	Chloride intracellular channel 1	Nucleus	Ion channel
−1.145	Q13813	SPTAN1	Spectrin, alpha, nonerythrocytic 1	Plasma membrane	Other
−1.144	P07900	HSP90AA1	Heat shock protein 90 kDa alpha (cytosolic), class A member 1	Cytoplasm	Enzyme
−1.143	P68363	TUBA1B	Tubulin, alpha 1b	Cytoplasm	Other
−1.14	Q5JP53	TUBB	Tubulin, beta class 1	Cytoplasm	Other
−1.137	P60174	TPI1	Triosephosphate isomerase 1	Cytoplasm	Enzyme
−1.136	P27482	CALML3	Calmodulin-like 3	Cytoplasm	Other
−1.135	P19338	NCL	Nucleolin	Nucleus	Other
−1.124	P18206	VCL	Vinculin	Plasma membrane	Enzyme
−1.117	P10809	HSPD1	Heat shock 60 kDa protein 1 (chaperonin)	Cytoplasm	Enzyme
−1.117	Q92598	HSPH1	Heat shock 105 kDa/110 kDa protein 1	Cytoplasm	Other
−1.114	K7ELL7	PRKCSH	Protein kinase C substrate 80K-H	Cytoplasm	Enzyme
−1.112	P05198	EIF2S1	Eukaryotic translation initiation factor 2, subunit 1 alpha, 35 kDa	Cytoplasm	Translation regulator
−1.111	P30050	RPL12	Ribosomal protein L12	Nucleus	Other
−1.108	F8W6I7	HNRNPA1	Heterogeneous nuclear ribonucleoprotein A1	Nucleus	Other
−1.108	P00338	LDHA	Lactate dehydrogenase A	Cytoplasm	Enzyme
−1.106	Q16658	FSCN1	Fascin actin-bundling protein 1	Cytoplasm	Other
−1.103	P78371	CCT2	Chaperonin containing TCP1, subunit 2 (beta)	Cytoplasm	Kinase
−1.102	P68133	ACTA1	Actin, alpha 1, skeletal muscle	Cytoplasm	Other
−1.095	P29728	OAS2	2′-5′-oligoadenylate synthetase 2, 69/71 kDa	Cytoplasm	Enzyme
−1.092	P13797	PLS3	Plastin 3	Cytoplasm	Other
−1.09	D6RFM5	SDHA	Succinate dehydrogenase complex, subunit A, flavoprotein (Fp)	Cytoplasm	Enzyme
−1.082	B4E022	TKT	Transketolase	Cytoplasm	Enzyme
−1.081	O95433	AHSA1	AHA1, activator of heat shock 90 kDa protein ATPase homologue 1 (yeast)	Cytoplasm	Other
−1.077	E7EX73	EIF4G1	Eukaryotic translation initiation factor 4 gamma, 1	Cytoplasm	Translation regulator
−1.076	P04406	GAPDH	Glyceraldehyde-3-phosphate dehydrogenase	Cytoplasm	Enzyme
−1.076	P26599	PTBP1	Polypyrimidine tract binding protein 1	Nucleus	Enzyme
−1.076	P11216	PYGB	Phosphorylase, glycogen; brain	Cytoplasm	Enzyme
−1.072	Q13838	DDX39B	DEAD (Asp-Glu-Ala-Asp) box polypeptide 39B	Nucleus	Enzyme
−1.072	Q99733	NAP1L4	Nucleosome assembly protein 1-like 4	Cytoplasm	Other
−1.068	P29692	EEF1D	Eukaryotic translation elongation factor 1 delta (guanine nucleotide exchange protein)	Cytoplasm	Translation regulator

(*Continued*)

Table 2 (*Continued*)

Fold change	ID	Symbol	Entrez gene name	Location	Type(s)
−1.067	O00151	PDLIM1	PDZ and LIM domain 1	Cytoplasm	Transcription regulator
−1.065	O75369	FLNB	Filamin B, beta	Cytoplasm	Other
−1.063	P62191	PSMC1	Proteasome (prosome, macropain) 26S subunit, ATPase, 1	Nucleus	Peptidase
−1.059	P00558	PGK1	Phosphoglycerate kinase 1	Cytoplasm	Kinase
−1.055	P50990	CCT8	Chaperonin containing TCP1, subunit 8 (theta)	Cytoplasm	Enzyme
−1.052	F5H7V9	TNC	Tenascin C	Extracellular space	Other
−1.049	Q99613	EIF3C	Eukaryotic translation initiation factor 3, subunit C	Other	Translation regulator
−1.048	P45880	VDAC2	Voltage-dependent anion channel 2	Cytoplasm	Ion channel
−1.043	P26641	EEF1G	Eukaryotic translation elongation factor 1 gamma	Cytoplasm	Translation regulator
−1.043	P00441	SOD1	Superoxide dismutase 1, soluble	Cytoplasm	Enzyme
−1.039	E9PFD7	EGFR	Epidermal growth factor receptor	Plasma membrane	Kinase
−1.039	Q9NQC3	RTN4	Reticulon 4	Cytoplasm	Other
−1.037	Q9NUQ9	FAM49B	Family with sequence similarity 49, member B	Extracellular space	Other
−1.037	P08729	KRT7	Keratin 7	Cytoplasm	Other
−1.037	P25398	RPS12	Ribosomal protein S12	Cytoplasm	Other
−1.034	Q13347	EIF3I	Eukaryotic translation initiation factor 3, subunit I	Cytoplasm	Translation regulator
−1.034	F8VQE1	TRMT1	tRNA methyltransferase 1 homolog (*S. cerevisiae*)	Extracellular space	Enzyme
−1.031	P63261	ACTG1	Actin, gamma 1	Cytoplasm	Other
−1.027	O43707	ACTN4	Actinin, alpha 4	Cytoplasm	Other
−1.027	P13796	LCP1	Lymphocyte cytosolic protein 1 (L-plastin)	Cytoplasm	Other
−1.027	E7EUY0	PRKDC	Protein kinase, DNA-activated, catalytic polypeptide	Nucleus	Kinase
−1.025	Q8NC51	SERBP1	SERPINE1 mRNA binding protein 1	Cytoplasm	Other
−1.025	Q13263	TRIM28	Tripartite motif containing 28	Nucleus	Transcription regulator
−1.023	Q00610	CLTC	Clathrin, heavy chain (Hc)	Plasma membrane	Other
−1.022	P40227	CCT6A	Chaperonin containing TCP1, subunit 6A (zeta 1)	Cytoplasm	Other
−1.021	P63104	YWHAZ	Tyrosine 3-monooxygenase/tryptophan 5-monooxygenase activation protein, zeta	Cytoplasm	Enzyme
−1.02	P51149	RAB7A	RAB7A, member RAS oncogene family	Cytoplasm	Enzyme
−1.018	P25787	PSMA2	Proteasome (prosome, macropain) subunit, alpha type, 2	Cytoplasm	Peptidase
−1.016	P35268	RPL22	Ribosomal protein L22	Nucleus	Other
−1.012	Q04828	AKR1C1/ AKR1C2	Aldo-keto reductase family 1, member C2	Cytoplasm	Enzyme
−1.01	P08758	ANXA5	Annexin A5	Plasma membrane	Other
−1.01	Q5VU59	TPM3	Tropomyosin 3	Cytoplasm	Other
−1.009	Q15233	NONO	Non-POU domain containing, octamer-binding	Nucleus	Other
−1.009	P62258	YWHAE	Tyrosine 3-monooxygenase/tryptophan 5-monooxygenase activation protein, epsilon	Cytoplasm	Other
−1.008	P35579	MYH9	Myosin, heavy chain 9, nonmuscle	Cytoplasm	Enzyme
−1.005	P16144	ITGB4	Integrin, beta 4	Plasma membrane	Transmembrane receptor
−1.001	Q15149	PLEC	Plectin	Cytoplasm	Other

Abbreviation: PLB, plumbagin.

pathways were EIF2 signaling pathway, regulation of eIF4 and p70S6K signaling, remodeling of epithelial adherens junctions pathway, mTOR signaling pathway, protein ubiquitination pathway, Nrf2-mediated oxidative stress response signaling pathway, epithelial adherens junction signaling pathway, caveolar-mediated endocytosis signaling pathway, RhoA signaling pathway, and oxidative phosphorylation pathway (Table 3). Notably, a number of molecules were involved in cell survival, cell proliferation, redox homeostasis, cell metabolism, cell migration, and cell death, such as p53, CDK1/cdc2, FADD, Nrf2, MAPK, mTOR, p70S6K, E-cadherin, and vimentin.

PLB regulates cell cycle regulators of SCC25 cells

The cell cycle arresting effect of PLB is considered as a critical contributor to its anticancer activities. We treated SCC25 cells with 5 μM PLB for 24 hours, and then, cell samples were subject to quantitative proteomic analysis. The results showed that PLB regulated cell cycle at G_2/M

Table 3 Potential signaling pathways regulated by PLB in SCC25 cells

Ingenuity canonical pathways	–logP	Protein molecules
EIF2 signaling	3.31E01	EIF2S1, EIF2S2, EIF2S3, EIF3B, EIF3C, EIF3D, EIF3E, EIF3F, EIF3G, EIF3I, EIF3M, EIF4A1, EIF4G1, PABPC1, PPP1CA, RPL3, RPL4, RPL5, RPL6, RPL7, RPL8, RPL9, RPL10, RPL12, RPL22, RPL27, RPL10A, RPLP0, RPLP1, RPLP1, RPLP2, RPS5, RPS7, RPS8, RPS12, RPS14, RPS15, RPS17, RPS19, RPS24, RPS27A, RPS3A, RPS4X, RPSA
Regulation of eIF4 and p70S6k signaling	2.03E01	EIF2S1, EIF2S2, EIF2S3, EIF3B, EIF3C, EIF3D, EIF3E, EIF3F, EIF3G, EIF3I, EIF3M, EIF4A1, EIF4G1, ITGB1, PABPC1, PPP2R1A, RPS5, RPS7, RPS8, RPS12, RPS14, RPS15, RPS17, RPS19, RPS24, RPS27A, RPS3A, RPS4X, RPSA
Remodeling of epithelial adherens junctions	1.52E01	ACTA1, ACTG1, ACTN1, ACTN4, ACTR3, ARPC1B, CTNNA1, CTNND1, DNM1L, IQGAP1, RAB7A, TUBA1B, TUBA1C, TUBA4A, TUBB, TUBB4B, VCL, ZYX
mTOR signaling	1.43E01	EIF3B, EIF3C, EIF3D, EIF3E, EIF3F, EIF3G, EIF3I, EIF3M, EIF4A1, EIF4B, EIF4G1, PPPAR1A, RHOA, RPS5, RPS7, RPS8, RPS12, RPS14, RPS15, RPS17, RPS19, RPS24, RPS27A, RPS3A, RPS4X, RPSA
Protein ubiquitination pathway	1.36E01	HLA-A, HSP90AA1, HSP90AB1, HSP90B1, HSPA4, HSPA5, HSPA8, HSPA9, HSPB1, HSPD1, HSPH1, PSMA1, PSMA2, PSMA4, PSMA5, PSMB1, PSMB5, PSMC1, PSMC2, PSMC3, PSMC4, PSMD1, PSMD2, PSME2, UBA1, UBE2N, UCHL1, UCHL3, USP5
Nrf2-mediated oxidative stress response	5.42E00	ACTA1, ACTG1, CBR1, DNAJA2, GSTP1, NQO1, HSP90AA1, PPIB, PRDX1, SOD1, STIP1, VCP
Epithelial adherens junction signaling	5.21E00	ACTA1, ACTG1, ACTN1, ACTN4, ACTR3, ARPC1B, CTNNA1, CTNND1, EGFR, IQGAP1, JUP, MYH9, RHO1, TUBA1B, TUBA1C, TUBA4A, TUBB, TUBB4B, VAL, ZYX
Caveolar-mediated endocytosis signaling	5.18E00	ACTA1, ACTG1, CAV1, COPA, COPB2, COPE, EGFR, FLNA, FLNB, HLA-A, ITGA6, ITGB1, ITGB4, PTRF
RhoA signaling	5.10E00	ACTA1, ACTG1, ACTR3, ARPC1B, CFL1, EZR, KTN1, MAN, MYL12A, PFN1, RHOA, SEPT9
Oxidative phosphorylation	5.08E00	UQCRH, ATP5D, ATP5L, UQCRB, MT-CO2, ATP5H, NDUFA5, NDUFAB1, NDUFB6, ATP5F1, COX4I1, SDHA, ATP5J, COX7A2, COX6B1, COX17, ATP5O, ATP5A1, NDUFS3, ATP5C1, MT-ND1, NDUFB11, ATP5B, NDUFS8, UQCR10, CYC1, UQCRC2, COX5A, CYCS, UQCRC1, COX5B
TCA cycle II (eukaryotic)	4.85E00	SDHA, SUCLA2, CS, SUCLG1, DLST, ACO2, DLD, IDH3A, OGDH, MDH2, FH, MDH1, IDH3B
Germ cell–Sertoli cell junction signaling	4.76E00	ACTA1, ACTG1, ACTN1, ACTN4, CFL1, CTNNA1, CTNND1, GSN, IQGAP1, ITGA6, ITGB1, JUP, PAK2, PAC2, RHOA, TUBA1B, TUBA1C, TUBA4A, TUBB, TUBB4B, ZYX
Actin nucleation by ARP-WASP complex	4.64E00	RHOA, ARPC3
Aspartate degradation II	4.11E00	GOT2
Superpathway of methionine degradation	4.08E00	GOT2
Tight junction signaling	4.08E00	MYL6, PPP2CA, HSF1, ACTA2, VAPA, PRKAR2A, RAC1, YBX3, CDC42, ACTG1, CPSF6, PPP2R1A, CLDN4, MYH9, SAFB, VCL, SPTAN1, CTNNA1, CSTF3, VASP, RHOA
2-Ketoglutarate dehydrogenase complex	3.89E00	DLST, DLD, OGDH
Integrin signaling	3.87E00	ACTA1, ACTG1, ACTN1, ACTN4, ACTR3, ARF1, ARPC1B, CAPN1, CAPN2, CAPNS1, CAV1, CTTN, ITGA6, ITGB1, ITGB4, MYL12A, PAK2, RAC2, RHOA, VCL, ZYX
Clathrin-mediated endocytosis signaling	3.80E00	ACTA1, ACTG1, ACTR3, AP2B1, ARPC1B, CLTC, CTTN, DNM1L, HSPA8, ITGB1, ITGB4, RAB7A, TFRC
Cell cycle: G_2/M DNA damage checkpoint regulation	3.78E00	YWHAQ, PRKDC, YWHAG, YWHAE, YWHAH, YWHAB, YWHAZ, SFN, SKP1, CDK1
Glycolysis I	3.75E00	ALDOA, ALD0C, ENO1, GAPDH, GPI, PGAM1, PGAM1, PKG1, PKM, TPI1

(*Continued*)

Table 3 (*Continued*)

Ingenuity canonical pathways	–logP	Protein molecules
Ephrin receptor signaling	3.73E00	RHOA, AKT2, ARPC3, RAC2, ACTR3, MAPK1
Unfolded protein response	3.66E00	CALR, CANX, DNAJA2, HSP90B1, HSPA4, HSPA5, HSPA8, HSPA9, HSPH1, P4HB, VCP
Actin cytoskeleton signaling	3.64E00	ACTA1, ACTG1, ACTN1, ACTN4, ACTR3, ARPC1B, CFL1, FLNA, GSN, IQGAP1, ITGB1, MSN, MYH9, MYL12A, PAK2, PFN1, RAC2, RHOA, VCL
Semaphorin signaling in neurons	3.47E00	RHOA, DPYSL2, PAK2, CFL2, MAPK1, CFL1, RHOC, RAC1
Gluconeogenesis I	3.46E00	ALDOA, ALDOC, ENO1, GAPDH, GPI, MDH2, PGAM1, PGK1
Virus entry via endocytic pathways	3.32E00	ACTA1, ACTG1, AP2B1 CAV1, CLTC, FLNA, FLNB, HLA-A, ITGA6, ITGB1, ITGB4, RAC2, TFRC
Regulation of actin-based motility by rho	3.31E00	ACTA1, ACTR3, ARHGDIA, ARPC1B, CFL1, GSN, ITGB1, MYL12A, PAK2, PFN1, RAC2, RHOA
Mechanisms of viral exit from host cells	3.27E00	CHMP4B, ACTA2, XPO1, LMNB2, PDCD6IP, ACTG1, LMNB1
14-3-3-Mediated signaling	2.95E00	PDIA3, SFN, TUBA1B, TUBA1C, TUBA4A, TUBB, TUBB4B, VIM, YWHAB, YWHAE, YWHAG, YWHAQ, YWHAZ
Superoxide radicals degradation	2.87E00	SOD1, SOD2, NQO1
Spliceosomal cycle	2.86E00	U2AF2, U2AF1
ILK signaling	2.84E00	ACTA1, ACTG1, ACTN1, ACTN4, CDL1, DSP, FLNA, FLNB, ITGB1, ITGB4, KRT18, MYH9, NACA, PPP2R1A, RHOA, VIM
Aryl hydrocarbon receptor signaling	2.76E00	NQO1, GSTP1, ALDH, HSP27
Ethanol degradation II	2.75E00	ADH5, HSD17B10, AKR1A1, ACSL3, DHRS9, ALDH1A3, ALDH3A2, ALDH9A1
Noradrenaline and adrenaline degradation	2.74E00	ADH5, HSD17B10, AKR1A1, DHRS9, ALDH1A3, ALDH3A2, ALDH9A1
Glycogen degradation III	2.72E00	PGM3, PGM1, PYGB, PYGL
Palmitate biosynthesis I (animals)	2.71E00	FASN
Granzyme B signaling	2.64E00	NUMA1, LMNB2, CYCS, LMNB1, PARP1
Regulation of cellular mechanics by caplain protease	2.55E00	ACTN1, ACTN4, CAPN1, CAPN2, CAPNS1, EGFR, EZR, ITGB1, VCL
Pentose phosphate pathway	2.51E00	PGD, TKT, PGLS, TALDO1
BER pathway	2.44E00	PCNA, PARP1, APEX1
RhoGDI signaling	2.43E00	ACTA1, ACTG1, ACTR3, ARHGDIA, ARHGDIB, ARPC1B, CFL1, EZR, GDI2, GNB2L1, ITGB1, MSN, MYL12A, PAK2, RHOA
IGF-1 signaling	2.42E00	SFN, STAT3
Erk/MAPK signaling	2.41E00	RAP1B, ITGB1, PPP1CC, PXN, YWHAG, PAK2, YWHAH, MAPK1, YWHAB, PPP2CA, RRAS, ITGA2, YWHAZ, RAC1, PRKAR2A, TLN1, PPP1R14B, YWHAQ, PPP2R1A, HSPB1, PRKAR1A
Adenine and adenosine salvage I	2.39E00	PNP
Purine nucleotides de novo biosynthesis II	2.36E00	ATIC, GART, GMPS, IMPDH2, PAICS
Hypoxia signaling in the cardiovascular system	2.34E00	HSP90AA1, HSP90AB1, HSP90B1, LDHA, NQO1, P4HB, UBE2N
Glycogen degradation II	2.31E00	PGM3, PGM1, PYGB, PYGL
Sertoli cell–Sertoli cell junction signaling	2.26E00	ACTA1, ACTG1, ACTN1, ACTN4, CTNNA1, ITGB1, JUP, SPTAN1, SPTBN1, TUBA1B, TUBA1C, TUBA4A, TUBB, TUBB4B, YBX3
Lipid antigen presentation by CD1	2.22E00	CALR, AP2A1, PDIA3, CANX
Guanine and guanosine salvage I	2.18E00	PNP
Myc mediated apoptosis signaling	2.17E00	FADD, SFN, YWHAB, YWHAE, YWHAG, YWHAQ, YWHAZ
Ephrin B signaling	2.14E00	CDC42, GNB1, CFL2, RAC2, RHOA

DNA double-strand break repair by nonhomologous end joining	2.13E00	XRCC1, XRCC4, PARP1
Urate biosynthesis/inosine 5′-phosphate degradation	2.12E00	PRKDC, XRCC6, XRCC5, PARP1
Telomere extension by Telomerase	2.11E00	HNRNPA1, HNRNPA2B1, XRCC5, XRCC6
Rac signaling	2.09E00	PAK2, CFL1, MAPK1, ARPC1B, RRAS, ITGA2, RAC1, IQGAP1, CDC42, CFL2, CD44, ARPC3, ARPC4, RHOA
VEGF signaling	2.08E00	ACTA1, ACTG1, ACTN1, ACTN4, EIF2S1, EIF2S2, EIF2S3, SFN, VCL, YWHAE
Formaldehyde oxidation II (glutathione-dependent)	2.05E00	ADH5, ESD
p53 signaling	2.03E00	PCNA, MAPK1
Apoptosis signaling	1.77E00	ACIN1, CAPNS1, MAPK1, RRAS, LMNA, CAPN2, SPTAN1, CYCS, CDK1, PARP1, AIFM1
Inosine-5′-phosphate biosynthesis II	1.73E00	PAICS, ATIC
Gap junction signaling	1.67E00	ACTA1, ACTG1, CAV1, EGFR, PDIA3, TUBA1B, TUBA1C, TUBA4A, TUBB, TUBB4B
Antigen presentation pathway	1.64E00	CALR, CANX, HLA-A, PDIA3, PSMB5
RAN signaling	1.62E00	CSE1L, KPNA2, KPNB1, RAN
eNOS signaling	1.51E00	HSP90AA1, CAV1
Pyruvate fermentation to lactate	1.45E00	LDHA, LDHB
Breast cancer regulation by Stathmin1	1.38E00	RHOA, PPP2R1A, TUBB6, RHOA, TUBA4A, PPP1CA
ERK5 signaling	1.35E00	EGFR, SFN, YWHAB, YWHAE, YWHAG, YWHAQ, YWHAZ
tRNA charging	1.26E00	AARS, GARS, RARS, TARS, WARS
Arginine biosynthesis IV	1.26E00	OAT, GLUD1
Mitotic roles of polo-like kinase	1.25E00	SLK, HSP90B1, PPP2R1A, HSP90AB1, PPP2CA, HSP90AA1, CAPN1
Death receptor signaling	1.23E00	ACIN1, CYCS, ACTB, FADD
Sucrose degradation V (Mammalian)	1.09E00	ALDOA, ALDOC, TPI1
Cdc42 signaling	1.08E00	ITGB1, ACTR2, PAK2, MYL6, ARPC1B, MAPK1, CFL1, HLA-A, ITGA2, IQGAP1, CDC42, ACTR3, CFL2, MYL12B, ARPC3, ARPC4
Xanthine and xanthosine salvage	1.02E00	PNP
Glutamate biosynthesis II	8.15E-01	GLUD1
Mitochondrial dysfunction	7.5E-01	CYTB, VDAC2
PTEN signaling	7.32E-01	MAPK1, YWHAH, RRAS, CSNK2A1, RAC1, CSNK2B, CDC42
Glutamate degradation X	7.01E-01	GLUD1
Fatty acid biosynthesis initiation II	6.5E-01	FASN
Neuregulin signaling	6.39E-01	EGFR, RPS6, HSP90B1, MAPK1, HSP90AB1, RRAS, ITGA2, HSP90AA1
Endoplasmic reticulum stress pathway	5.98E-01	CALR, EIF2S1, HSP90B1, HSPA5
Telomerase signaling	5.78E-01	EGFR, HSP90AA1, PPP2R1A
CDK5 signaling	5.46E-01	PPP2R1A, PPP1CA
Role of tissue factor in cancer	5.15E-01	EGFR, AKT2, CFL2, MAPK1
Isoleucine degradation I	5.06E-01	IMPDH2, PNP
P70S6K signaling	4.74E-01	EEF2, EGFR, PDIA3, PPP2R1A, SFN, YWHAB, YWHAE, YWHAG, YWHAQ, YWHAZ

(*Continued*)

Table 3 (*Continued*)

Ingenuity canonical pathways	–logP	Protein molecules
Axonal guidance signaling	4.51E-01	DPYSL2, RAC2, AKT2, MYL6, PDIA3, TUBA4A, ACTR3, TUBB6, CFL2, RHOA, RTN4, ARPC3, PFN2, PFN1, PSMD14
Role of PKR in interferon induction and antiviral response	4.16E-01	CYCS
Protein kinase A signaling	3.54E-01	APEX1, FLNA, FLNB, GNB2L1, HSF3A/H3F3B, MYL12A, PDE6H, PDIA3, PPP1CA, PYGB, PYGL, RHOA, SFN, YWHAB, YWHAE, YWHAG, YWHAQ, YWHAZ
Macropinocytosis signaling	3.53E-01	RHOA, ITGB1, RRAS, RAC1, ACTN4
HIPPO signaling	3.27E-01	PPP1CA, PPP2R1A, SFN, YWHAB, YWHAE, YWHAG, YWHAQ, YWHAZ
Nitric oxide signaling in the cardiovascular system	2.86E-01	CAV1, HSP90AB1
Glucocorticoid receptor signaling	2.82E-01	HMGB1, AKT2, HSP90AA1, STAT1
Fcy receptor-mediated phagocytosis in macrophages and monocytes	2.5E-01	RAC, CDC42
Tec kinase signaling	2.49E-01	RHO, STAT, FADD
Activation of IRF by cytosolic pattern recognition receptors	2.45E-01	PPIB, MAVS, ADAR, ISG15, STAT2, CYPB
Prostate cancer signaling	2.22E-01	HSP90B1, MAPK1, PA2G4, HSP90AB1, RRAS, HSP90AA1, CTNNB1, GSTP1
HGF signaling	1.78E-01	AKT2

Abbreviations: ACT, actin; ACTN, actinin; ACTR3, ACTR3 actin-related 3 homolog; Akt, protein kinase B; ALDH, aldehyde dehydrogenase; ARPC, actin related protein 2/3 complex; CAV1, caveolin 1; CDC, cell division cycle; CDK, cyclin-dependent kinase; COPA, coatomer protein complex subunit alpha; CTNN, cadherin-associated protein; DNM1L, dynamin 1-like; EGFR, epidermal growth factor receptor; EIF, eukaryotic initiation factor; eNOS, endothelial nitric oxide synthase; FADD, Fas (TNFRSF6)-associated via death domain; FLN, filamin; GSTP1, glutathione S-transferase pi 1; HLA-A, major histocompatibility complex class I; HGF, hepatocyte growth factor; HMGB1, high mobility group protein B1; HSP, heat shock protein; IQGAP1, IQ motif containing GTPase activating protein 1; ITGB, intergrin beta; NQO1, NAD(P)H: quinone oxidoreductase 1; MAPK, mitogen-activated protein kinase; mTOR, mammalian target of rapamycin; Nrf2, Nuclear factor erythroid 2-related factor 2; PA2G4, proliferation-associated 2G4; PAK, p21-activated kinase; PABPC1, poly(A) binding protein cytoplasmic 1; PI3K, phosphoinositide 3-kinase; PLB, plumbagin; PPIB, peptidylprolyl isomerase B; PSM, proteasome subunit; PTEN, phosphatase and tensin-like protein; RAR, retinoic acid receptor; RHO, Ras homolog gene family; RhoGDI, Rho GDP-dissociation inhibitor; RPS, ribosomal protein S; RPL, ribosomal protein L; S6K, S6 kinase; SOD, superoxide dismutase; STAT, signal transducer and activator of transcription; TUBA, tubulin alpha; VEGF, vascular endothelial growth factor; VIM, vimentin.

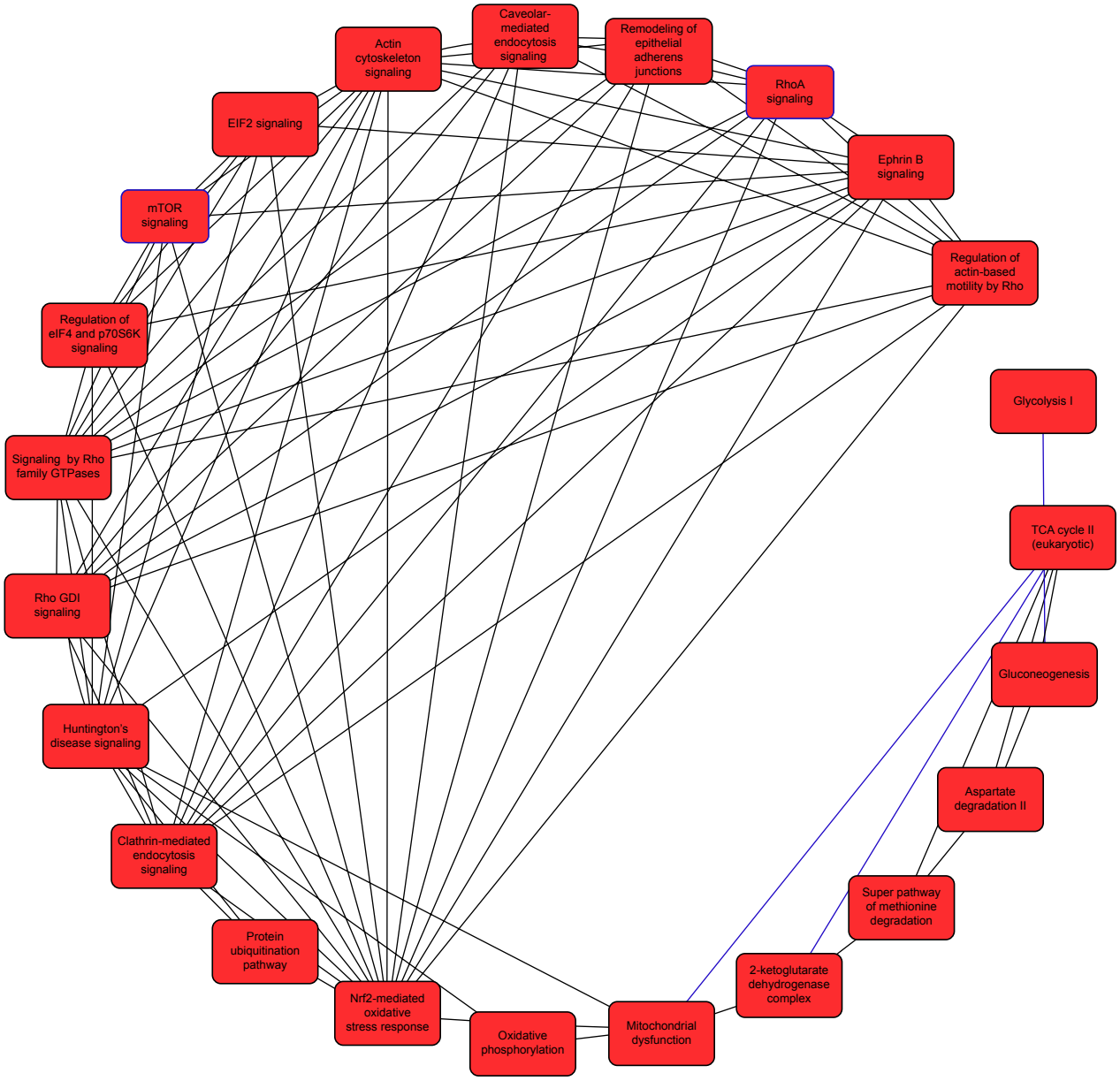

Figure 1 Proteomic analysis reveals a network of signaling pathways regulated by PLB in SCC25 cells.
Notes: A network of signaling pathways was analyzed by IPA according to the 398 molecules and 101 related pathways that were regulated by PLB in SCC25 cells.
Abbreviations: IPA, Ingenuity Pathway Analysis; PLB, plumbagin.

DNA damage checkpoint in SCC25 cells with the involvement of multiple functional proteins (Table 3). These included YWHAQ, PRKDC, YWHAG, YWHAE, YWHAH, YWHAB, YWHAZ, SFN, SKP1, and CDK1 at G_2/M checkpoint (Figure 2).

PLB regulates apoptosis in SCC25 cells

Apoptosis is the type I programmed cell death pathway and has been considered as a promising target for the treatment of cancer either via intrinsic (mitochondrial-mediated) or extrinsic (death receptor-mediated) apoptosis pathways. As listed in Table 3, PLB regulated apoptotic signaling pathway and death receptor signaling pathway involving a number of functional proteins. These included ACIN1, CAPNS1, MAPK1, RRAS, LMNA, CAPN2, SPTAN1, CYCS, CDK1, PARP1, AIFM1, FADD, and ACTB. Moreover, the IPA results showed that mTOR signaling pathway played a central role in the regulation of cell metabolism, growth, proliferation, and survival through the integration of both intracellular and extracellular signals (Table 3). We subsequently investigated extrinsic apoptosis mediated by FADD in SCC25 cells with the treatment of PLB.

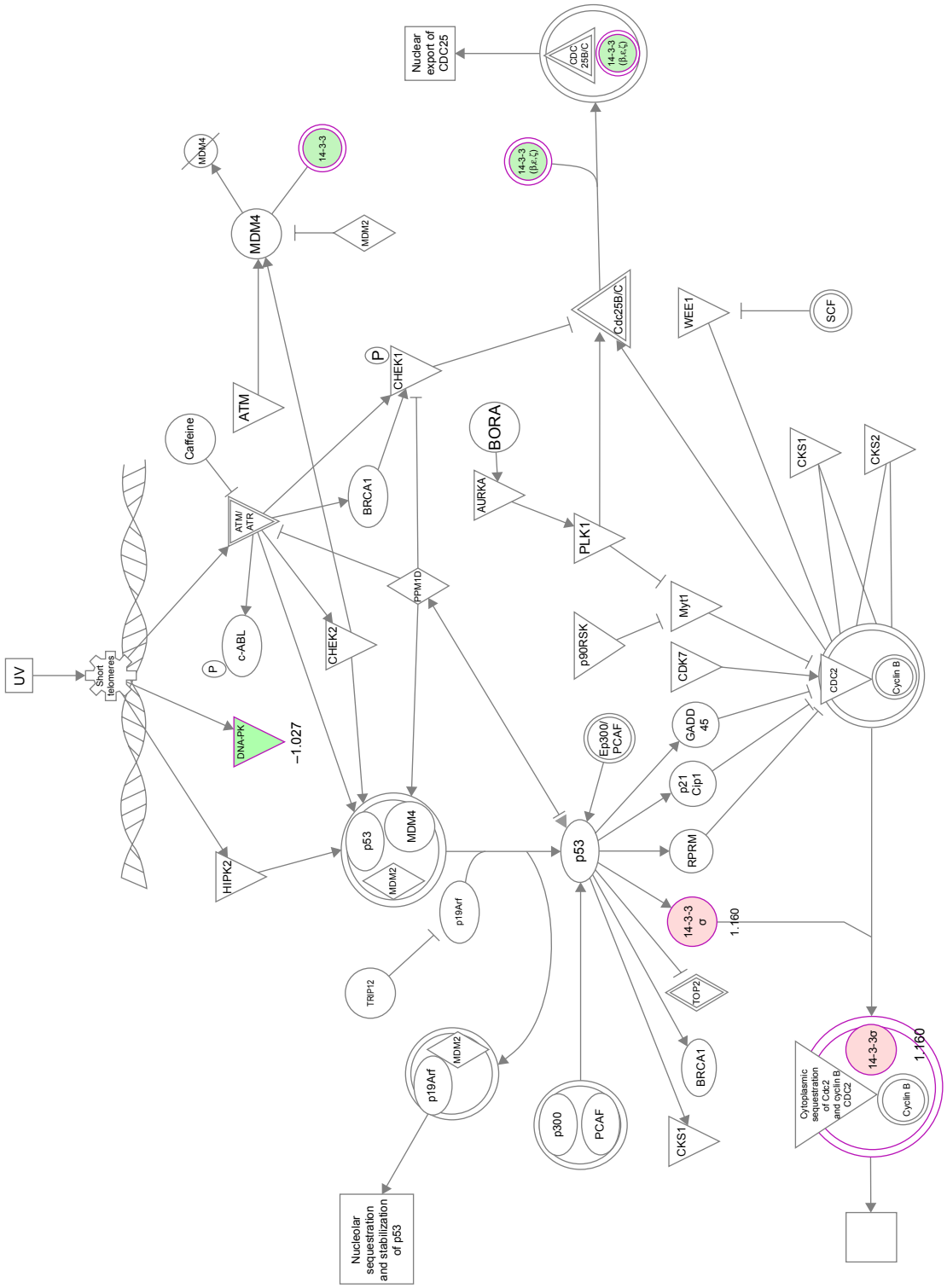

Figure 2 PLB regulates cell cycle at G_2/M checkpoint in SCC25 cells.
Notes: SCC25 cells were treated with 5 μM PLB for 24 hours and the protein samples were subject to quantitative proteomic analysis. Red indicates upregulation; green indicates a downregulation. The intensity of green and red molecule colors indicates the degree of down- or upregulation, respectively. Solid arrows indicate direct interaction.
Abbreviations: PLB, plumbagin; UV, ultraviolet.

PLB regulates EMT pathways in SCC25 cells

EMT has a close association with cell migration, invasion, and stemness. Suppressing the progress of EMT is thought to be clinically helpful for cancer therapy. We analyzed the effect of PLB on EMT-related proteins and signaling pathways using SILAC-based proteomic approach. The proteomic data showed that PLB regulated epithelial adherens junction signaling pathway in SCC25 cells involving a number of functional proteins, including ACTA1, ACTG1, ACTN1, ACTN4, ACTR3, ARPC1B, CTNNA1, CTNND1, DNM1L, EGFR, IQGAP1, JUP, MYH9, RAB7A, RHO1, TUBA1B, TUBA1C, TUBA4A, TUBB, TUBB4B, VAL, VCL, and ZYX.

PLB regulates redox homeostasis involving Nrf2-mediated signaling pathways in SCC25 cells

Induction of ROS generation plays a critical role in the cytokine production, contributing to the cancer cell killing effect of PLB. However, the regulatory effect of PLB on ROS generation-related molecules and signaling pathways has not been fully understood. In this study, we observed that PLB regulated several critical signaling pathways related to ROS generation and redox homeostasis in SCC25 cells. Our quantitative proteomic study showed that PLB treatment regulated Nrf2-mediated oxidative stress response and oxidative phosphorylation in SCC25 cells (Table 2). A number of functional proteins were found to be involved in these pathways, including ACTA1, ACTG1, CBR, DNAJA2, GSTP1, NQO1, HSP90AA1, PPIB, SOD1, STIP1, and VCP (Table 2). Of note, Nrf2-mediated signaling pathways have critical roles in the maintenance of intracellular redox homeostasis in response to various stimuli via regulating antioxidant responsive elements. The quantitative proteomic data suggest that modulation of the expression of functional proteins involved in Nrf2-mediated signaling pathways may contribute to the anticancer effect of PLB in the treatment of TSCC. The results showed that PLB can efficiently induce ROS generation and that this can be abolished by NAC and GSH. Hence, we subsequently studied the relationship of ROS-generation-inducing effect of PLB with other cellular biological functions, including cell cycle arrest, cell apoptosis, and EMT.

Verification of molecular targets of PLB in SCC25 cells by Western blotting assay

Our aforementioned quantitative proteomic studies have predicted and shown that PLB can modulate a number of signaling pathways and functional proteins related to cell proliferation, cell migration, cell death, and cell survival. On the basis of our previous experimental and present proteomic data in SCC25 cells, we further examined the effect of PLB with a focus on cell cycle, apoptosis, EMT, and redox homeostasis and its related signaling pathways to delineate the underlying mechanisms.

PLB induces G_2/M arrest in SCC25 cells via downregulation of cyclin B1, CDK1/cdc2, and cdc25

First, we examined the effect of PLB on cell cycle distribution of SCC25 cells using a flow cytometer. PLB markedly induced a G_2/M phase arrest ($P<0.05$, 0.01, or 0.001; Figure 3). Compared with the control cells (2.4%), the percentage of SCC25 cells in G_2/M phase was increased in a concentration-dependent manner after PLB treatment (Figure 3A and B). The percentage of cells in G_2/M phase was 5.8%, 9.1%, and 13.1% when treated with PLB at 0.1, 1, and 5 μM, respectively. On the other hand, PLB significantly decreased the percentage of SCC25 cells in G_1 phase when treated with 5 μM in comparison to the control cells ($P<0.001$; Figure 3B). In a separate experiment, the effect of 5 μM PLB on cell cycle distribution was examined in SCC25 cells over 48 hours (Figure 3C and D). Compared to the control cells, the percentage of SCC25 cells in the G_2/M phase was increased from 2.7% at basal level to 8.1%, 9.4%, and 11.1% after 6-, 24-, and 48-hour treatment with 5 μM PLB, respectively ($P<0.001$; Figure 3D), whereas 5 μM PLB treatment decreased the percentage of SCC25 cells in G_1 phase from 48.8% at basal level to 41.3% after 48 hours of treatment ($P<0.05$; Figure 3D).

To explore the mechanisms for PLB-induced cell cycle arrest in SCC25 cells, the expression level of key regulators responsible for G_2/M checkpoint was examined using Western blotting assay. CDK1/cdc2, cyclin B1, and cdc25 are important regulators for G_2 to M phase transition and thus their expression level was determined in SCC25 cells. The expression level of cdc2 was marked suppressed in SCC25 cells after treatment with PLB at concentrations of 0.1, 1, and 5 μM for 24 hours ($P<0.001$; Figure 4A and C). Compared with the control cells, the expression level of cyclin B1 was decreased by 18.3%, 46.0%, and 62.3% when SCC25 cells were treated with 0.1, 1, and 5 μM PLB for 24 hours, respectively ($P<0.01$ or 0.001; Figure 4A and C). There was a 10.7%, 14.0%, and 35.3% reduction in the expression level of cdc25 in SCC25 cells when treated with PLB at 0.1, 1, and 5 μM for 24 hours, respectively ($P<0.05$, 0.01, or 0.001; Figure 4A and C).

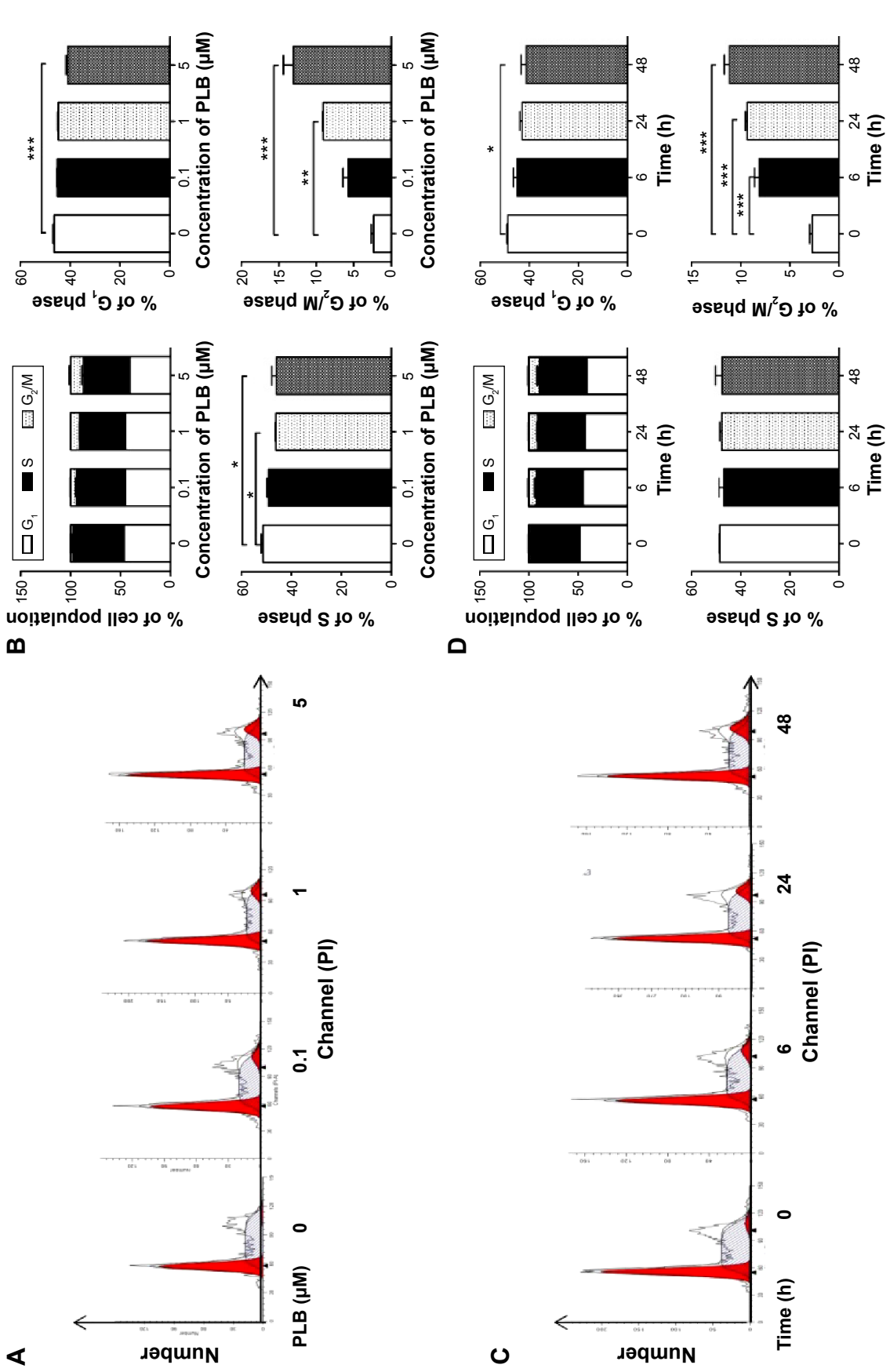

Figure 3 PLB induces G_2/M arrest in SCC25 cells.

Notes: Cell cycle distribution of SCC25 cells after the treatment of PLB in the concentration and time course experiments. (**A**) Representative flow cytometric plots of cell cycle distribution of SCC25 cells and (**B**) bar graphs showing the percentage of SCC25 cells in G_1, S, and G_2/M phases after the treatment of 0.1, 1, and 5 μM PLB for 24 hours. (**C**) Representative flow cytometric plots of cell cycle distribution of SCC25 cells and (**D**) bar graphs showing the percentage of SCC25 cells in G_1, S and G_2/M phases after the treatment of 5 μM PLB for 6, 24, and 48 hours. Data are the mean ± SD of three independent experiments. *$P<0.05$; **$P<0.01$; and ***$P<0.001$ by one-way ANOVA.

Abbreviations: PLB, plumbagin; ANOVA, analysis of variance; SD, standard deviation; PI, propidium iodide.

Next, we conducted separate experiment over 48 hours. In comparison to the control cells, the expression level of cdc2 was decreased by 18.3% and 19.0% when SCC25 cells were treated with 5 μM PLB for 24 and 48 hours, respectively ($P<0.001$; Figure 4B and D); there was a 34.3% and 49.3% reduction in the expression level of cyclin B1 when SCC25 cells were incubated with 5 μM PLB for 24 and 28 hours, respectively ($P<0.001$; Figure 4B and D); and the expression level of cdc25 was also markedly suppressed ($P<0.01$ or 0.001; Figure 4B and D). These results demonstrate that PLB downregulates cyclin B1, CDK1/cdc2, and cdc25 in SCC25 cells. Importantly, these results have confirmed the regulatory effect of PLB on cell proliferation-related signaling pathways, which was predicted by our proteomic studies.

PLB induces apoptosis via FADD-mediated extrinsic signaling pathway

Apoptosis is a typical type of programmed cell death that plays an important role in PLB-induced cancer cell death. Previously, we observed that PLB significantly induced intrinsic apoptosis in SCC25 cells in a concentration- and time-dependent manner.[20] On the basis of the results hinted at by the proteomic results

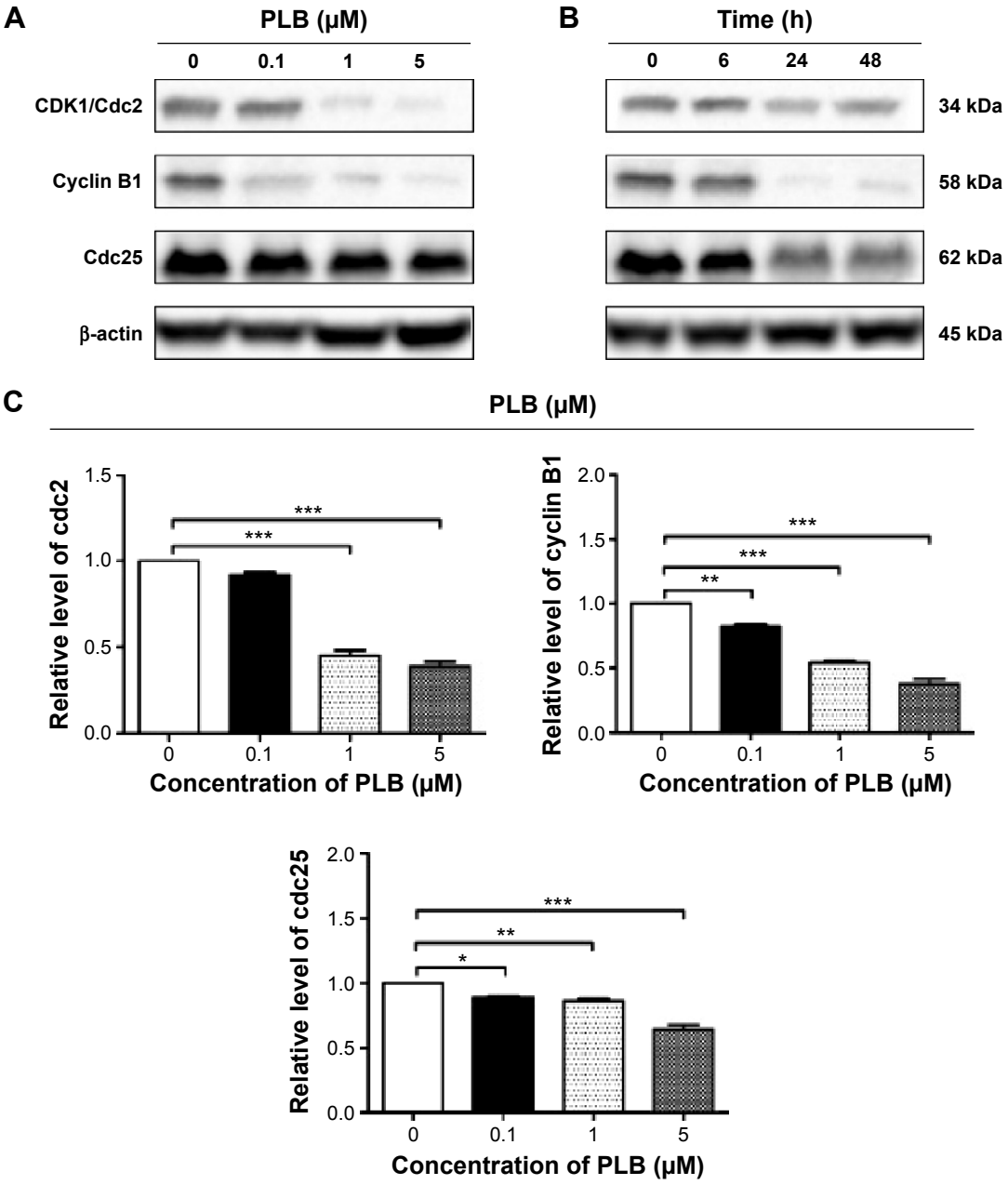

Figure 4 (*Continued*)

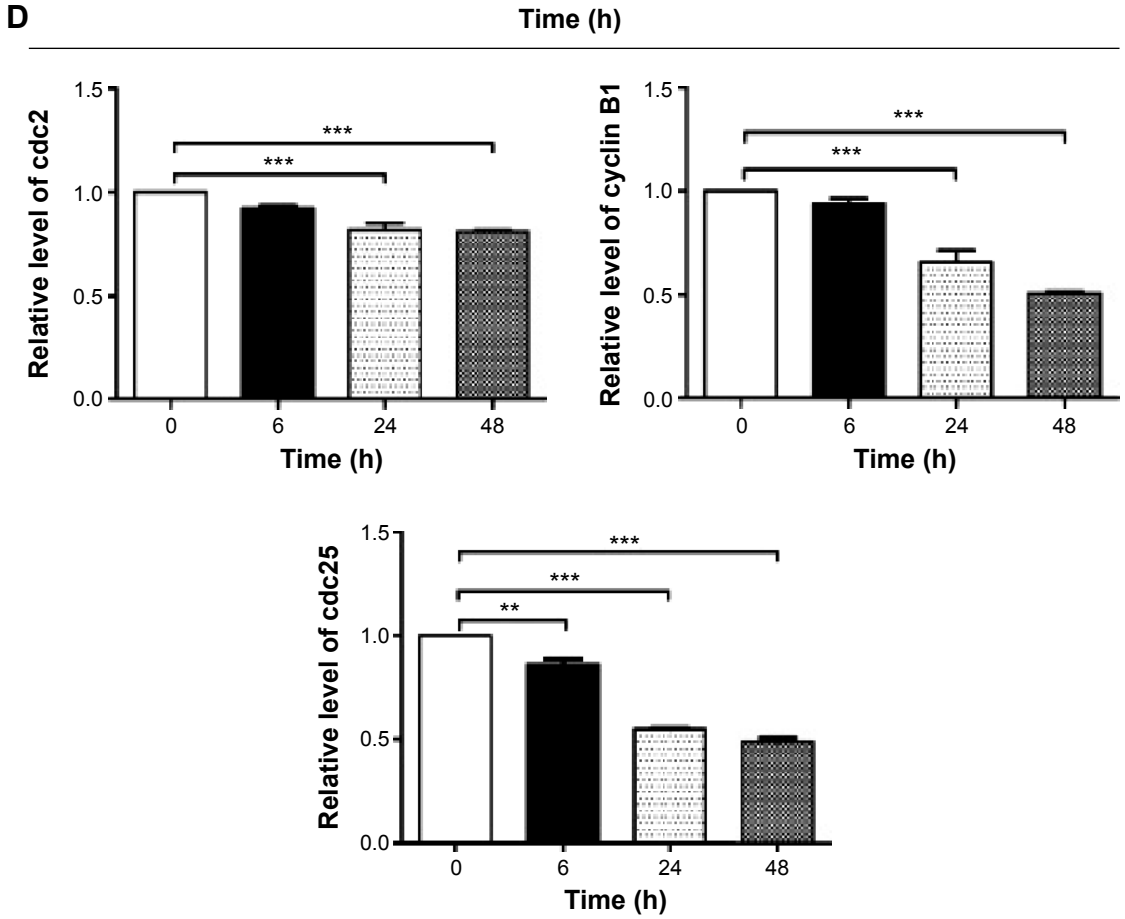

Figure 4 PLB regulates the expression of CDK1/cdc2, cyclin B1, and cdc25 in SCC25 cells.
Notes: SCC25 cells were treated with PLB in the concentration and time course experiments and the protein samples were subject to Western blotting assay. (**A**) Representative blots of CDK1/cdc2, cyclin B1, and cdc25 in SCC25 cells after the treatment of 0.1, 1, and 5 μM PLB for 24 hours, and (**B**) representative blots of CDK1/cdc2, cyclin B1, and cdc25 in SCC25 cells after the treatment of 5 μM PLB for 6, 24, and 48 hours. (**C**) Bar graphs showing the relative levels of CDK1/cdc2, cyclin B1, and cdc25 in SCC25 cells after the treatment of 0.1, 1, and 5 μM PLB for 24 hours, and (**D**) bar graphs showing the relative level of CDK1/cdc2, cyclin B1, and cdc25 in SCC25 cells after the treatment of 5 μM PLB for 6, 24, and 48 hours. Data are the mean ± SD of three independent experiments. *$P<0.05$; **$P<0.01$; and ***$P<0.001$ by one-way ANOVA.
Abbreviations: PLB, plumbagin; ANOVA, analysis of variance; SD, standard deviation.

(Figure 5), we further tested the apoptosis inducing effect of PLB with a focus on FADD-mediated signaling pathway. First, we employed flow cytometry to analyze the apoptosis-inducing effect of PLB in SCC25 cells. Subsequently, the modulation effect of PLB on the expression of FADD, TRADD, DR5, and cleaved caspase 3 in SCC25 cells was measured with a consideration to fully understand the apoptosis-inducing effect of PLB via FADD-mediated extrinsic signaling pathway. Cells were treated with PLB at concentrations of 0.1, 1, and 5 μM for 24 hours. The apoptosis level was increased from 3.0% to 6.1%, 8.2%, and 20.3% when SCC25 cells were treated with 0.1, 1, and 5 μM for 24 hours, respectively ($P<0.05$, 0.01, or 0.001; Figure 6A and B). Next, we conducted the time course experiment, and the results showed that the apoptosis level was increased from 3.5% at basal level to 11.4%, 21.2%, and 35.7% when SCC25 cells were treated with 5 μM PLB for 6, 24, and 48 hours, respectively ($P<0.001$; Figure 6C and D). Furthermore, There was a 1.3- and 1.6-fold increase in the expression level of FADD after SCC25 cells were treated with 1 and 5 μM PLB for 24 hours, respectively ($P<0.01$ or 0.001; Figure 7A and C). The expression level of TRADD and DR5 was also increased when cells were treated with PLB ($P<0.01$ or 0.001; Figure 7A and C). The cleavage of caspase 3 is the determinant process in both intrinsic and extrinsic apoptosis. We found that PLB markedly increased the level of cleaved caspase 3 to 1.2- and 1.3-fold when SCC25 cells were treated with 1 and 5 μM for 24 hours, respectively ($P<0.01$ or 0.001; Figure 7A and C). In a separate experiment, we examined the apoptosis-inducing effect of PLB over 48 hours. The expression level of FADD was increased 1.5-, 1.5-, and 1.6-fold when SCC25 cells were treated with 5 μM for 6, 24, and 48 hours, respectively ($P<0.001$; Figure 7B and D). The expression level of DR5 was also markedly increased in comparison with the control cells ($P<0.05$ or 0.001; Figure 7B and D). Meanwhile,

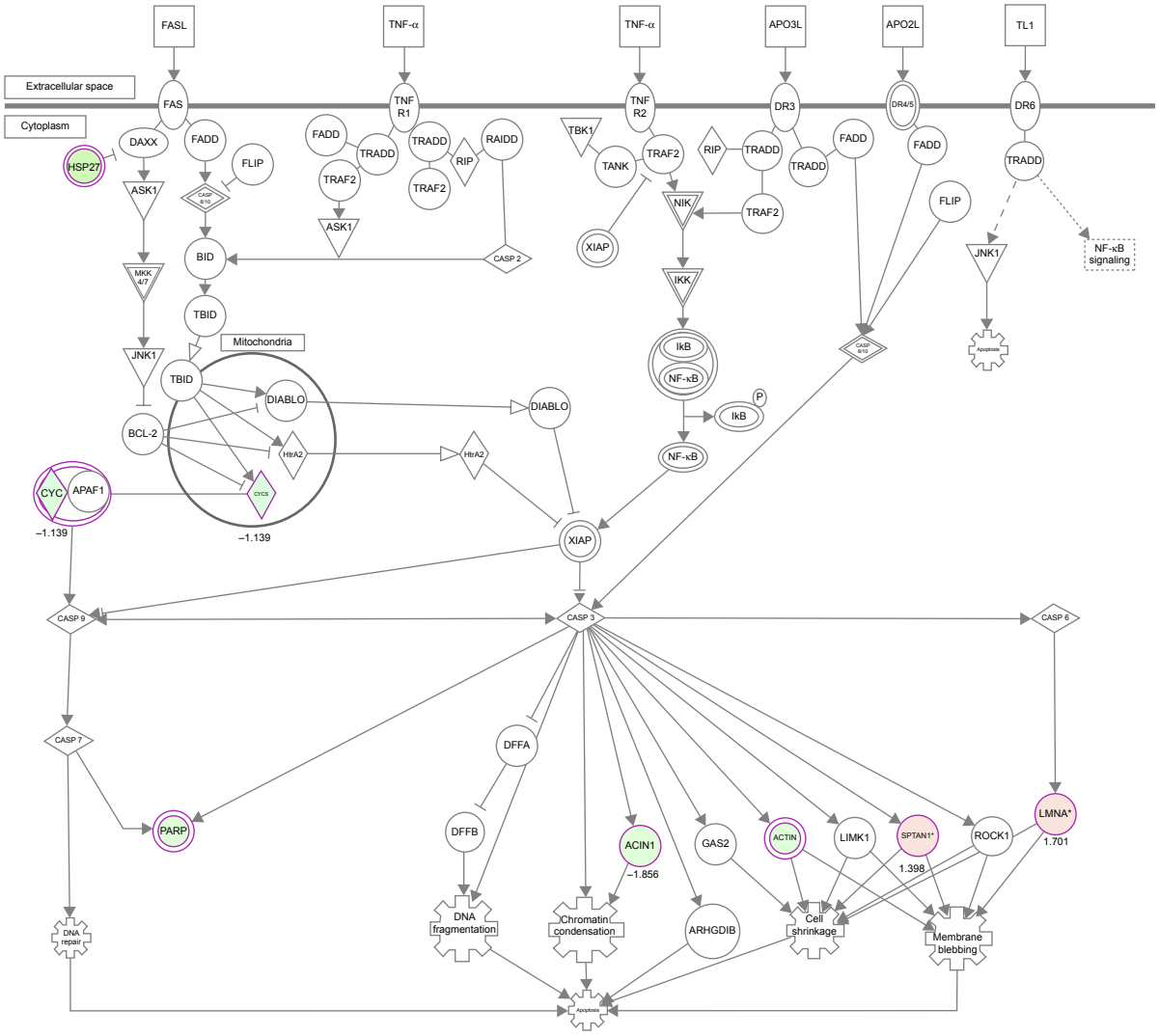

Figure 5 PLB regulates death receptor signaling in SCC25 cells.

Notes: SCC25 cells were treated with 5 μM PLB for 24 hours and the protein samples were subject to quantitative proteomic analysis. Red indicates upregulation; green indicates downregulation. The intensity of green and red molecule colors indicates the degree of down- or upregulation, respectively. Solid arrows indicate direct interaction and dashed arrows indicate indirect interaction. The arrow with white head indicates translocation. The arrow with gray head indicates activation, causation, expression, localization, membership, modification, molecular cleavage, phosphorylation, protein-DNA interactions, protein-RNA interactions, regulation of binding, transcription.

Abbreviation: PLB, plumbagin.

there was a 1.1-, 1.3-, and 1-2 fold rise in the expression level of cleaved caspase 3, when SCC25 cells were treated with 5 μM PLB for 6, 24, and 48 hours, respectively ($P<0.01$ or 0.001; Figure 7B and D). The expression level of TRADD was also remarkably increased when SCC25 cells were treated with 5 μM PLB for 48 hours. These results clearly show that PLB induces apoptosis by involving the FADD-mediated extrinsic pathway in SCC25 cells, and these data are in agreement with our proteomic findings.

PLB inhibits EMT and stemness in SCC25 cells

EMT is a critical process involved in the invasion, metastasis, and stemness of cancer.[35] EMT depends on a reduction in expression of cell adhesion molecules. Tight junctions function as complete barriers between epithelium and endothelium and contribute to the maintenance of cell polarity. Claudin and occludin proteins are integral structural and functional components of tight junctions.[36,37] ZO-1, 2, and 3 are peripheral membrane adaptor proteins that link junctional transmembrane proteins to the actin cytoskeleton.[38–40] Cadherins are a superfamily of transmembrane glycoproteins, which include N-, P-, R-, B-, and E-cadherins.[41] E-cadherin is considered an active suppressor of invasion in many epithelial cancers.[42] Cancer cells often have upregulated N-cadherin in addition to loss of E-cadherin.[43] Furthermore, the cytoplasmic domain of classical cadherins interacts with β-catenin, γ-catenin, and p120 catenin.[44,45] It is reported that snail can interact with

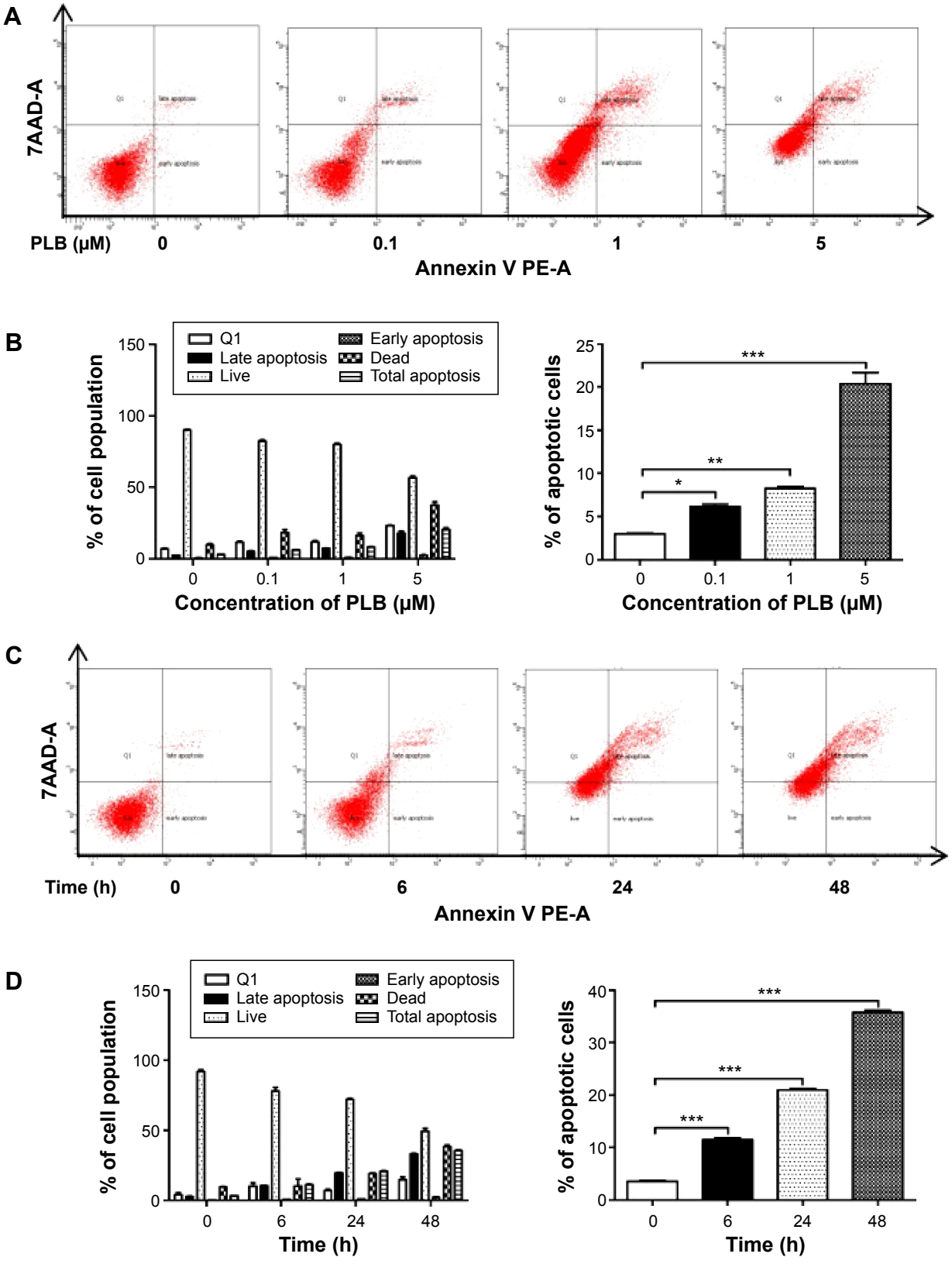

Figure 6 PLB induces apoptosis in SCC25 cells.

Notes: Apoptosis induction effect of PLB in SCC25 cells was examined. (**A**) Representative flow cytometric plots of apoptosis in SCC25 cells and (**B**) bar graphs showing the percentage of total apoptosis in SCC25 cells after the treatment of 0.1, 1, and 5 μM PLB for 24 hours. (**C**) Representative flow cytometric plots of apoptosis in SCC25 cells and (**D**) bar graphs showing the total apoptosis in SCC25 cells after the treatment of 5 μM PLB for 6, 24, and 48 hours. Data are the mean ± SD of three independent experiments. *$P<0.05$; **$P<0.01$; and ***$P<0.001$ by one-way ANOVA.

Abbreviations: PLB, plumbagin; ANOVA, analysis of variance; SD, standard deviation.

β-catenin via Wnt signaling pathway.[46] Herein, on the basis of the proteomic results (Figure 8), we verified the effect of PLB treatment on EMT-associated markers in SCC25 cells using Western blotting assay. Incubation of SCC25 cells with PLB resulted in a concentration- and time-dependent increase in the expression level of E-cadherin and a decrease in the expression level of N-cadherin (Figure 9A–D). There was a 1.2- and 1.8-fold increase in the expression of E-cadherin when treated with 1 and 5 μM PLB for 24 hours, respectively, whereas 5 μM PLB suppressed expression level of N-cadherin 23% ($P<0.05$ or 0.001; Figure 9A and C). When SCC25 cells were treated with 5 μM PLB over 48 hours, the expression level of E-cadherin was increased 1.2-, 1.4-, and 1.8-fold after the treatment of 5 μM PLB for 6, 24, and 48 hours, respectively ($P<0.01$ or 0.001; Figure 9B and D). The expression level of N-cadherin was decreased by 23.3% and 45.0% when SCC 25 cells were treated with 5 μM PLB for 24 and 48 hours, respectively ($P<0.05$ or 0.001; Figure 9B and D).

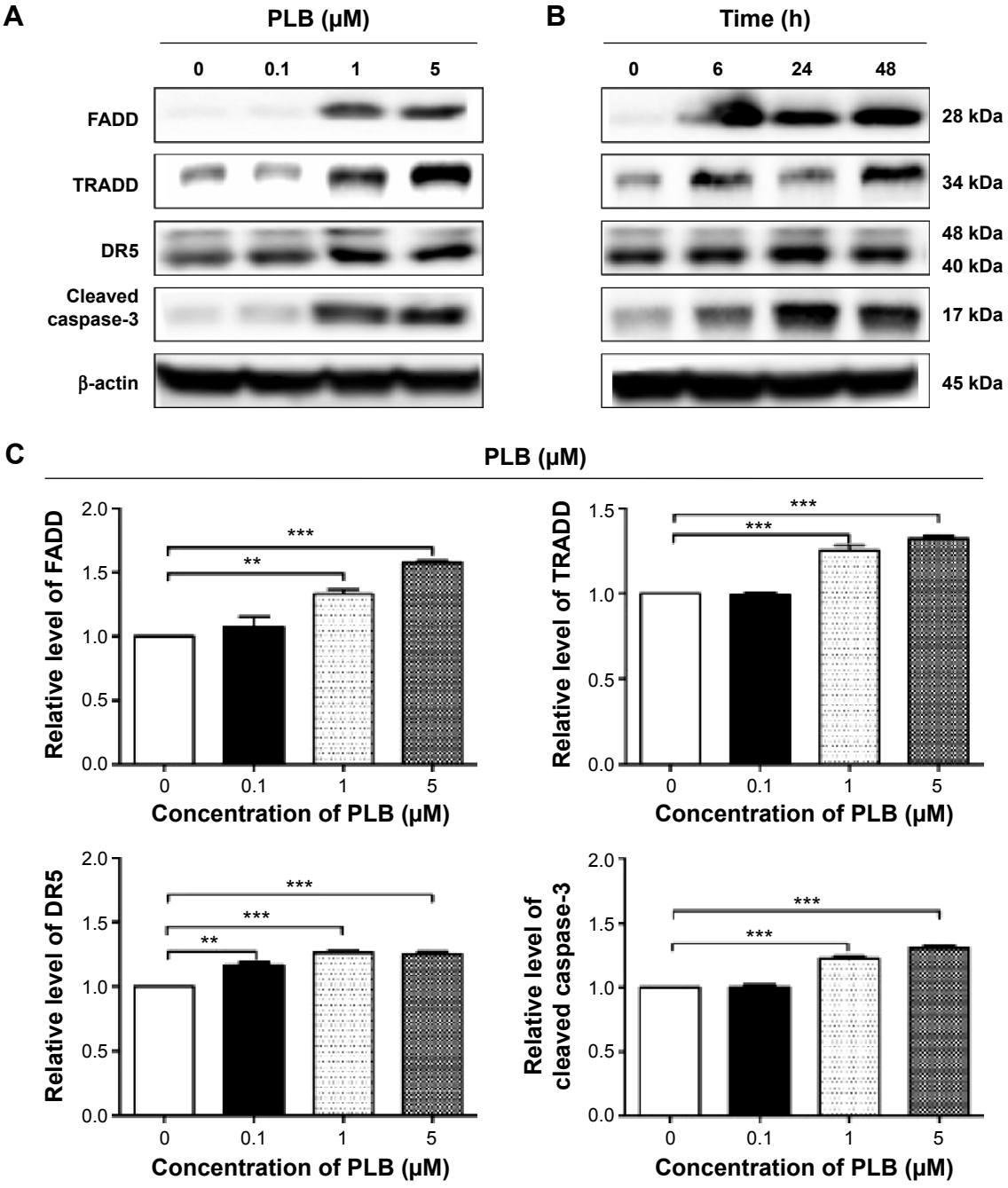

Figure 7 (*Continued*)

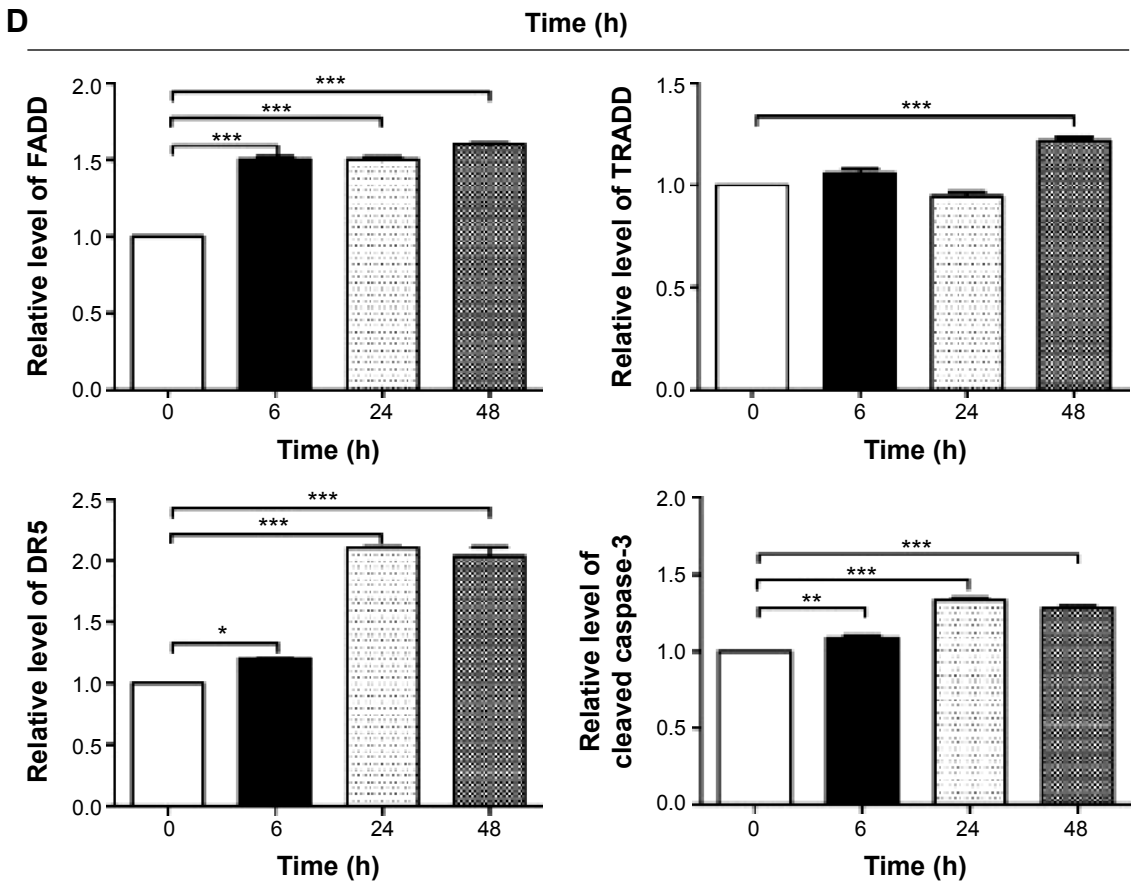

Figure 7 PLB regulates the expression of FADD, TRADD, and DR5 in SCC25 cells.

Notes: SCC25 cells were treated with PLB in the concentration and time course experiments and protein samples were subject to Western blotting assay. (**A**) Representative blots of FADD, TRADD, and DR5 in SCC25 cells after the treatment of 0.1, 1, and 5 μM PLB for 24 hours, and (**B**) representative blots of FADD, TRADD, and DR5 in SCC25 cells after the treatment of 5 μM PLB for 6, 24, and 48 hours. (**C**) Bar graphs showing the relative level of FADD, TRADD, and DR5 in SCC25 cells after the treatment of 0.1, 1, and 5 μM PLB for 24 hours, and (**D**) bar graphs showing the relative level of FADD, TRADD, and DR5 in SCC25 cells after the treatment of 5 μM PLB for 6, 24, and 48 hours. Data are the mean ± SD of three independent experiments. *$P<0.05$; **$P<0.01$; and ***$P<0.001$ by one-way ANOVA.

Abbreviations: PLB, plumbagin; ANOVA, analysis of variance; SD, standard deviation; FADD, Fas (TNFRSF6)-associated via death domain; TRADD, TNF1 receptor-associated death domain.

In order to further examine the effect of PLB on EMT in SCC25 cells, we measured the expression level of several key regulators of E-cadherin. Snail and slug (both zinc finger transcriptional factors) together with TCF8/ZEB1 are suppressors of E-cadherin in EMT. PLB significantly reduced the expression level of snail and slug in SCC25 (Figure 9A and C). When SCC25 cells were treated with 5 μM PLB for 24 hours, the expression level of snail and slug was decreased by 46% and 41%, respectively (Figure 9A and C). Furthermore, PLB induced a time-dependent reduction in the expression level of TCF-8/ZEB1 in SCC25 cells. The expression level of TCF-8/ZEB1 was decreased by 22.0%, 27.0%, and 70.3% when SCC25 cells were treated with 5 μM PLB for 6, 24, and 48 hours, respectively (Figure 9B and D).

Vimentin is a type III intermediate filament protein in mesenchymal cells. β-Catenin can act as an integral component of a protein complex in adherens junctions that helps cells maintain epithelial layers, and β-catenin participates in the Wnt signaling pathway as a downstream target. In SCC25 cells, PLB inhibited the expression of vimentin in a concentration- and time-dependent manner. The expression level of vimentin was decreased by 19.3% and 24.7% when cells were treated with 1 and 5 μM PLB for 24 hours, respectively ($P<0.01$; Figure 9A and C). Consistently, the expression level of vimentin was decreased by 21.0% and 51.3% when SCC25 cells were incubated with 5 μM PLB for 24 and 48 hours, respectively ($P<0.01$ or 0.001; Figure 9B and D). There was also a significant reduction in the expression level of β-catenin in both the concentration and time course experiment when SCC25 cells were treated with 5 μM PLB. PLB at 5 μM markedly decreased the expression level of β-catenin by 24.7% with a 24-hour incubation period ($P<0.01$; Figure 9A and C). Finally, the expression of tight junction proteins ZO-1 and claudin-1

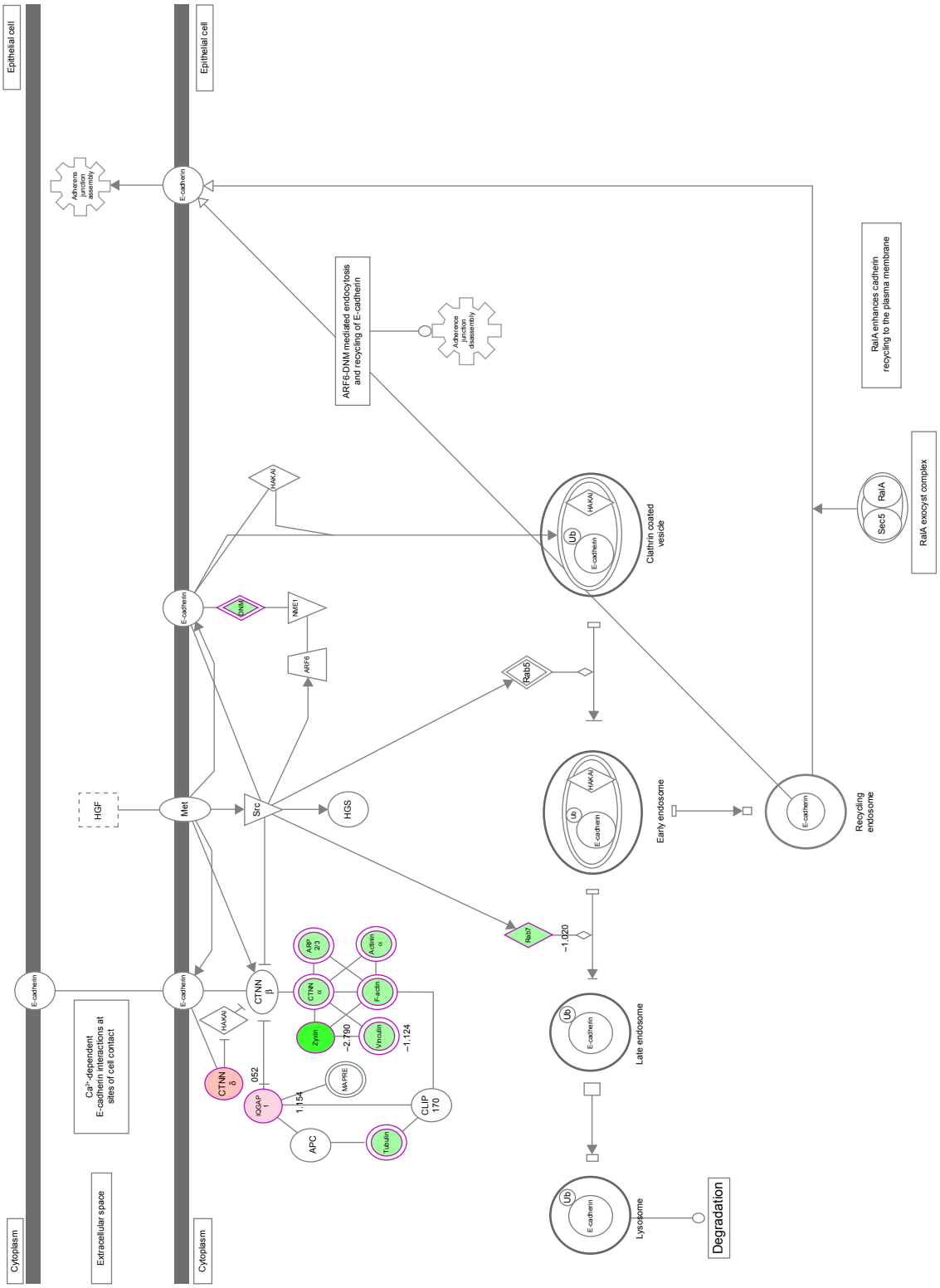

Figure 8 PLB regulates remodeling of epithelial adherens junctions pathway in SCC25 cells.
Notes: SCC25 cells were treated with 5 μM PLB for 24 hours and the protein samples were subject to quantitative proteomic analysis. Red indicates upregulation; green indicates downregulation. The intensity of green and red molecule colors indicates the degree of down or upregulation, respectively. Solid arrows indicate direct interaction. The arrow with white head indicates translocation. The arrow with gray head indicates activation, causation, expression, localization, membership, modification, molecular cleavage, phosphorylation, protein-DNA interactions, protein-RNA interactions, regulation of binding, transcription.
Abbreviation: PLB, plumbagin.

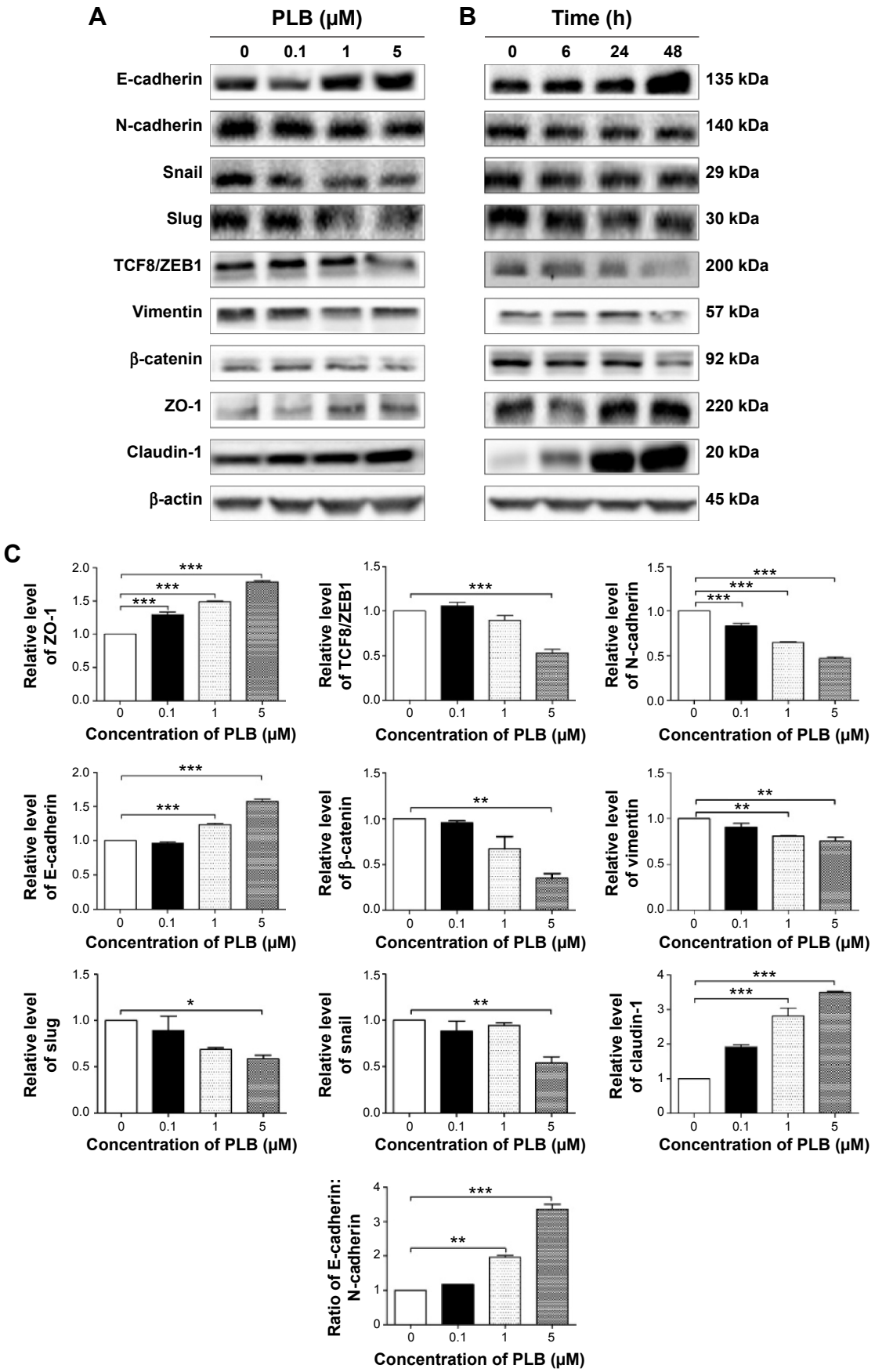

Figure 9 (*Continued*)

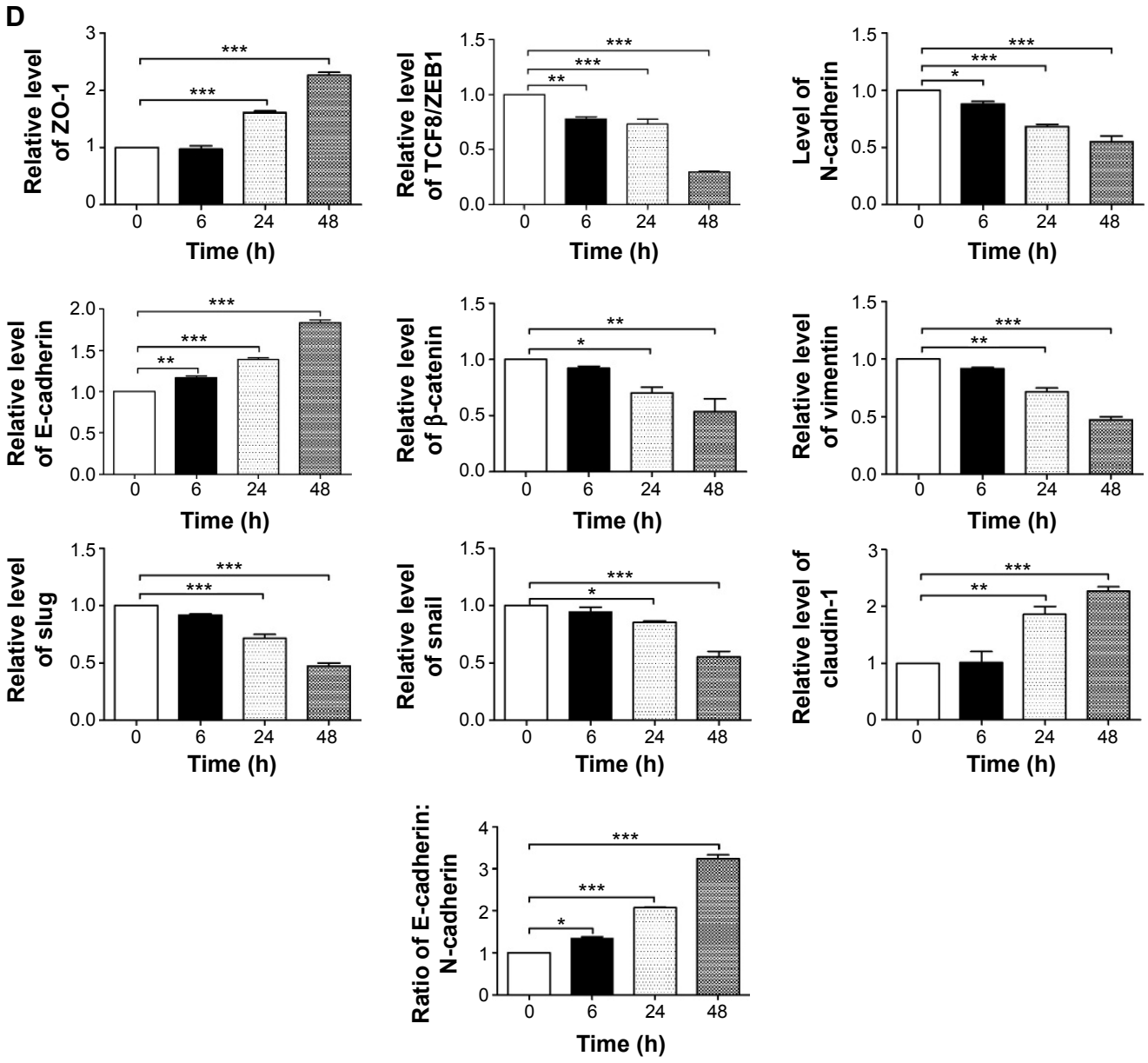

Figure 9 PLB regulates the expression of EMT-related markers in SCC25 cells.

Notes: SCC25 cells were treated with PLB in the concentration and time course experiments and protein samples were subject to Western blotting assay. (**A**) Representative blots of E-cadherin, N-cadherin, snail, slug, TCF8/ZEB1, vimentin, β-catenin, ZO-1, and claudin-1 in SCC25 cells after the treatment of 0.1, 1, and 5 μM PLB for 24 hours; (**B**) representative blots of E-cadherin, N-cadherin, snail, slug, TCF8/ZEB1, vimentin, β-catenin, ZO-1, and claudin-1 in SCC25 cells after the treatment of 5 μM PLB for 6, 24, and 48 hours. (**C**) Bar graphs showing the relative level of E-cadherin, N-cadherin, snail, slug, TCF8/ZEB1, vimentin, β-catenin, ZO-1, and claudin-1 in SCC25 cells after the treatment of 0.1, 1, and 5 μM PLB for 24 hours, and (**D**) bar graphs showing the relative level of E-cadherin, N-cadherin, snail, slug, TCF8/ZEB1, vimentin, β-catenin, ZO-1, and claudin-1 in SCC25 cells after the treatment of 5 μM PLB for 6, 24, and 48 hours. Data are the mean ± SD of three independent experiments. *$P<0.05$; **$P<0.01$; and ***$P<0.001$ by one-way ANOVA.

Abbreviations: PLB, plumbagin; ANOVA, analysis of variance; SD, standard deviation.

were examined in SCC25 cells after the treatment of PLB. ZO-1 and -2 are required for tight junction formation and function. The effect of PLB on the expression of ZO-1 and claudin-1 in SCC25 cells increased significantly in a concentration- and time-dependent manner (Figure 9A and B). Treatment of cells with 5 μM PLB for 24 hours led to a 1.8- and 3.5-fold rise in the expression level of ZO-1 and claudin-1, compared to the control cells, respectively ($P<0.001$; Figure 9A and C). These results from Western blotting assay verified our proteomic data.

In addition, there is increasing evidence showing that CSCs can display EMT characteristics such as loss of the adhesion protein E-cadherin. This relationship drives us to think about the stemness-attenuating effect of PLB in SCC25 cells. Therefore, we primarily conducted the Western blotting assay to examine the key stemness markers, including

Oct-4, Bmi-1, Nanog, and Sox-2. Oct-4, also known as Oct-3, belongs to the POU (Pit-Oct-Unc) transcription factor family and plays an important role during early embryogenesis.[47] Sox-2 is a member of the *Sox* gene family that encodes transcription factors and plays an important role in the maintenance of stemness.[48] Nanog transcription factor cooperates with Oct-4 and Sox-2 and is identified as a key CSCs marker.[49] Bmi-1 is a transcriptional repressor that belongs to the polycomb-group family of proteins that determine the proliferation and senescence of normal and CSCs.[50] The Western blotting results showed that PLB significantly decreased the expression level of Oct-4, Sox-2, Nanog, and Bmi-1. Incubation of SCC25 cells with 5 μM PLB remarkably decreased the expression level of Oct-4, Sox-2, Nanog, and Bni-1 by 35.7%, 27.0%, 70.7%, and 38.3%, respectively, compared with the control cells ($P<0.001$; Figure 10A and C). In a separate experiment, we evaluated the effect of different incubation times with 5 μM PLB. Totally, the expression levels of Bmi-1, Nanog, and Sox-2 were decreased significantly after 6 hours of incubation, while the Oct-4 expression level was decreased significantly after 24 hours of incubation (Figure 10B and D). These results indicate that PLB suppresses the stemness of human TSCC cells.

PLB induces intracellular ROS generation and regulates redox homeostasis via suppressing Nrf2-mediated oxidative signaling pathway in SCC25 cells

As shown in the proteomic results, PLB exhibited a regulating effect on intracellular redox homeostasis in SCC25 cells, which may possibly contribute to the cell cycle arresting, apoptosis inducing, EMT inhibiting, and stemness-attenuating effects of PLB. Herein, we examined the role of Nrf2-mediated signaling pathway in PLB's beneficial action in SCC25 cells. Nrf2, also known as Nfe2I2, is a nuclear factor that controls the expression of various detoxifying enzymes, ROS elimination proteins, drug transporters, and antiapoptotic proteins. Normally, Nrf2 is suppressed in the cytoplasm by the interaction with Kelch-like ECH-associated protein 1 (Keap1) and Cullin3. Once exposed to the antioxidant response element (ARE)-mediated inducers, Nrf2 will translocate to the nucleus where it forms a heterodimer with a small Maf protein and binds to other nuclear factors and initiates the transcription of antioxidative genes.[51,52] As noted earlier, the proteomic results indicated that Nrf2-oxidative signaling pathway responded to the PLB treatment in SCC25 cells (Figure 11). Therefore, we analyzed this pathway using Western blotting assay. First, SCC25 cells were treated with 0.1, 1, and 5 μM PLB for 24 hours and their nuclear proteins were extracted. The results showed that the expression levels of nuclear (n)-Nrf2, NQO1, GST, and HSP90 were all decreased, while the expression level of cytosolic (c)-Nrf2 was increased in SCC25 cells, compared with the control cells (Figure 12A). The ratio of n-Nrf2 to c-Nrf2 was decreased by 13.3% and 37.0% when SCC25 cells were incubated with 1 and 5 μM PLB for 24 hours, respectively ($P<0.01$ or 0.001; Figure 12C). In addition, the expression levels of c-Nrf2, n-Nrf2, NQO1, GST, and HSP90 were also examined with the treatment of 5 μM PLB over a 48-hour treatment period. The ratio of n-Nrf2 to c-Nrf2 was decreased by 28.3% and 39.0% when SCC25 cells were incubated with 5 μM PLB for 24 and 48 hours, respectively ($P<0.001$; Figure 12D). The expression levels of NQO1, GST, and HSP90 were all markedly decreased ($P<0.05$ or 0.001; Figure 12D). Taken together, the results show that Nrf2-oxidative signaling pathway is involved in the ROS-generation-inducing effect of PLB, contributing to the regulatory activities of PLB on intracellular redox homeostasis in SCC25 cells (Figure 13).

Relationship between PLB-induced ROS generation and PLB-mediated cell cycle arrest, apoptosis induction, EMT inhibition, and stemness attenuation

The relationship between PLB-induced ROS generation and PLB-mediated cell cycle arrest, apoptosis induction, EMT inhibition, and stemness attenuation was further examined in SCC25 cells with the application of ROS scavengers (NAC and GSH). SCC25 cells were treated with 5 μM PLB, 100 μM NAC, 1 mM GSH, 5 μM PLB plus 100 μM NAC, and 5 μM PLB plus 1 mM GSH, respectively. As shown in Figures 14–16, the cell cycle arresting, apoptosis inducing, EMT inhibiting, and stemness-attenuating effects of PLB were abolished by NAC and GSH. The percentage of cells in G_2/M phase was decreased by 53.2% and 61.4% in SCC25 cells when cells were coincubated with NAC and PLB or GSH and PLB, compared to PLB-treated cells, respectively ($P<0.01$ or 0.001; Figure 14B). In addition, in comparison to PLB-treated cells, NAC and GSH ablated PLB-induced apoptosis 53.3% and 55.6%, respectively ($P<0.001$; Figure 15B). Furthermore, the expression of EMT and stemness representative markers were measured (Figure 16). Compared to PLB-treated cells, the expression level of E-cadherin was decreased by 30.4% and 36.2% when cells were cotreated with NAC and PLB or GSH and PLB, respectively ($P<0.001$; Figure 16A and B). On the contrary, the expression level of N-cadherin, Oct-4, Bmi-1, and

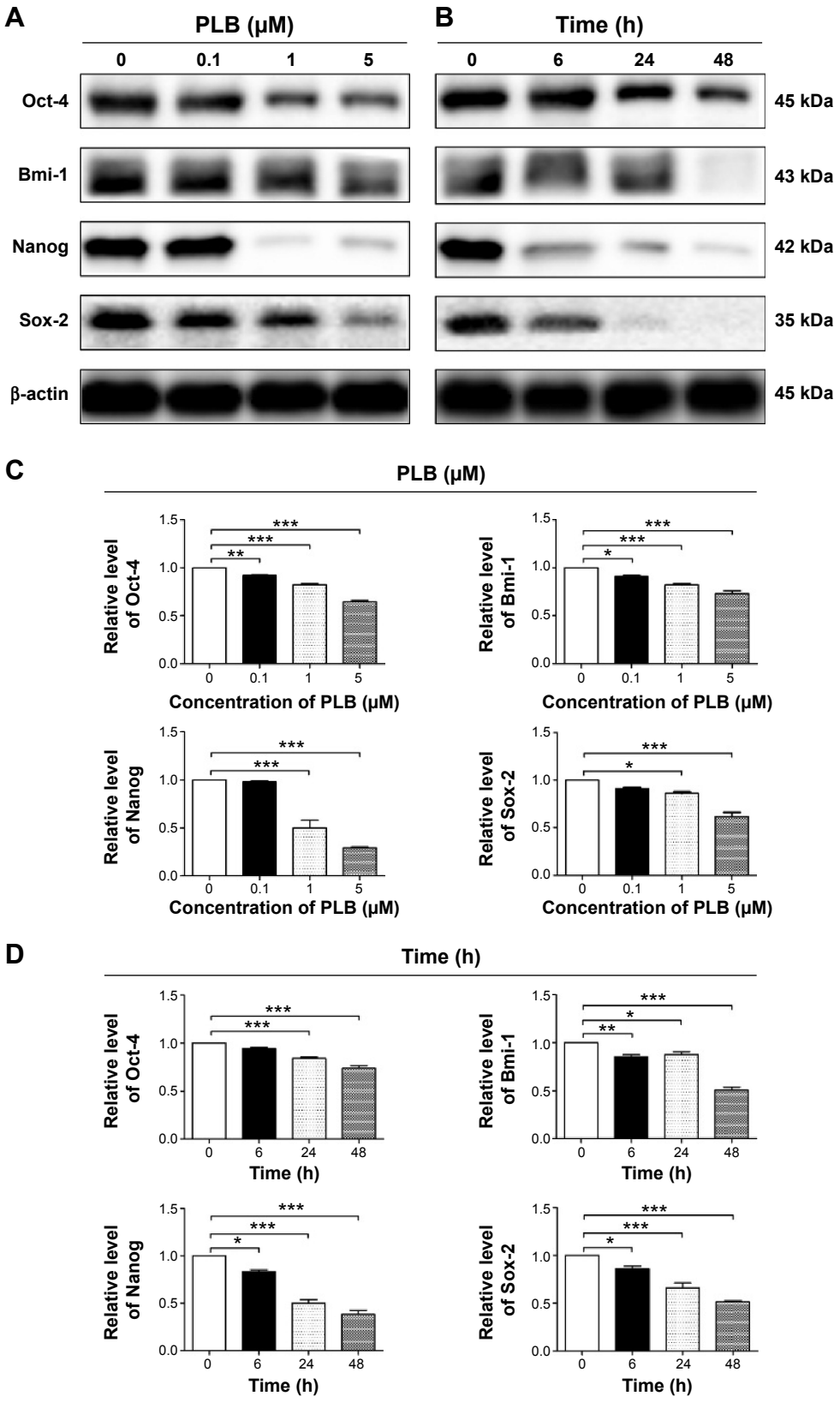

Figure 10 PLB regulates the expression of stemness markers in SCC25 cells.

Notes: SCC25 cells were treated with PLB in the concentration and time course experiments and protein samples were subject to Western blotting assay. (**A**) Representative blots of Oct-4, Bmi-1, Nanog, and Sox-2 in SCC25 cells after the treatment of 0.1, 1, and 5 μM PLB for 24 hours, and (**B**) representative blots of Oct-4, Bmi-1, Nanog, and Sox-2 in SCC25 cells after the treatment of 5 μM PLB for 6, 24, and 48 hours. (**C**) Bar graphs showing the relative levels of Oct-4, Bmi-1, Nanog, and Sox-2 in SCC25 cells after the treatment of 0.1, 1, and 5 μM PLB for 24 hours, and (**D**) bar graphs showing the relative levels of Oct-4, Bmi-1, Nanog, and Sox-2 in SCC25 cells after the treatment of 5 μM PLB for 6, 24, and 48 hours. Data are the mean ± SD of three independent experiments. *$P<0.05$; **$P<0.01$; and ***$P<0.001$ by one-way ANOVA.

Abbreviations: PLB, plumbagin; ANOVA, analysis of variance; SD, standard deviation.

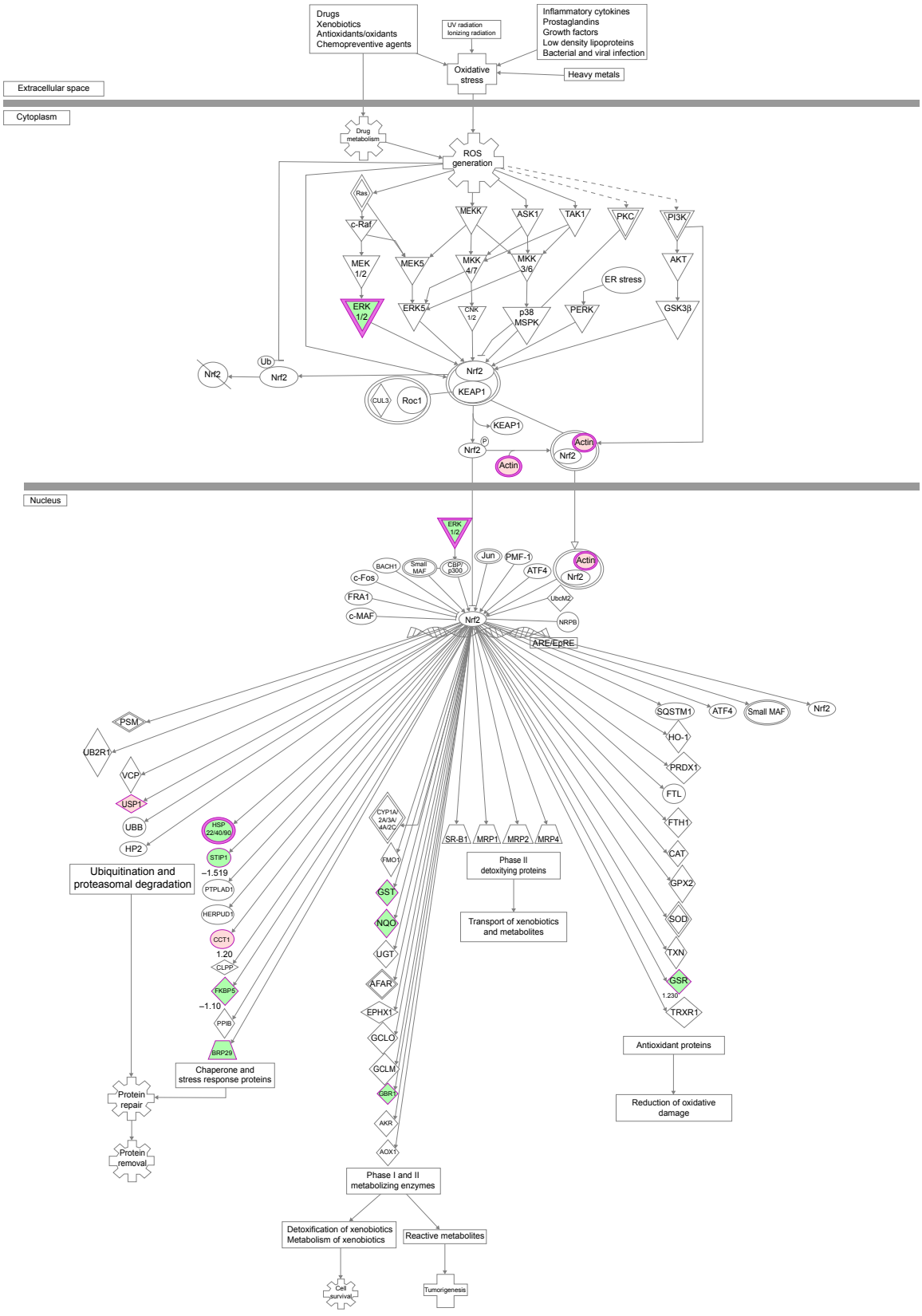

Figure 11 PLB regulates Nrf2 oxidative signaling pathway in SCC25 cells.

Notes: SCC25 cells were treated with 5 μM PLB for 24 hours and the protein samples were subject to quantitative proteomic analysis. Red indicates upregulation; green indicates downregulation. The intensity of green and red molecule colors indicates the degree of down or upregulation, respectively. Solid arrows indicate direct interaction and dashed arrows indicate indirect interaction.

Abbreviations: PLB, plumbagin; UV, ultraviolet.

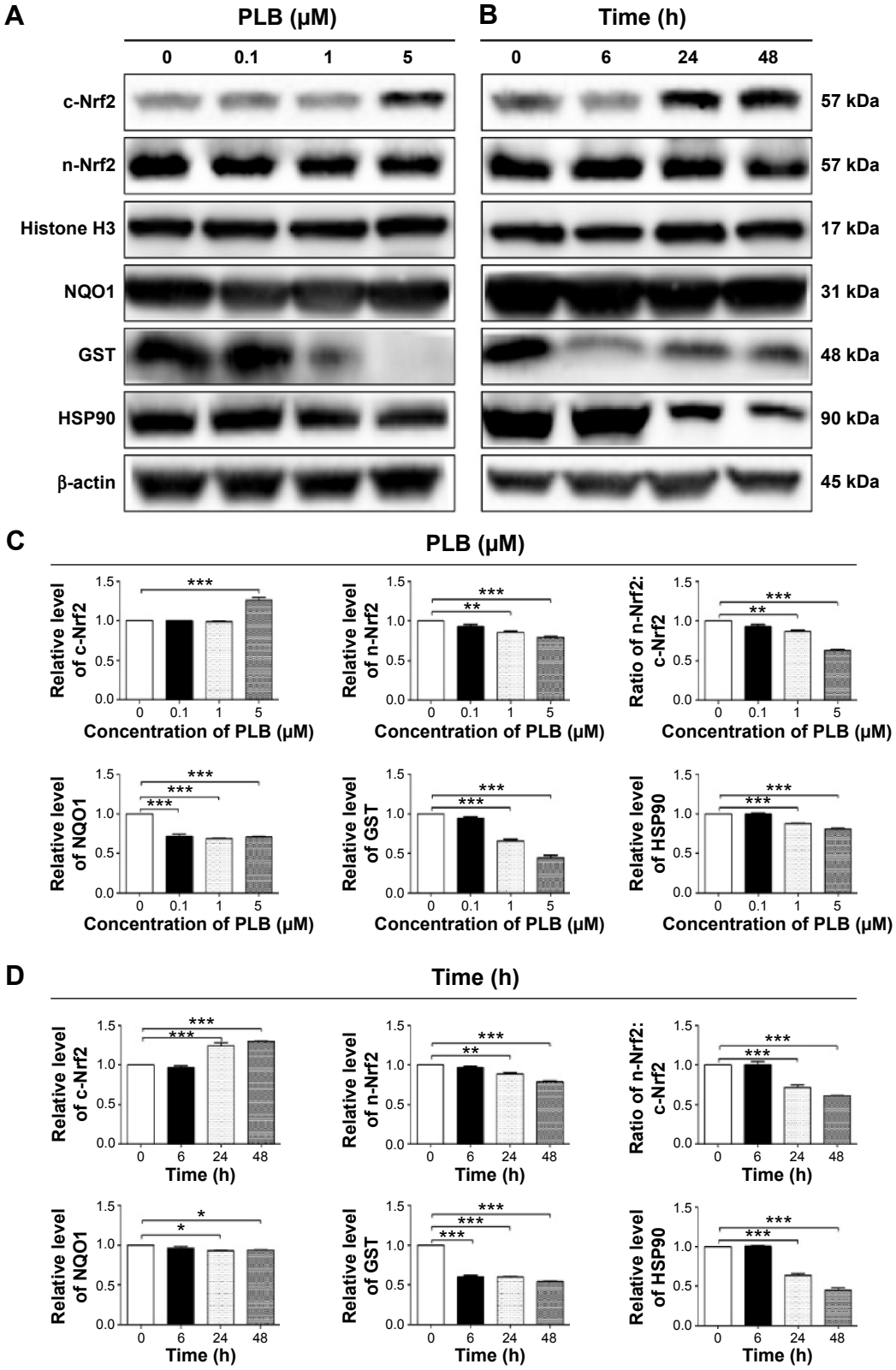

Figure 12 PLB regulates the expression of Nrf2, NQO1, GST, and HSP90 in SCC25 cells.

Notes: SCC25 cells were treated with PLB in the concentration and time course experiments and protein samples were subject to Western blotting assay. (**A**) Representative blots of c-Nrf2, n-Nrf2, NQO1, GST, and HSP90 in SCC25 cells after the treatment of 0.1, 1, and 5 μM PLB for 24 hours, and (**B**) representative blots of Nrf2, NQO1, GST, and HSP90 in SCC25 cells after the treatment of 5 μM PLB for 6, 24, and 48 hours. (**C**) Bar graphs showing the relative level of Nrf2, NQO1, GST, and HSP90 in SCC25 cells after the treatment of 0.1, 1, and 5 μM PLB for 24 hours, and (**D**) bar graphs showing the relative levels of Nrf2, NQO1, GST, and HSP90 in SCC25 cells after the treatment of 5 μM PLB for 6, 24, and 48 hours. Data are the mean ± SD of three independent experiments. *$P<0.05$; **$P<0.01$; and ***$P<0.001$ by one-way ANOVA.

Abbreviations: PLB, plumbagin; ANOVA, analysis of variance; SD, standard deviation.

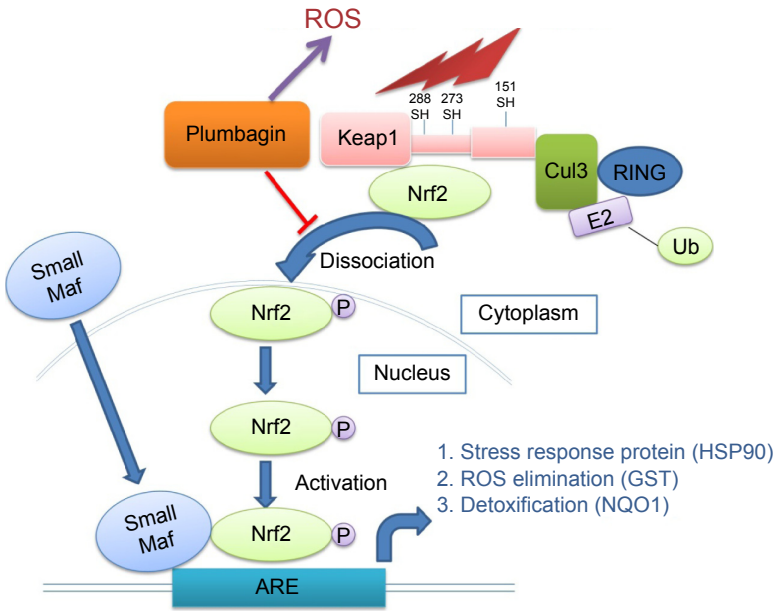

Figure 13 Schematic diagram shows that PLB regulates the Nrf2-mediated oxidative signaling pathway and its downstream proteins NQO1, GST, and HSP90 in SCC25 cells.
Abbreviations: ROS, reactive oxygen species; GST, glutathione S-transferase.

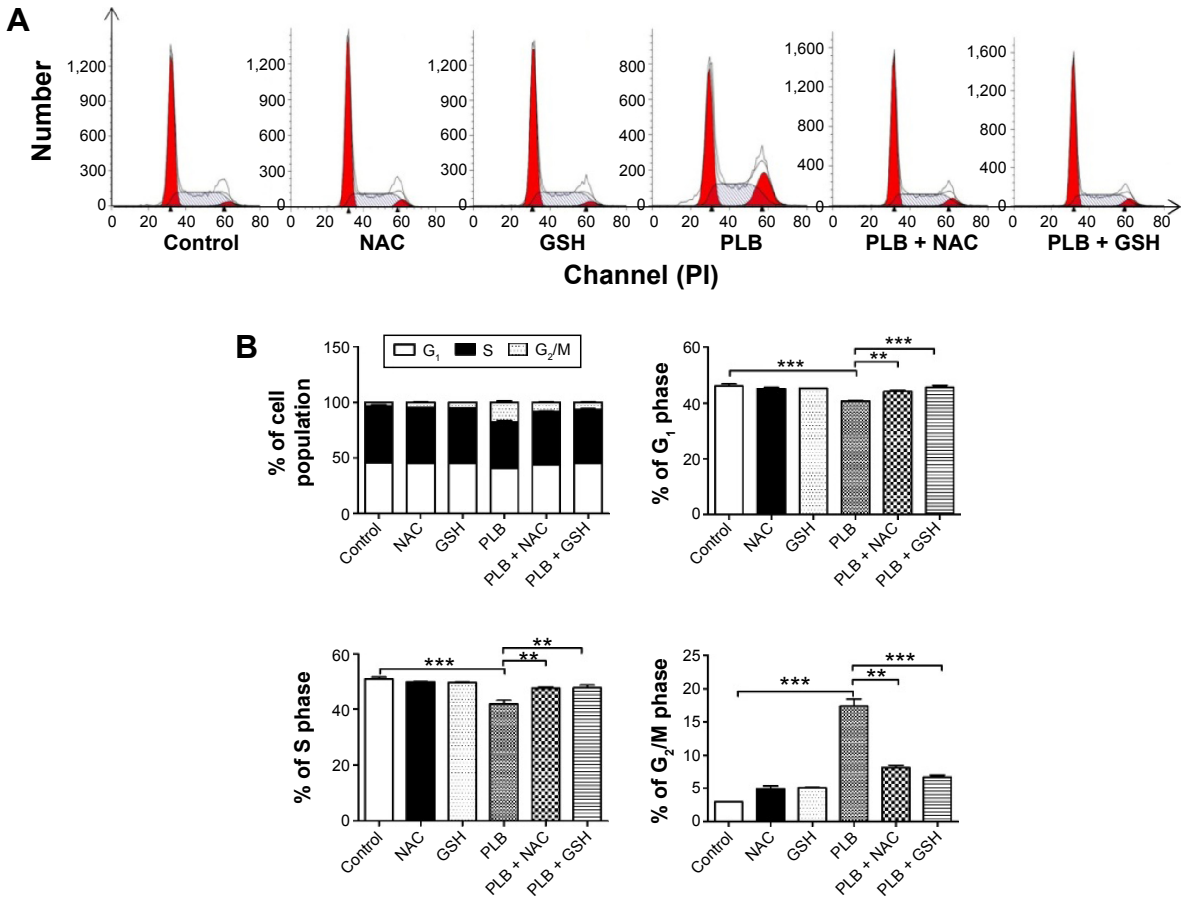

Figure 14 The effect of ROS scavengers NAC and GSH in PLB-induced G_2/M arrest in SCC25 cells.
Notes: (**A**) Representative flow cytometric plots of cell cycle distribution of SCC25 and (**B**) bar graphs showing the percentage of SCC25 cells in G_1, S and G_2/M phases after the treatment of 5 μM PLB, 100 μM NAC, 1 mM GSH, 5 μM PLB plus 100 μM NAC, and 5 μM PLB plus 1 mM GSH for 24 hours. Data are the mean ± SD of three independent experiments. $^{**}P<0.01$; and $^{***}P<0.001$ by one-way ANOVA.
Abbreviations: ROS, reactive oxygen species; NAC, *N*-acetyl-L-cysteine; GSH, L-glutathione; PLB, plumbagin; ANOVA, analysis of variance; SD, standard deviation.

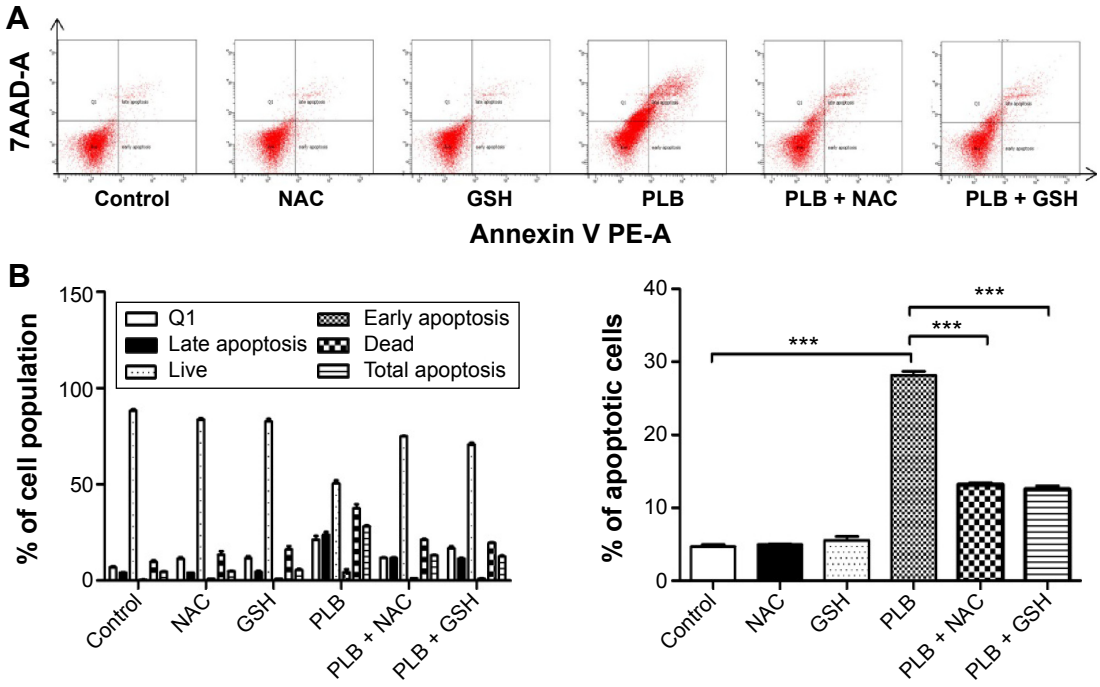

Figure 15 The effect of ROS scavengers NAC and GSH in PLB-induced apoptosis in SCC25 cells.
Notes: (**A**) Representative flow cytometric plots of apoptosis in SCC25 and (**B**) bar graphs showing the apoptotic percentage of SCC25 cells after the treatment of 5 μM PLB, 100 μM NAC, 1 mM GSH, 5 μM PLB plus 100 μM NAC, and 5 μM PLB plus 1 mM GSH for 24 hours. Data are the mean ± SD of three independent experiments. ***$P<0.001$ by one-way ANOVA.
Abbreviations: ROS, reactive oxygen species; NAC, *N*-acetyl-L-cysteine; GSH, L-glutathione; PLB, plumbagin; ANOVA, analysis of variance; SD, standard deviation.

Nanog was increased when cells were coincubated with NAC and PLB or GSH and PLB (Figure 16A and B). However, the expression level of Sox-2 did not show statistical significance (Figure 16A and B). This may be partially ascribed to PLB-mediated other pathways that downregulate the Sox-2 level. Taken together, PLB-induced ROS generation may interact with the actions of PLB-mediated cell cycle arrest, apoptosis induction, EMT inhibition, and stemness attenuation.

Discussion

TSCC remains one of the devastating malignancies in oral and maxillofacial tumors. TSCC is notorious for its lymphatic metastasis and relapse. Although sequential treatments are available, including radiotherapy, surgery, and chemotherapy, the therapeutic efficacy is not so optimistic.[1] This is partially due to hyperactive cell survival pathways and radiotherapy/chemotherapy resistance.[53,54] It is urgent to probe into the

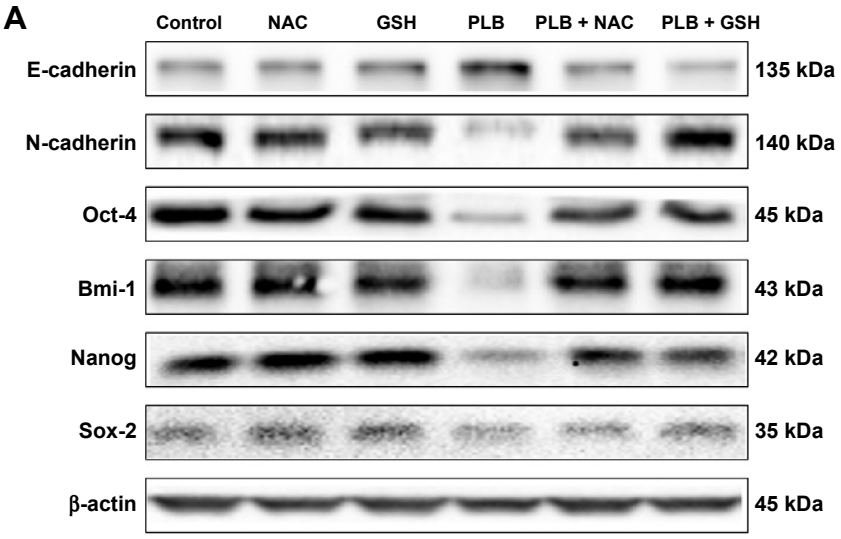

Figure 16 (*Continued*)

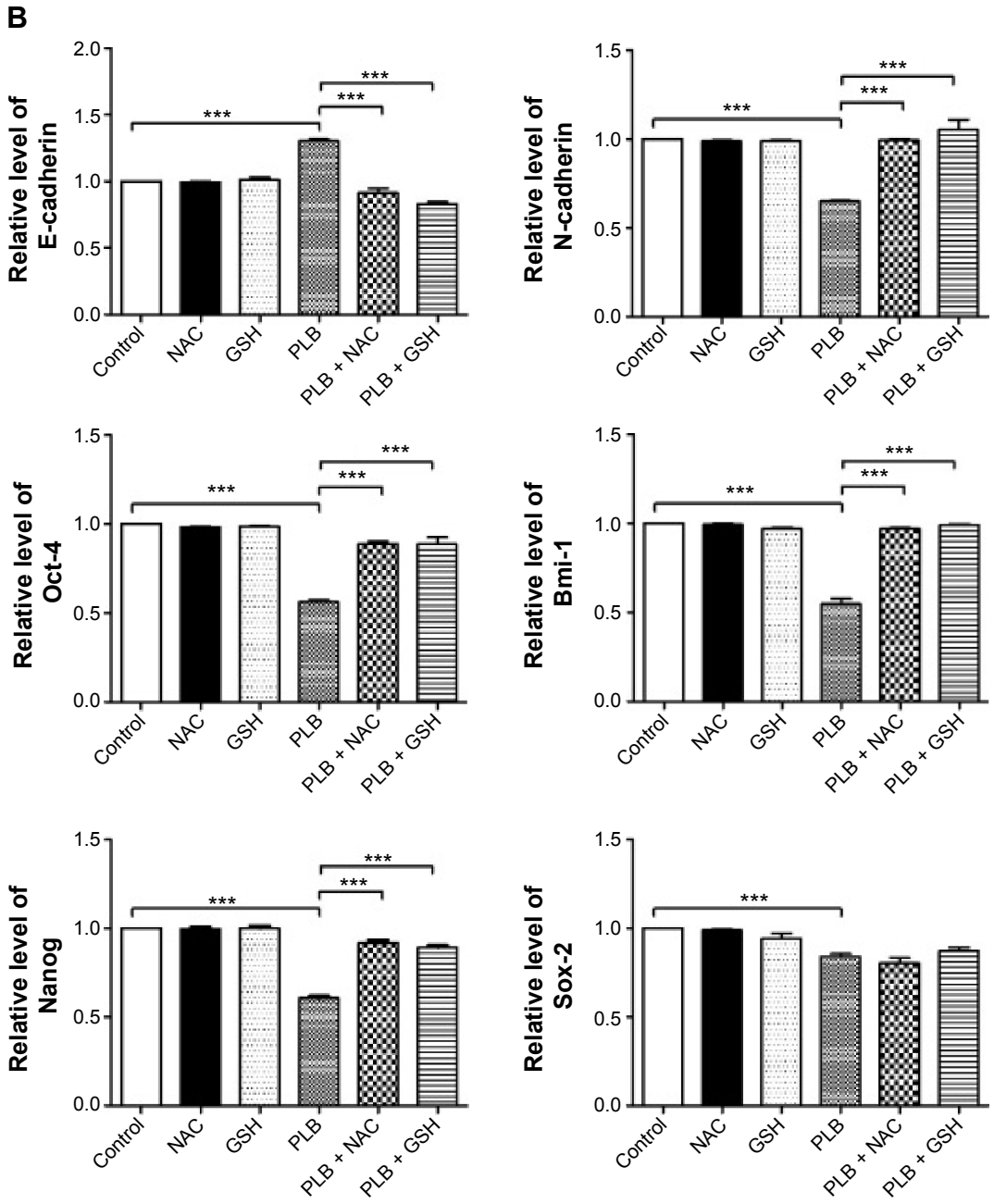

Figure 16 The effect of ROS scavengers NAC and GSH in PLB-mediated EMT inhibition and stemness attenuation in SCC25 cells.
Notes: (**A**) Representative blots of E-cadherin, N-cadherin, Oct-4, Bmi-1, Nanog, and Sox-2 in SCC25 cells and (**B**) bar graphs showing the relative level of E-cadherin, N-cadherin, Oct-4, Bmi-1, Nanog, and Sox-2 in SCC25 cells after the treatment of 5 μM PLB, 100 μM NAC, 1 mM GSH, 5 μM PLB plus 100 μM NAC, and 5 μM PLB plus 1 mM GSH for 24 hours. Data are the mean ± SD of three independent experiments. ***$P<0.001$ by one-way ANOVA.
Abbreviations: ROS, reactive oxygen species; NAC, *N*-acetyl-L-cysteine; GSH, L-glutathione; EMT, epithelial to mesenchymal transition; PLB, plumbagin; ANOVA, analysis of variance; SD, standard deviation.

corresponding molecular alterations and seek novel effective drugs for TSCC treatment. PLB is an active naphthoquinone constituent isolated from the roots of *Plumbaginaceae* plants.[17] It has been reported that PLB exhibits anticancer activities with minimal side effect in vitro and in vivo, which is greatly ascribed to its effects on multiple signaling pathways related to ROS generation, apoptosis, and autophagy.[23,55,56] In this study, we employed a SILAC-based quantitative proteomic study to obtain a comprehensive view of the proteomic response to PLB treatment in TSCC cell line SCC25, and the findings have shown that PLB regulates a variety of functional protein molecules and signaling pathways involved in critical cellular processes. Further validation results have shown that PLB induces G_2/M arrest and extrinsic apoptosis, but inhibits EMT and stemness via ROS generation through Nrf2-mediated oxidative signaling pathway in TSCC cell line SCC25 cells.

The SILAC-based proteomic approach can provide a system-level analysis to tackle the challenges in cancer treatment, such as chemoresistance. One study applied SILAC-based quantitative proteomic approach to analyze differences in protein expression level between parental hepatocellular carcinoma cell line HuH-7 and sorafenib-acquired resistance HuH-7 (HuH-7R) cells. Results indicated that galectin-1 is a predictive marker of sorafenib resistance and a downstream target of the Akt/mTOR/HIF-1a signaling pathway.[57] The SILAC-based proteomic approach can also quantitatively evaluate the effect of a given compound or drug and identify its potential molecular targets and related signaling pathways.[58–60] For example, the SILAC-based proteomic approach was used to screen the therapeutic targets of histone deacetylases inhibitor vorinostat in human breast cancer MDA-MB-231 cell line, and the results found that 61 proteins were lysine acetylated by vironostat.[30] This study demonstrated that PLB modulated a plethora of protein molecules, of which the expression levels of 143 protein molecules were increased while the levels of 255 protein molecules were decreased. Furthermore, 101 signaling pathways were potentially regulated by PLB in SCC25 cells. The following proteins are widely involved in cell survival, cell proliferation, redox homeostasis, cell metabolism, cell migration, and cell death: YWHAQ, PRKDC, YWHAG, YWHAE, YWHAH, YWHAB, YWHAZ, SFN, SKP1, CDK1, ACIN1, CAPNS1, MAPK1, RRAS, LMNA, CAPN2, SPTAN1, CYCS, PARP1, AIFM1, FADD, ACTB, ACTA1, ACTG1, ACTN1, ACTN4, ACTR3, ARPC1B, CTNNA1, CTNND1, DNM1L, EGFR, IQGAP1, JUP, MYH9, RAB7A, RHO1, TUBA1B, TUBA1C, TUBA4A, TUBB, TUBB4B, VAL, VCL, ZYX, CBR, DNAJA2, GSTP1, NQO1, HSP90AA1, PPIB, SOD1, STIP1, and VCP. The network of signaling pathways was mainly related to cell cycle distribution, cell migration, redox hemostasis, and cell death. The top ten targeted signaling pathways were EIF2 signaling pathway, regulation of eIF4 and p70S6K signaling, remodeling of epithelial adherens junctions pathway, mTOR signaling pathway, protein ubiquitination pathway, Nrf2-mediated oxidative stress response signaling pathway, epithelial adherens junction signaling pathway, caveolar-mediated endocytosis signaling pathway, RhoA signaling pathway, and oxidative phosphorylation pathway. The proteomic results indicate that PLB may target these molecules and related signaling pathways to elicit its anticancer effects in the treatment of TSCC. Notably, we have observed a differential effect of PLB on turmoral and nontumoral cells, with a higher half-maximal inhibitory concentration toward to nontumoral cells than that to the corresponding tumoral cells,[20] which renders PLB a promising anticancer drug candidate.

Subsequently, we further validated the proteomic responses to PLB in SCC25 cells. We found that PLB induced G_2/M arrest in SCC25 cells in a concentration- and time-dependent manner. Meanwhile, the expression level of key regulators of G_2/M phase, such as cdc2, cyclin B1, and cdc25, were decreased after the treatment of PLB. It has been reported that cell cycle progression is tightly regulated by cyclins and CDKs.[61] The complex formed by the association of CDK1/cdc2 and Cyclin B1 plays a major role in the entry of cells into mitosis. Phosphorylation of CDK1/cdc2 at Thr161 by CDK-activating kinase is essential for CDK1/cdc2 kinase activity. The process of the CDK1/cdc2 phosphorylation and dephosphorylation are mediated by the nuclear kinase Wee1 and the dual-specificity phosphatase cdc25. Wee1 can stop mitosis by inhibiting the CDK1/cdc2 phosphorylation, while cdc25 can help entry into mitosis by eliminating the inhibitory phosphorylation.[61] Thus, taking the proteomic, flow cytometric, and Western blotting results into consideration, PLB-induced cell cycle arrest may be mediated through the regulation of key modulators controlling the G_2/M check point in SCC25 cells.

Apoptosis is a conserved physiological mechanism that is important during embryogenesis and homeostasis of tissue. Dysregulated apoptosis has been implicated in many diseases including cancer.[62] The successful execution of apoptosis is crucial for many chemotherapy drugs.[63] It is widely accepted that there are two types of apoptosis: intrinsic apoptosis and extrinsic apoptosis. Mitochondrial disruption and the subsequent cytochrome c release can initiate the caspase-dependent apoptosis. Bcl-2 family plays an important role during this process.[64,65] Previously, our findings showed that PLB triggered the mitochondrial-mediated apoptosis in SCC25 cells.[20] In this study, the proteomic study showed that PLB regulated mitochondrial function and death receptor signaling pathway. We found that PLB could induce FADD-mediated extrinsic apoptosis in SCC25 cells. The proteomic results hinted that PLB regulated the death receptor signaling and that the protein molecule FADD was upregulated by PLB. FADD is a key adaptor protein for death receptor-mediated apoptosis. The death domain of FADD binds to the death domain of death receptor. Subsequently, procaspase-8 is recruited and caspase 3, 6, and 7 are cleaved. Finally, apoptosis is induced; and both intrinsic and extrinsic apoptosis converge into the cleavage of caspase 3. TRADD is a tumor necrosis factor receptor 1 (TNFR1) associated signal transducer that enhances association of FADD with TNFR1.[66,67] DR5, also

known as TRAIL-R2, can bind to adaptor molecules FADD and TRADD.[68] In this study, we found that PLB increased the level of FADD, TRADD, and DR5. This indicated the extrinsic apoptosis-inducing effect of PLB in SCC25. Together with the results from our previous paper,[20] it seems that PLB can efficiently induce both intrinsic and extrinsic apoptosis in SCC25 cells.

TSCC is notorious for its metastasis and relapse, and acquisition of EMT and induction of CSC-like properties are inevitably responsible for the metastasis and relapse.[69] EMT is a highly conserved biological process that converts epithelial cells into mesenchymal cells via the modulation of various transcription factors.[70–73] EMT has been classified into three types according to specific physiological context. Type I EMT plays an important role in embryogenesis and organ development. Type II EMT functions in wound healing and tissue regeneration. Type III EMT, the one we focus on, is involved in cancer metastasis and CSC formation.[35,74] The EMT process is characterized by loss of epithelial markers such as E-cadherin, claudin, and occludin, and acquisition of mesenchymal markers such as N-cadherin, vimentin, snail, slug, and ZO-1.[75,76] Many signaling pathways, such as Wnt, TGF-β, and STAT3, can mediate the EMT process via activating a plethora of transcriptional regulators of mesenchymal markers.[75,76] Furthermore, CSCs can display EMT characteristics such as loss of adhesion protein E-cadherin.[11] Static CSCs that have moved to distant sites might be responsible for metastases and relapse, especially after curative surgical treatment of a primary tumor.[77] Seminal findings demonstrate that EMT activators, such as Twist1 and Prrx1, can serve as a direct molecular link between EMT and stemness.[78,79] Our proteomic study showed that PLB could regulate the epithelial adherens junctions pathway in SCC25 cells. The Western blotting assay validated that PLB could increase the expression level of E-cadherin and decrease the level of N-cadherin in SCC25 cells. Furthermore, we examined other key regulators of EMT. We found that PLB significantly reduced the expression level of snail, slug, TCF-8/ZEB1, β-catenin, and vimentin, while increasing the expression level of claudin-1 and ZO-1. All these implied the EMT-inhibiting role of PLB in SCC25 cells. Subsequently, CSCs markers were also measured, and the expression levels of Oct-4, Bmi-1, Nanog, and Sox-2 were all found to be decreased by PLB in a concentration- and time-dependent manner in SCC25 cells. Taken together, PLB can inhibit EMT and attenuate stemness in SCC25 cells. We can speculate that there are interconnections between EMT and stemness, such as the loss of E-cadherin. Given that PLB can regulate the key factors in EMT, the stemness property may more or less be affected. However, the exact network between EMT and stemness needs further investigation. Importantly, it has been reported that ROS may link the EMT and stemness via glucose metabolism.[80] In our previous paper,[20] we found that PLB can efficiently induce ROS generation, which can be abolished by ROS scavengers NAC and GSH. On the basis of the results of the present proteomic analysis, PLB can efficiently regulate the Nrf2-mediated oxidative stress response signaling pathway. Nrf2, also known as Nfe2l2, is a nuclear factor that controls the expression of various detoxifying enzymes, ROS elimination proteins, drug transporters, and antiapoptotic proteins. Normally, Nrf2 is suppressed in the cytoplasm by combination with Keap1 and Cullin3. Once exposed to the ARE-mediated inducers, Nrf2 will translocate to the nucleus where it forms a heterodimer with a small Maf protein and binds to other nuclear factors and initiates the transcription of antioxidative genes.[51,52] The Western blotting results showed that the ratio of n-Nrf2 to c-Nrf2 was significantly decreased. Furthermore, the downstream effectors NQO1, GST, and HSP90 were examined. These effectors are involved in ROS elimination and detoxification.[81–83] Results showed that PLB can decrease the expression level of NQO1, GST, and HSP90 in SCC25 cells. We can carefully draw a conclusion that PLB can kill TSCC cells via ROS generation and attenuation of ROS elimination factors. Finally, we employed the ROS scavengers NAC and GSH to further examine the effect of PLB in cell cycle arrest, apoptosis induction, EMT inhibition, and stemness attenuation. Interestingly, results showed that the cell cycle arresting, apoptosis inducing, EMT inhibiting, and stemness-attenuating effect of PLB can be efficiently abolished by NAC and GSH. This highlights the ROS-generation-inducing effect of PLB as an upstream effector to regulate other downstream biological activities such as cell cycle arrest and apoptosis.

In summary, the quantitative SILAC-based proteomic approach showed that PLB inhibited cell proliferation, activated death receptor-mediated apoptotic pathway, remodeled epithelial adherens junctions pathway, and increased intracellular level of ROS via Nrf2-mediated oxidative stress response signaling pathway in human SCC25 cells involving a number of key functional proteins. This study may provide a clue to fully identify the molecular targets and elucidate the underlying mechanisms of PLB in the treatment of TSCC.

Acknowledgments

The authors appreciate the financial support by the National Natural Science Foundation of China (grant number: 81560440)

and the Key Project of Chinese Medicine Research Plan of Jiangxi province (grant number: 2013Z010).

Disclosure

The authors report no conflicts of interest in the work.

References

1. Siegel RL, Miller KD, Jemal A. Cancer statistics, 2015. *CA Cancer J Clin*. 2015;65(1):5–29.
2. Li R, Koch WM, Fakhry C, Gourin CG. Distinct epidemiologic characteristics of oral tongue cancer patients. *Otolaryngol Head Neck Surg*. 2013;148(5):792–796.
3. Joseph LJ, Goodman M, Higgins K, et al. Racial disparities in squamous cell carcinoma of the oral tongue among women: a SEER data analysis. *Oral Oncol*. 2015;51(6):586–592.
4. Markopoulos AK. Current aspects on oral squamous cell carcinoma. *Open Dent J*. 2012;6:126–130.
5. Dogan E, Cetinayak HO, Sarioglu S, Erdag TK, Ikiz AO. Patterns of cervical lymph node metastases in oral tongue squamous cell carcinoma: implications for elective and therapeutic neck dissection. *J Laryngol Otol*. 2014;128(3):268–273.
6. Liu F, Kong X, Lv L, Gao J. TGF-beta1 acts through miR-155 to down-regulate TP53INP1 in promoting epithelial-mesenchymal transition and cancer stem cell phenotypes. *Cancer Lett*. 2015;359(2):288–298.
7. Donnenberg VS, Donnenberg AD. Stem cell state and the epithelial-to-mesenchymal transition: implications for cancer therapy. *J Clin Pharmacol*. 2015;55(6):603–619.
8. Perdigao-Henriques R, Petrocca F, Altschuler G, et al. miR-200 promotes the mesenchymal to epithelial transition by suppressing multiple members of the Zeb2 and Snail1 transcriptional repressor complexes. *Oncogene*. Epub 2015.
9. Brabletz T. EMT and MET in metastasis: where are the cancer stem cells? *Cancer Cell*. 2012;22(6):699–701.
10. Morrison SJ, Kimble J. Asymmetric and symmetric stem-cell divisions in development and cancer. *Nature*. 2006;441(7097):1068–1074.
11. Martin-Belmonte F, Perez-Moreno M. Epithelial cell polarity, stem cells and cancer. *Nat Rev Cancer*. 2012;12(1):23–38.
12. Boumahdi S, Driessens G, Lapouge G, et al. SOX2 controls tumour initiation and cancer stem-cell functions in squamous-cell carcinoma. *Nature*. 2014;511(7508):246–250.
13. Chiou SH, Yu CC, Huang CY, et al. Positive correlations of Oct-4 and Nanog in oral cancer stem-like cells and high-grade oral squamous cell carcinoma. *Clin Cancer Res*. 2008;14(13):4085–4095.
14. Molofsky AV, Pardal R, Iwashita T, et al. Bmi-1 dependence distinguishes neural stem cell self-renewal from progenitor proliferation. *Nature*. 2003;425(6961):962–967.
15. Kagias K, Ahier A, Fischer N, Jarriault S. Members of the NODE (Nanog and Oct4-associated deacetylase) complex and SOX-2 promote the initiation of a natural cellular reprogramming event in vivo. *Proc Natl Acad Sci U S A*. 2012;109(17):6596–6601.
16. Stuckey DW, Shah K. Stem cell-based therapies for cancer treatment: separating hope from hype. *Nat Rev Cancer*. 2014;14(10):683–691.
17. Padhye S, Dandawate P, Yusufi M, Ahmad A, Sarkar FH. Perspectives on medicinal properties of plumbagin and its analogs. *Med Res Rev*. 2012;32(6):1131–1158.
18. Sung B, Oyajobi B, Aggarwal BB. Plumbagin inhibits osteoclastogenesis and reduces human breast cancer-induced osteolytic bone metastasis in mice through suppression of RANKL signaling. *Mol Cancer Ther*. 2012;11(2):350–359.
19. Sinha S, Pal K, Elkhanany A, et al. Plumbagin inhibits tumorigenesis and angiogenesis of ovarian cancer cells in vivo. *Int J Cancer*. 2013;132(5):1201–1212.
20. Pan ST, Qin Y, Zhou ZW, et al. Plumbagin induces G2/M arrest, apoptosis, and autophagy via p38 MAPK- and PI3K/Akt/mTOR-mediated pathways in human tongue squamous cell carcinoma cells. *Drug Des Devel Ther*. 2015;9:1601–1626.
21. Li YC, He SM, He ZX, et al. Plumbagin induces apoptotic and autophagic cell death through inhibition of the PI3K/Akt/mTOR pathway in human non-small cell lung cancer cells. *Cancer Lett*. 2014;344(2):239–259.
22. Sandur SK, Ichikawa H, Sethi G, Ahn KS, Aggarwal BB. Plumbagin (5-hydroxy-2-methyl-1,4-naphthoquinone) suppresses NF-kappaB activation and NF-kappaB-regulated gene products through modulation of p65 and IkappaBalpha kinase activation, leading to potentiation of apoptosis induced by cytokine and chemotherapeutic agents. *J Biol Chem*. 2006;281(25):17023–17033.
23. Kuo PL, Hsu YL, Cho CY. Plumbagin induces G2-M arrest and autophagy by inhibiting the AKT/mammalian target of rapamycin pathway in breast cancer cells. *Mol Cancer Ther*. 2006;5(12):3209–3221.
24. Wang F, Wang Q, Zhou ZW, et al. Plumbagin induces cell cycle arrest and autophagy and suppresses epithelial to mesenchymal transition involving PI3K/Akt/mTOR-mediated pathway in human pancreatic cancer cells. *Drug Des Devel Ther*. 2015;9:537–560.
25. Zhou ZW, Li XX, He ZX, et al. Induction of apoptosis and autophagy via sirtuin1- and PI3K/Akt/mTOR-mediated pathways by plumbagin in human prostate cancer cells. *Drug Des Devel Ther*. 2015;9:1511–1554.
26. Sun J, McKallip RJ. Plumbagin treatment leads to apoptosis in human K562 leukemia cells through increased ROS and elevated TRAIL receptor expression. *Leuk Res*. 2011;35(10):1402–1408.
27. Xu KH, Lu DP. Plumbagin induces ROS-mediated apoptosis in human promyelocytic leukemia cells in vivo. *Leuk Res*. 2010;34(5):658–665.
28. Lee JH, Yeon JH, Kim H, et al. The natural anticancer agent plumbagin induces potent cytotoxicity in MCF-7 human breast cancer cells by inhibiting a PI-5 kinase for ROS generation. *PLoS One*. 2012;7(9):e45023.
29. Edelmann MJ, Shack LA, Naske CD, Walters KB, Nanduri B. SILAC-based quantitative proteomic analysis of human lung cell response to copper oxide nanoparticles. *PLoS One*. 2014;9(12):e114390.
30. Zhou Q, Chaerkady R, Shaw PG, et al. Screening for therapeutic targets of vorinostat by SILAC-based proteomic analysis in human breast cancer cells. *Proteomics*. 2010;10(5):1029–1039.
31. Ong SE, Mann M. A practical recipe for stable isotope labeling by amino acids in cell culture (SILAC). *Nat Protoc*. 2006;1(6):2650–2660.
32. Pan ST, Zhou ZW, He ZX, et al. Proteomic response to 5,6-dimethylxanthenone 4-acetic acid (DMXAA, vadimezan) in human non-small cell lung cancer A549 cells determined by the stable-isotope labeling by amino acids in cell culture (SILAC) approach. *Drug Des Devel Ther*. 2015;9:937–968.
33. Qiu JX, Zhou ZW, He ZX, et al. Plumbagin elicits differential proteomic responses mainly involving cell cycle, apoptosis, autophagy, and epithelial-to-mesenchymal transition pathways in human prostate cancer PC-3 and DU145 cells. *Drug Des Devel Ther*. 2015;9:349–417.
34. Qin Y, Zhou ZW, Pan ST, et al. Graphene quantum dots induce apoptosis, autophagy, and inflammatory response via p38 mitogen-activated protein kinase and nuclear factor-kappaB mediated signaling pathways in activated THP-1 macrophages. *Toxicology*. 2015;327:62–76.
35. Thiery JP, Lim CT. Tumor dissemination: an EMT affair. *Cancer Cell*. 2013;23(3):272–273.
36. Stebbing J, Filipovic A, Giamas G. Claudin-1 as a promoter of EMT in hepatocellular carcinoma. *Oncogene*. 2013;32(41):4871–4872.
37. Furuse M, Hirase T, Itoh M, et al. Occludin: a novel integral membrane protein localizing at tight junctions. *J Cell Biol*. 1993;123(6 Pt 2):1777–1788.
38. Furuse M, Itoh M, Hirase T, et al. Direct association of occludin with ZO-1 and its possible involvement in the localization of occludin at tight junctions. *J Cell Biol*. 1994;127(6 Pt 1):1617–1626.

39. Haskins J, Gu L, Wittchen ES, Hibbard J, Stevenson BR. ZO-3, a novel member of the MAGUK protein family found at the tight junction, interacts with ZO-1 and occludin. *J Cell Biol*. 1998;141(1):199–208.
40. Umeda K, Ikenouchi J, Katahira-Tayama S, et al. ZO-1 and ZO-2 independently determine where claudins are polymerized in tight-junction strand formation. *Cell*. 2006;126(4):741–754.
41. Gheldof A, Berx G. Cadherins and epithelial-to-mesenchymal transition. *Prog Mol Biol Transl Sci*. 2013;116:317–336.
42. Janda E, Nevolo M, Lehmann K, et al. Raf plus TGFbeta-dependent EMT is initiated by endocytosis and lysosomal degradation of E-cadherin. *Oncogene*. 2006;25(54):7117–7130.
43. Zhang X, Liu G, Kang Y, et al. N-cadherin expression is associated with acquisition of EMT phenotype and with enhanced invasion in erlotinib-resistant lung cancer cell lines. *PLoS One*. 2013;8(3):e57692.
44. Polakis P. More than one way to skin a catenin. *Cell*. 2001;105(5):563–566.
45. Eger A, Stockinger A, Park J, et al. Beta-Catenin and TGFbeta signalling cooperate to maintain a mesenchymal phenotype after FosER-induced epithelial to mesenchymal transition. *Oncogene*. 2004;23(15):2672–2680.
46. Stemmer V, de Craene B, Berx G, Behrens J. Snail promotes Wnt target gene expression and interacts with beta-catenin. *Oncogene*. 2008;27(37):5075–5080.
47. Koo BS, Lee SH, Kim JM, et al. Oct4 is a critical regulator of stemness in head and neck squamous carcinoma cells. *Oncogene*. 2015;34(18):2317–2324.
48. Sarkar A, Hochedlinger K. The sox family of transcription factors: versatile regulators of stem and progenitor cell fate. *Cell Stem Cell*. 2013;12(1):15–30.
49. Hayashi Y, Caboni L, Das D, et al. Structure-based discovery of NANOG variant with enhanced properties to promote self-renewal and reprogramming of pluripotent stem cells. *Proc Natl Acad Sci U S A*. 2015;112(15):4666–4671.
50. Lessard J, Sauvageau G. Bmi-1 determines the proliferative capacity of normal and leukaemic stem cells. *Nature*. 2003;423(6937):255–260.
51. DeNicola GM, Karreth FA, Humpton TJ, et al. Oncogene-induced Nrf2 transcription promotes ROS detoxification and tumorigenesis. *Nature*. 2011;475(7354):106–109.
52. Zhang Y, Gordon GB. A strategy for cancer prevention: stimulation of the Nrf2-ARE signaling pathway. *Mol Cancer Ther*. 2004;3(7):885–893.
53. Tsurutani J, West KA, Sayyah J, Gills JJ, Dennis PA. Inhibition of the phosphatidylinositol 3-kinase/Akt/mammalian target of rapamycin pathway but not the MEK/ERK pathway attenuates laminin-mediated small cell lung cancer cellular survival and resistance to imatinib mesylate or chemotherapy. *Cancer Res*. 2005;65(18):8423–8432.
54. Zhao G, Cai C, Yang T, et al. MicroRNA-221 induces cell survival and cisplatin resistance through PI3K/Akt pathway in human osteosarcoma. *PLoS One*. 2013;8(1):e53906.
55. Aziz MH, Dreckschmidt NE, Verma AK. Plumbagin, a medicinal plant-derived naphthoquinone, is a novel inhibitor of the growth and invasion of hormone-refractory prostate cancer. *Cancer Res*. 2008;68(21):9024–9032.
56. Wang CC, Chiang YM, Sung SC, et al. Plumbagin induces cell cycle arrest and apoptosis through reactive oxygen species/c-Jun N-terminal kinase pathways in human melanoma A375.S2 cells. *Cancer Lett*. 2008;259(1):82–98.
57. Yeh CC, Hsu CH, Shao YY, et al. Integrated SILAC and iTRAQ quantitative proteomic analysis identifies galectin-1 as a potential biomarker for predicting sorafenib resistance in liver cancer. *Mol Cell Proteomics*. 2015;14(6):1527–1545.
58. Dolai S, Xu Q, Liu F, Molloy MP. Quantitative chemical proteomics in small-scale culture of phorbol ester stimulated basal breast cancer cells. *Proteomics*. 2011;11(13):2683–2692.
59. Geiger T, Cox J, Ostasiewicz P, Wisniewski JR, Mann M. Super-SILAC mix for quantitative proteomics of human tumor tissue. *Nat Methods*. 2010;7(5):383–385.
60. Everley PA, Krijgsveld J, Zetter BR, Gygi SP. Quantitative cancer proteomics: stable isotope labeling with amino acids in cell culture (SILAC) as a tool for prostate cancer research. *Mol Cell Proteomics*. 2004;3(7):729–735.
61. Hunter T. Protein kinases and phosphatases: the yin and yang of protein phosphorylation and signaling. *Cell*. 1995;80(2):225–236.
62. Evan GI, Vousden KH. Proliferation, cell cycle and apoptosis in cancer. *Nature*. 2001;411(6835):342–348.
63. Reed JC. Apoptosis-based therapies. *Nat Rev Drug Discov*. 2002;1(2):111–121.
64. Boehning D, Patterson RL, Sedaghat L, et al. Cytochrome c binds to inositol (1,4,5) trisphosphate receptors, amplifying calcium-dependent apoptosis. *Nat Cell Biol*. 2003;5(12):1051–1061.
65. Yang J, Liu X, Bhalla K, et al. Prevention of apoptosis by Bcl-2: release of cytochrome c from mitochondria blocked. *Science*. 1997;275(5303):1129–1132.
66. Pobezinskaya YL, Liu Z. The role of TRADD in death receptor signaling. *Cell Cycle*. 2012;11(5):871–876.
67. Park YC, Ye H, Hsia C, et al. A novel mechanism of TRAF signaling revealed by structural and functional analyses of the TRADD-TRAF2 interaction. *Cell*. 2000;101(7):777–787.
68. Zlotorynski E. Apoptosis. DR5 unfolds ER stress. *Nat Rev Mol Cell Biol*. 2014;15(8):498–499.
69. Biddle A, Mackenzie IC. Cancer stem cells and EMT in carcinoma. *Cancer Metastasis Rev*. 2012;31(1–2):285–293.
70. Okada T, Sinha S, Esposito I, et al. The Rho GTPase Rnd1 suppresses mammary tumorigenesis and EMT by restraining Ras-MAPK signalling. *Nat Cell Biol*. 2015;17(1):81–94.
71. Kudo-Saito C, Shirako H, Takeuchi T, Kawakami Y. Cancer metastasis is accelerated through immunosuppression during Snail-induced EMT of cancer cells. *Cancer Cell*. 2009;15(3):195–206.
72. Ansieau S, Bastid J, Doreau A, et al. Induction of EMT by twist proteins as a collateral effect of tumor-promoting inactivation of premature senescence. *Cancer Cell*. 2008;14(1):79–89.
73. Waerner T, Alacakaptan M, Tamir I, et al. ILEI: a cytokine essential for EMT, tumor formation, and late events in metastasis in epithelial cells. *Cancer Cell*. 2006;10(3):227–239.
74. Qureshi R, Arora H, Rizvi MA. EMT in cervical cancer: its role in tumour progression and response to therapy. *Cancer Lett*. 2015;356(2 Pt B):321–331.
75. De Craene B, Berx G. Regulatory networks defining EMT during cancer initiation and progression. *Nat Rev Cancer*. 2013;13(2):97–110.
76. Rhim AD, Mirek ET, Aiello NM, et al. EMT and dissemination precede pancreatic tumor formation. *Cell*. 2012;148(1–2):349–361.
77. Clevers H. The cancer stem cell: premises, promises and challenges. *Nat Med*. 2011;17(3):313–319.
78. Mani SA, Guo W, Liao MJ, et al. The epithelial-mesenchymal transition generates cells with properties of stem cells. *Cell*. 2008;133(4):704–715.
79. Ocana OH, Corcoles R, Fabra A, et al. Metastatic colonization requires the repression of the epithelial-mesenchymal transition inducer Prrx1. *Cancer Cell*. 2012;22(6):709–724.
80. Schieber MS, Chandel NS. ROS links glucose metabolism to breast cancer stem cell and EMT phenotype. *Cancer Cell*. 2013;23(3):265–267.
81. Matsui A, Ikeda T, Enomoto K, et al. Increased formation of oxidative DNA damage, 8-hydroxy-2′-deoxyguanosine, in human breast cancer tissue and its relationship to GSTP1 and COMT genotypes. *Cancer Lett*. 2000;151(1):87–95.
82. Beck R, Dejeans N, Glorieux C, et al. Hsp90 is cleaved by reactive oxygen species at a highly conserved N-terminal amino acid motif. *PLoS One*. 2012;7(7):e40795.
83. Li L, Dong H, Song E, et al. Nrf2/ARE pathway activation, HO-1 and NQO1 induction by polychlorinated biphenyl quinone is associated with reactive oxygen species and PI3K/AKT signaling. *Chem Biol Interact*. 2014;209:56–67.